

Manohar Badger

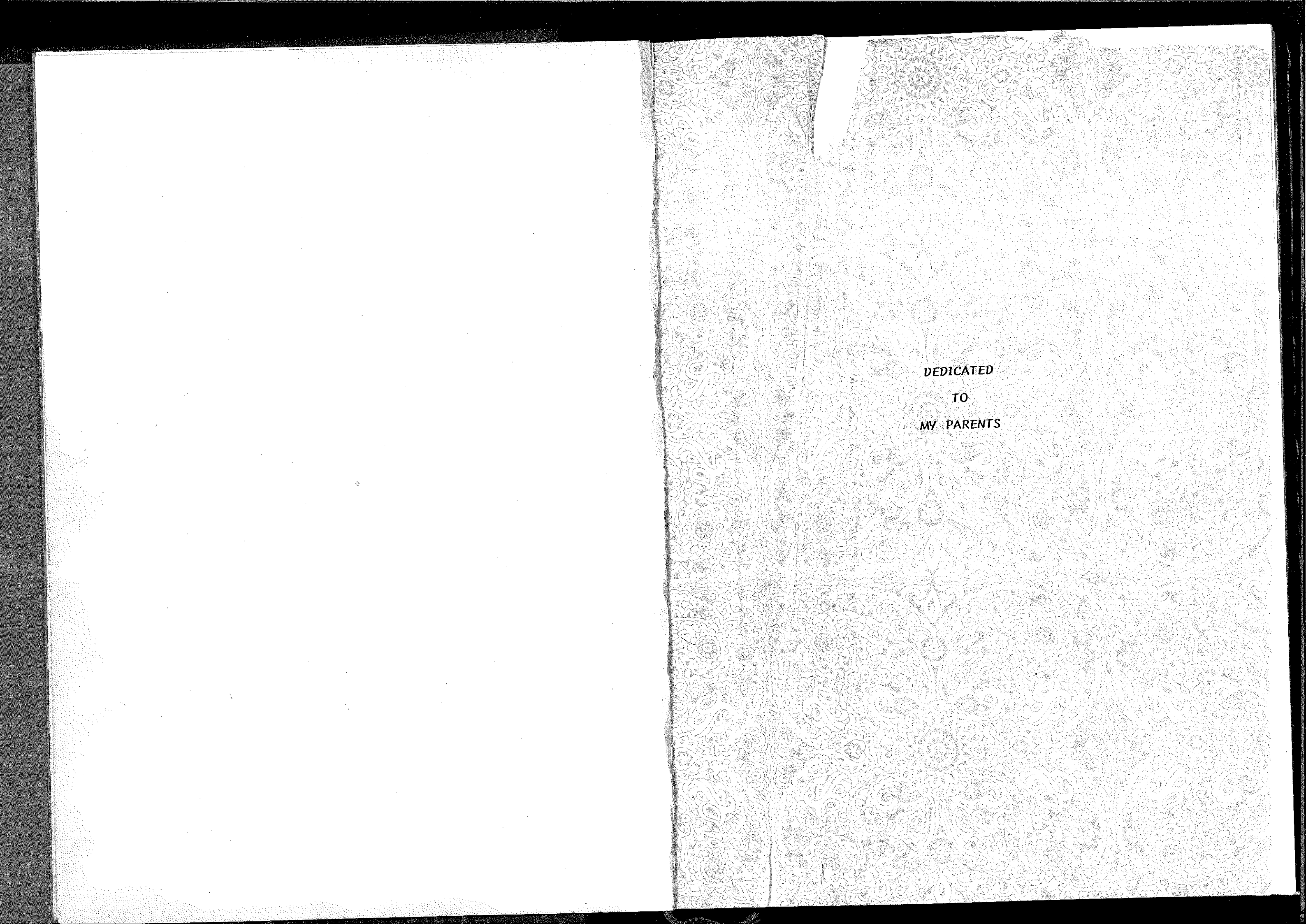
**TRANSPORT PHENOMENA IN
POLYMERIC MEDIA**

A THESIS
SUBMITTED TO THE
UNIVERSITY OF BOMBAY
FOR THE DEGREE OF
DOCTOR OF PHILOSOPHY
(IN CHEMISTRY)

BY
M. V. BADIGER
B. Sc., (Tech.)

DIVISION OF CHEMICAL ENGINEERING
NATIONAL CHEMICAL LABORATORY
PUNE - 411 008 (INDIA)

1988



DEDICATED
TO
MY PARENTS

ACKNOWLEDGEMENTS

It is an honour to acknowledge my debt of gratitude to my research supervisor, Dr. R.A. Mashelkar, Deputy Director and Head of the Chemical Engineering Division, National Chemical Laboratory, Pune, for his inspiring guidance and encouragement in the course of this work.

I am grateful to Drs. M.G. Kulkarni and S. Ganapathy for their keen interest and valuable suggestions.

I would like to thank Drs. S. Radhakrishnan and S.N. Shintre for their generous help.

My grateful thanks are due to Prof. L.K. Doraiswamy, Director, NCL for permitting me to work in NCL and to submit this thesis to the University of Bombay.

Thanks are due to Mr. K.G. Joshi and Mr. A.C. Detankar for typing the thesis.

It is a pleasure to acknowledge the cooperation and encouragement received from my colleagues in the group.



(M.V. BADIGER)

October 4, 1988

C O N T E N T S

Page No.

SCOPE OF THE WORK

1

CHAPTER - I

AN OVERVIEW OF SUPERABSORBENT POLYMERS

INTRODUCTION

4

- A brief overview of gels.

5

- Sol-gel transition.

6

- Swelling of gels.

7

PHASE TRANSITION

10

- Volume phase transition in polymers.

13

- Manifestations of volume phase transition.

20

- Criteria for volume phase transition in gels.

23

INVESTIGATION OF GEL STRUCTURE BY NMR

38

RHEOLOGY OF GELS

40

SEPARATION PROCESSES BASED ON GELS

41

REFERENCES

43

NOTATION

47

SYNTHESIS AND CHARACTERIZATION OF SUPER-
ABSORBENT POLYMERSSUPER ABSORBENTS BASED ON CROSS-LINKED
POLYSTYRENE SULFONATE

INTRODUCTION	48
EXPERIMENTAL	49
- Synthesis of cross-linked polystyrene gels by : Suspension polymerization. : Bulk polymerization.	51
- Sulfonation of cross-linked polystyrene gels.	53
- Estimation of degree of sulfonation.	54
- Swelling ratio measurements.	54
RESULTS AND DISCUSSION	55
- Effect of degree of cross-linking and degree of sulfonation on swelling ratio.	55
- Estimation of average molecular weight between cross-links (Mc).	59
- Determination of average mesh-size of the network (ξ).	61
- Determination of V_2 , Mc and ξ for bulk polymerized polystyrene - DVB gels.	62
- Effect of electrolytes and pH on swelling ratio.	63
- Swelling behaviour of polystyrene sulfonate gel in non-aqueous media.	68
CONCLUSIONS	76

	Page No.
<u>SUPERABSORBENTS BASED ON POLY-2-ACRYLAMIDO-2-METHYL PROPANE SULFONATE (PAMPS)</u>	
INTRODUCTION	77
SYNTHESIS AND CHARACTERIZATION	78
CONCLUSIONS	81
REFERENCES	82
NOTATION	84
<u>CHAPTER - III</u>	
<u>NMR STUDIES IN SUPERABSORBENT POLYMERS</u>	
<u>FUNDAMENTALS OF NMR</u>	94
- Nuclear Magnetic Resonance (NMR) Phenomena.	94
- NMR Spectrometer.	96
- Fourier - Transform NMR (FT-NMR).	98
<u>STATE OF WATER IN SUPERABSORBENT POLYMERS</u>	99
INTRODUCTION	99
EXPERIMENTAL	
- Relaxation time measurements.	101
RESULTS AND DISCUSSION	
- Interpretation of data.	105
CONCLUSIONS	111
<u>HIGH RESOLUTION SOLID-STATE PROTON MAGIC ANGLE SAMPLE SPINNING (MASS) NMR OF SUPER-ABSORBENT POLYMERS</u>	
INTRODUCTION	113
EXPERIMENTAL	115

	Page No.
RESULTS AND DISCUSSION	116
CONCLUSIONS	120
 <u>EFFECT OF CROSS-LINKING ON CARBON-13 NMR OF SUPERABSORBENT POLYMER</u>	
INTRODUCTION	120
EXPERIMENTAL	121
RESULTS AND DISCUSSION	122
CONCLUSIONS	125
REFERENCES	126
NOTATION	129
 <u>CHAPTER - IV</u>	
<u>DEFORMATION DEPENDENT SUPERABSORPTION AND PHASE TRANSITIONS IN SUPERABSORBENT POLYMERS.</u>	
INTRODUCTION	132
EXPERIMENTAL	134
RESULTS AND DISCUSSION	136
- Enhancement of superabsorbing capacity.	136
- NMR and Molecular basis for Deformation dependent superabsorption.	141
- Deformation induced by centrifugal Action.	148
- Deformation dependent phase transitions.	149
- Memory effects in superabsorbent polymers.	154
IMPLICATIONS OF THE PRESENT WORK	156
REFERENCES	157

CHAPTER - V

RHEOLOGY OF SUPERABSORBENT POLYMERS

Page No.

INTRODUCTION	161
RHEOLOGICAL BEHAVIOUR OF GELS	161
RHEOLOGICAL BEHAVIOUR OF SUPERABSORBENT POLYMERS	163
EXPERIMENTAL	165
RESULTS	166
MODEL DEVELOPMENT	166
EVALUATION OF MODEL PARAMETERS.	171
CONCLUSIONS	173
REFERENCES	174
NOTATION	175

CHAPTER - VI

SUPERABSORBENT POLYMERS IN SEPARATIONS

INTRODUCTION	176
- Conventional separations.	177
- Towards alternative solutions to separation problems.	178
- Theoretical aspects.	184
- Design considerations.	186
EXPERIMENTAL.	189
- Concentration of dilute solutions.	189

RESULTS AND DISCUSSION	189
- Direct contact operation.	189
- Selectivity.	190
- Regeneration.	192
- Membrane/Gel composite processes.	192
INDUSTRIAL APPLICATION OF THE PROCESS	198
CONCLUSION	199
REFERENCES	200
SUMMARY AND CONCLUSIONS	208
SUGGESTIONS FOR FUTURE WORK	211

LIST OF TABLES

Page No.

CHAPTER - II

Table 2.1	Dependence of DVB content on swelling ratio : Sulfonated PS-DVB/H ₂ O (at constant degree of sulfonation).	85
Table 2.2	Effect of divinyl benzene (DVB) content on volume fraction of the network (V_2) and molecular weight between cross-links (Mc).	86
Table 2.3	Comparison of 'Mc' values by swelling ratio and Tg measurements.	87
Table 2.4	Effect of DVB content on mesh-sizes (ξ) of the polystyrene networks.	88
Table 2.5	Effect of very low DVB content on molecular parameters of PS-DVB resins.	89
Table 2.6	Swelling ratios for PSS-gels in non-aqueous solvents.	90
Table 2.7	Effect of Bis-acrylamide on swelling ratios of PAMPS gels.	91
Table 2.8	Dependence of χ on electrolyte (NaCl) concentration.	92
Table 2.9	Comparison of theoretical and experimental 'Mc' values of PAMPS gels.	93

CHAPTER - III

Page No.

Table 3.1	Spin-lattice relaxation time of (T_1) HSPAN superabsorbent polymer at different percentage - saturations of water.	130
Table 3.2	^{13}C chemical shifts of PAMPS superabsorbent polymer.	131

CHAPTER - IV

Table 4.1	Effect of percentage saturation on swelling ratio on spinning.	159
Table 4.2	Effect of spinning time on swelling ratio.	160

CHAPTER - VI

Table 6.1	Conventional techniques for concentration of biological macromolecules.	201
Table 6.2	Concentration of macromolecules using gel-stick method.	202
Table 6.3	Concentration of dilute aqueous solution using gel-bead batch operation.	203
Table 6.4	Macromolecular separation by continuous packed bed operation.	204
Table 6.5	Selectivity in continuous packed bed operation.	205

Table 6.6	Liquid gel-assisted dialysis/batch operation.	206
Table 6.7	Liquid gel-assisted dialysis/continuous operation.	207

LIST OF FIGURES

Page No.

CHAPTER - I

Figure 1.1	Pressure-volume isotherms of carbon dioxide.	11
Figure 1.2	Volume phase-transition in natural polymers.	15
Figure 1.3	Volume phase transition in HPAM gel evidenced by (a) refractive index (b) modulus and (c) stress-optical coefficient.	21
Figure 1.4	Osmotic pressure - volume isotherms for gels at various temperatures.	26
Figure 1.5	Transition in gels (—) coexistence curve (-----) spinodal curve (----) swelling volume curve.	27
Figure 1.6	Phase diagrams of gels at various values of S.	28
Figure 1.7	Effect of curing time on the phase transition of gels.	29
Figure 1.8	Effect of ionization on phase transition.	32

CHAPTER - II

Page No.

Figure 2.1	A rigid swellex superabsorbent.	50
Figure 2.2	Experimental set up for synthesizing superabsorbent polymers.	52
Figure 2.3	Effect of percentage DVB on swelling ratio (q).	56
Figure 2.4	Dependence of swelling ratio on mole fraction of DVB.	57
Figure 2.5	Effect of sulfonation on swelling ratio.	58
Figure 2.6	Effect of electrolyte concentration on swelling ratio.	64
Figure 2.7	Effect of presence of divalent electrolytes on swelling ratio.	66
Figure 2.8	Effect of pH on swelling ratio.	67
Figure 2.9	Swelling behaviour of PSS gels in the non-aqueous media.	71
Figure 2.10	Dependence of swelling ratio on solubility parameter.	73
Figure 2.11	Effect of degree of sulfonation on swelling ratio in non-aqueous media.	74

CHAPTER - III

Page No.

Figure 3.1	Block diagram of FT-NMR spectrometer.	97
Figure 3.2	Behaviour of disturbed magnetisation as a function of time.	102
Figure 3.3	Exchange model.	107
Figure 3.4	Single exponential decay.	108
Figure 3.5	Concentration dependence of relaxation rate.	110
Figure 3.6	Saturation dependence of relaxation rate.	112
Figure 3.7	Static proton NMR spectra of HSPAN.	114
Figure 3.8	^1H MASS spectra of HSPAN.	117
Figure 3.9	^{13}C spectra of PAMPS polymer.	123
Figure 3.10	^{13}C spectrum of PAMPS polymer.	124

CHAPTER - IV

Figure 4.1	In-situ superabsorption under deformation - Experimental setup.	135
Figure 4.2	Deformation dependent superabsorption HSPAN/Water (In-situ).	137

		Page No.
Figure 4.3	Deformation dependent superabsorption PAMPS/Water (In-situ).	138
Figure 4.4	Deformation dependent superabsorption-high speed device.	139
Figure 4.5	Line width transition with respect to (%) saturation .	142
Figure 4.6	¹³ C spectra of HSPAN polymer at different (%) saturation..	144
Figure 4.7	¹³ C spectra of unsheared and sheared HSPAN at low and high (%) saturation .	145
Figure 4.8	¹ H MASS and static spectra of unsheared and sheared HSPAN gels.	147
Figure 4.9	Deformation dependent phase transition-observation of second transition.	151
Figure 4.10	Deformation dependent phase transition-observation of reentrant phase transition.	153
Figure 4.11	Memory effect in superabsorbent polymers (HSPAN/Water system).	155
<u>CHAPTER - V</u>		
Figure 5.1	Viscosity vs time - HSPAN Polymer (100% saturation).	164
Figure 5.2	Viscosity vs time - HSPAN polymer (150% saturation).	167

Figure 5.3 Viscosity vs time - HSPAN polymer (200 % saturation). 168

CHAPTER - VI

Figure 6.1 Direct contact operation - use of gel-stick. 129

Figure 6.2 Swelling ratio controlled by variation of pH. 181

Figure 6.3 Regeneration strategy based on pH dependent swelling. 182

Figure 6.4 Conceptual design of direct contact separations. 183

Figure 6.5 Cross-linking agent controls 'Mc' and 'Q'. 191

Figure 6.6 Regeneration strategy for packed bed operation based on electrolyte elution. 193

Figure 6.7 Influence of regeneration by electrolyte elution on swelling capacity. 194

Figure 6.8 Indirect contact operation - batch dialysis. 196

Figure 6.9 Conceptual design for indirect contact separations. 197

SCOPE OF THE WORK

This work was undertaken with a view to elucidate the role of various structural attributes which govern the superabsorption in polymers and explore some novel applications.

The theory of swelling of polymeric gels was first put forth by Flory. Subsequently a number of researchers have tried to elucidate the nature of the phase transition in gels and the effect of various parameters such as solvent composition, temperature, pH etc. on the transition phenomena. Most of these approaches are based on the extension of the Flory's theory. A description of the transition phenomena in gels and the various approaches adopted in the past have been discussed in the first chapter.

Chapter two deals with the synthesis and characterization of cross-linked poly(styrene sulfonic acid) and poly(2-acrylamido-2-methyl propane sulfonic acid) based superabsorbent polymers which have been evaluated for applications in the separation processes.

NMR spectroscopy of polymers has emerged as a powerful tool to study molecular motions in polymers. The techniques such as cross-polarization (CP) and magic angle sample spinning (MASS) with high power proton

decoupling have further enhanced the value of carbon-13 NMR studies in these investigations. In the third chapter the state of water in the swollen polymers has been investigated by spin-lattice relaxation time measurements. High resolution proton NMR of superabsorbent polymers has been investigated by MASS technique. Investigations of this kind have been reported for the first time.

Deformation dependent superabsorption and phase transition have been discussed in the fourth chapter. The results have been explained on the basis of the existence of permanent and semipermanent cross-links in the polymer.

Superabsorbent polymeric gels, because of their large swelling power find extensive application as thickeners for printing pastes, oil drilling system etc. The viscosity and mechanical stability of these polymers in the swollen state depends on the chemical composition, degree of ionization and degree of cross-linking. The nature of swollen gel can vary from soft to a hard mass. An understanding of the rheological behaviour of these materials is therefore critical. Shear dependent viscosity of gels has been investigated. Cheng's model has been modified to explain the results qualitatively. A procedure for evaluating the model parameters has been described in chapter five.

Superabsorbent polymers offer potential applications in separation processes. Separation of biological macromolecules from dilute aqueous solution is becoming increasingly important. The sixth chapter reports a variety of techniques for separation and concentration of aqueous macromolecular solutions using superabsorbent polymers.

CHAPTER-I

AN OVERVIEW OF SUPERABSORBENT POLYMERS

Introduction

Superabsorbent polymers are basically polyelectrolytes containing a very small degree of cross-linking. These materials are commonly referred to as gels. They exhibit unique kinetic and equilibrium properties. Some of the materials such as cross-linked poly(acrylic acid) and poly(methacrylic acid) which belong to the family of the superabsorbent polymers have been investigated in great details since early sixties (1,2). However, the potential applications of the superabsorbent polymers in diverse fields were realized only in mid seventies (3). This spurred renewed interest in the fundamental investigation on gels (4), and elucidation of various factors affecting the superabsorbent behaviour of the polymers in quantitative terms. Apart from the volume-phase transition which is the most distinctive and widely investigated feature, these polymers also exhibit unique structural and rheological characteristics (5,6). However, these aspects have not received adequate attention in the past.

This chapter presents a brief overview of gels and their swelling behaviour. The volume phase transition phenomena have been described in details. The use of recently developed technique such as solid state NMR of polymers and magic angle sample spinning (MASS) to correlate the structure of the gels with the swelling behaviour is discussed. Finally, current state of art in the rheology

of superabsorbent polymers is also presented.

A brief overview of gels

The concept of gels was first proposed in the nineteenth century. A gel denoted a two phase system in which the dispersed phase, which constituted a very small volume fraction, formed a three dimensional network filled by a large quantity of dispersion medium. Although both amorphous and crystalline inorganic compounds were known to form gels, it was realized in early days that this was a characteristic feature of the high molecular weight organic compounds (9). A precise definition of 'gel' has eluded the workers in this area for more than a century. A recent review on gels has tried to bring out the most acceptable definition of gels and a scheme for the classification.(10)

Gels can in principle be classified into two categories (11). The first category includes gels which contain a network structure formed by the secondary forces. The gels which fall in this category are, soaps, phospholipids, reticular networks such as vanadium pentoxide gels, and the gels resulting from the aggregates in natural polymers such as gelatin, alginate etc. Gels in the second category consist of a three dimensional network structure formed by the covalent linkages. These gels are irreversible in the sense that they cannot be reversed unless the covalent cross-links are destroyed and the polymer degraded.

This category includes vulcanized rubbers, condensation polymers synthesized from multifunctional monomers and vinyl polymers containing small amounts of divinyl monomers.

The chemistry of gelation was extensively studied by Carothers (12) in early 1940s and the physical chemistry of the swelling of the gels was investigated by Flory (13). The interest in gels was rejuvenated in early seventies when the researchers at the USDA announced the development of a superabsorbent polymer based on hydrolysed starch-g-poly(acrylonitrile) (14). Parallely the Japanese developed synthetic superabsorbents based on acrylic acid/acrylamide copolymers. These polymers which formed aqueous gels containing less than 0.1 percent polymer, found wide ranging applications in agriculture, medicine, personal hygiene products, separations and controlled release delivery systems. While these technological developments were taking place, Tanaka and coworkers at MIT (15) investigated the elasticity of gel network, the volume phase transitions and the concomitant phenomena such as critical opalescence by laser light scattering. This behaviour could be elucidated on the basis of the interplay between the various forces influencing the polymer network.

Sol-gel transition

The most familiar example of the system which undergoes sol-gel transition is the dessert 'Jelly' which is chemically an animal protein. Other examples of gels of

this type are poly(vinyl alcohol) in water and poly(vinyl chloride) in dibutylphthalate. The gel formation in all these cases is due to the network formation. The network may result due to hydrogen bonding in polymer chains (16), polymer crystallite formation (17) and/or liquid-liquid phase transition. Recently, Kawanishi et al. (18) showed that all these factors operate in a sequential fashion which leads to gelation and the mode of superposition depends upon the kinetics of the individual process.

Swelling of gels

The theory of swelling of nonionic cross-linked network was first put forth by Flory, who subsequently modified it to take into account the effect of ionic substituents. When the network is swollen by the solvent, the network junctions and chains are forced to attain a strained conformation. The resulting strained conformation gives rise to a retractive force, which tends to bring the network chain into more probable conformation. An equilibrium is reached between these two forces as the volume fraction of the solvent increases and the equilibrium swelling is attained.

Flory proposed an analogy between the swelling equilibrium and osmotic equilibrium. The total osmotic pressure acting on the gel comprises the forces arising

from polymer-polymer affinity and rubber elasticity.

According to Flory the osmotic pressure of the gel is given by

$$\pi = \mu_1 - \mu_1^0 = RT \left[\ln(1-v_2) + v_2 + \chi v_2^2 + V_1 (v_e/v_0) (v_2^{1/3} - v_2/2) \right] \quad (1.1)$$

where, μ_1 and μ_1^0 are chemical potentials of solvent with in the gel and outside the gel, respectively, π is osmotic pressure, v_2 is the volume fraction of the network, which can be determined by swelling measurements, χ is the interaction parameter between the gel and the solvent,

R and T are gas constant and absolute temperature,

V_1 is the molar volume of the solvent and the term

(v_e/v_0) is the deformation factor, which arises due to the elasticity of the network. At equilibrium swelling we have $\pi = 0$. With some rearrangement equation (1.1) can be written as

$$-\left[\ln(1-v_2) + v_2 + \chi v_2^2 \right] = (V_1/\bar{v} M_c) (1 - 2 M_c/M_n) (v_2^{1/3} - v_2/2) \quad (1.2)$$

Where M_c is the molecular weight between cross links and M_n is the number average molecular weight. The term $(1 - 2 M_c/M_n)$ in the above equation is the correction factor for network imperfection resulting from chain ends.

With suitable approximations, this equation can be simplified to yield

$$q^{5/3} = (\bar{v} M_c / V_1) (1 - 2 M_c / M_n)^{-1} (1/2 - \chi) \quad (1.3)$$

This relationship shows how the swelling ratio (q) changes as a function of the extent of cross-linking and also the quality of the solvent. This equation has been experimentally confirmed for a number of systems.

The equilibrium between the swollen ionic gel and its surroundings can be considered by recognising that the osmotic pressure will arise from difference in mobile ion concentrations. Using appropriate approximations, two asymptotic limits can be calculated. The first one relates to the case when the electrolyte concentration outside the gel is negligible. We then have

$$q^{5/3} = \left[i \bar{v} / v_m + (0.5 - X) / v_1 \rho_p \right] M_c / (1 - 2 M_c / M_n) \quad (1.4)$$

Whereas in the presence of significant electrolyte concentration on the outside, the expression can be deduced as

$$q^{5/3} = \left[i^2 / 4 v_m^2 I_0 + (0.5 - X) / \rho_p v_1 \right] M_c / (1 - 2 M_c / M_n) \quad (1.5)$$

Where, 'i' is the degree of ionization, 'I₀' is the ionic strength of the external solvent and 'v_m' is the molar volume of the structural repeat unit of the network. The terms \bar{v} and ρ_p are specific volume and density of the network respectively.

From these equations it is apparent that the degree of swelling can be controlled by controlling factors such as the degree of ionization, ionic strength, solvent-polymer interactions, extent of cross-linking etc.

Phase transition

A single component chemically homogeneous system can assume a gas, liquid or solid phase depending upon its state characterized by temperature, pressure and volume. The phase diagrams provide valuable information about the molecular interactions in the system in each phase. At this stage it would be worthwhile to recapitulate our understanding of phase transitions in the more familiar gas-liquid systems.

Consider the pressure-volume isotherm of carbon dioxide at various temperatures as shown in Fig. 1.1. The deviations from ideal gas law behaviour become apparent as the temperature is progressively reduced. However, for temperatures above 31.1°C carbon dioxide can not be liquified. On the other hand isotherm of carbon dioxide at low temperature say 13°C shows some interesting features. At point A_1 carbon dioxide is entirely in gaseous

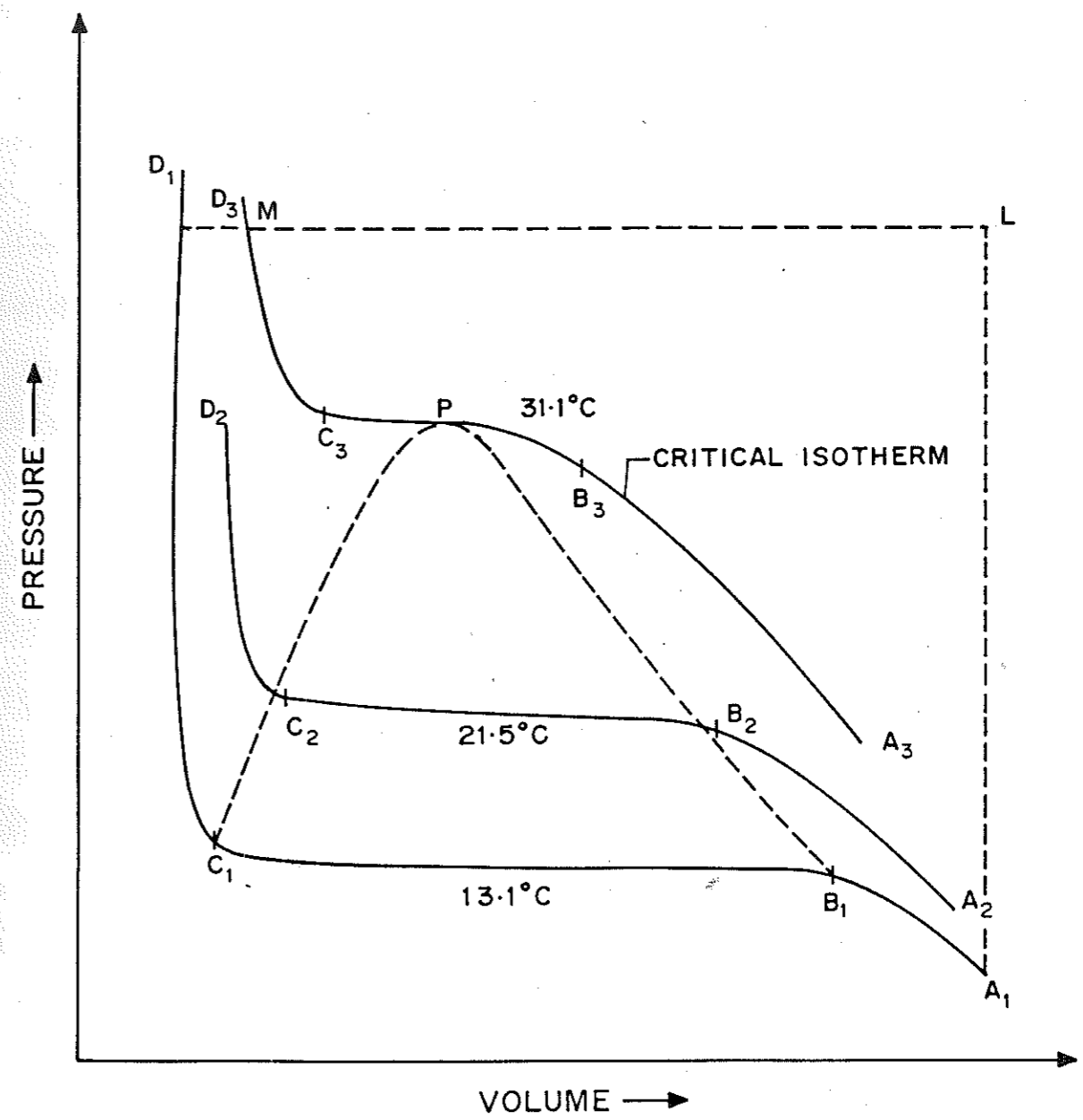


FIGURE 1.1: PRESSURE-VOLUME ISOTHERMS OF CARBON DIOXIDE

phase. As the pressure is increased, the isotherm A_1B_1 is followed, which to a certain extent is in accordance with the Boyle's law. At point B_1 liquefaction begins and the volume decreases rapidly as the gas is converted into a liquid of much higher density. At C_1 the liquefaction is complete and any further compression has negligible effect on the volume of the liquid since the liquids are practically incompressible. The portion A_1B_1 of the isotherm represents pure gas and the portion C_1D_1 pure liquid. Along the line B_1C_1 , gas and liquid coexist, the composition of the two phases changes while the total pressure remains constant. As the temperature is increased, the isotherms $A_2B_2C_2D_2$, $A_3B_3C_3D_3$ are followed in which the width of the horizontal region B_2C_2 , B_3C_3 etc. decreases with increasing temperature till it is reduced merely to a point P at temperature 31.1°C . Above this characteristic temperature called 'critical temperature' no liquefaction can take place. The pressure at which the gas can liquefy at critical temperature is termed as critical pressure, the volume occupied by one mole of gas at critical temperature and pressure denotes the critical volume and the pressure volume isotherm at the critical temperature is called the critical isotherm.

Alternatively the point D_1 can be reached starting from point A_1 by a different route. If a gas at A_1 is heated to a temperature above 31.1°C at constant volume the pressure increases as indicated by point L. The pres-

sure is held constant and the temperature reduced to 13.1°C .

This is accompanied by a decrease in volume upto D_1 , which denotes the liquid carbon dioxide which was gas at point A_1 . Upto point M on the right of the critical isotherm carbon dioxide is a gas but at D_1 which is towards its left it is a liquid. The point to be noted is that there is no sharp discontinuity inducing a transition and at no point during this transformation is more than one phase in existence.

Volume phase transition in polymers

A wide range of polymers are capable of exhibiting the transition phenomena similar to those described in preceding section. The necessary and sufficient conditions which need to be satisfied for the phenomena to be observable and the effects of various parameters on the transition behaviour can be correlated in terms of the equation of state for gels. The first observation of volume phase transition in the hydrolysed polyacrylamide gels was reported by Tanaka in 1978 (19). The phenomenon was explained in terms of the mean field theory based on Flory's theory of swelling. Subsequently it was shown that the volume phase transition (expressed in terms of swelling ratio (q) which is the ratio of swollen volume to unswollen volume) could be effected by variation of parameters such as temperature (20), solvent composition (21) and degree of ionization (22).

The volume phase transitions of the type described above can also be realized by a gel such as hydrolysed polyacrylamide swollen in 50% acetone-water mixture when subjected to an electric field of 500 mV/cm (23). Most of the transitions observed above are concerned with the anionic gels based on polyacrylamide. However, recent studies indicate that the phenomenon is quite general and could be observed for cationic gels (24), non-ionic gels (25) and natural gels such as gelatin, agarose, DNA etc. (26) (See Fig 1.2).

The volume-phase transition in superabsorbent polymers and the influence of the various parameters can be understood in terms of the osmotic pressure of the gel. This consists of three components, the rubber elasticity, the polymer-polymer affinity and the hydrogen ion pressure. As a result of the Brownian motion, a freely jointed chain assumes an equilibrium end-to-end distance equal to the square root of the number of segments multiplied by the length of the segment. For this value of the end-to-end distance, the average force acting on the chain is zero. The thermal motions of the segments give rise to a compressive force, when the chain extends and its end-to-end distance is greater than the equilibrium end-to-end distance. Alternatively if the end-to-end distance is smaller than the equilibrium end-to-end distance, a restoring force comes into play which tends to extend the chain.

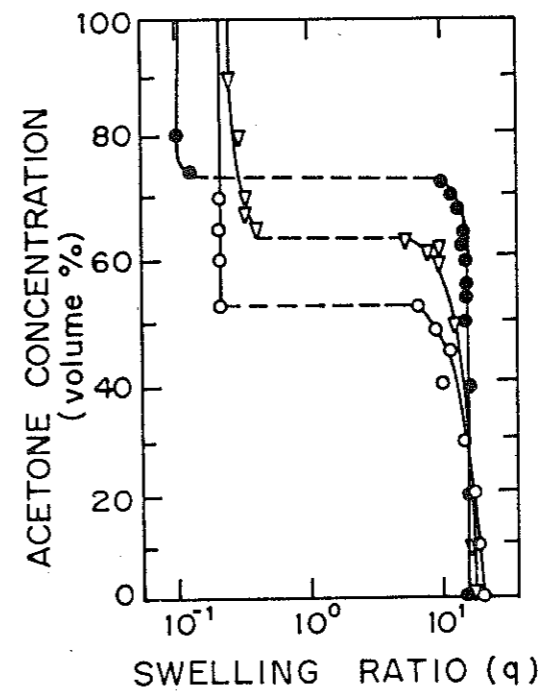



FIGURE 1.2 : VOLUME PHASE-TRANSITION IN NATURAL POLYMERS
(○) GELATIN , (▽) DNA AND (●) AGAROSE

The magnitude of this force is directly proportional to the temperature. This force, whether tensile or compressive, gives rise to a pressure, which by convention is considered to be positive if it results in swelling and negative if it tends to shrink the gel.

The interaction between the polymer chains gives rise to polymer-polymer affinity when the polymer-polymer interaction is favoured over the polymer-solvent interaction. The polymer-polymer affinity creates a negative pressure which tends to cause the collapse of the gel. The magnitude of the pressure increases as the solvent becomes poorer. Further, being a short range force, its magnitude also depends upon the volume of the gel. As the volume of the swollen gel increases, the polymer-polymer contacts becomes less favoured and the magnitude of this force decreases. On the contrary, as the solvent becomes poorer, the polymer chains tend to collapse and the magnitude of the negative pressure increases.

The third contribution to the osmotic pressure of the gel comes from the hydrogen ion pressure. The ionization of the polyelectrolyte gel releases H^+ ions in the gel. The repulsion of these ions is shielded by the negative charges bound to the polymer chain, which maintain the overall electrical neutrality. The mobility of the H^+ ions nonetheless, generates a positive pressure. At constant volume of the gel the pressure is directly propor-

tional to the temperature.

Thus, in principle, one can construct a plot of osmotic pressure versus gel volume at constant temperature or solvent composition. In practice, the gel always attains an equilibrium volume so that its total osmotic pressure is zero. If the pressure is positive, the gel takes up fluid and swells. If the pressure is negative it loses fluid and collapses. 

The continuous variation of the swelling ratio with temperature or solvent composition and the existence of the critical point can be explained on the basis of the variation of the three components of pressure with temperature and solvent composition. The region of negative compressibility in the P-V isotherm has been attributed to the forces arising from the polymer-polymer affinity. Above the critical point the osmotic pressure due to the rubber elasticity and hydrogen ion pressure are positive and their magnitude decreases as the gel expands.

What about the... This expansion also results in a decrease in the negative pressure due to polymer-polymer affinity. However, the rate of decrease is slower than the decreases in the other two components of the osmotic pressure. As a result, the total osmotic pressure decreases with increasing gel volume. Below the critical temperature the decrease in the osmotic pressure due to polymer-polymer affinity is

faster than the decrease due to polymer elasticity and hydrogen ion pressure. As a result the net osmotic pressure increases with increasing gel volume. While this explanation is true in principle, the local minimum is not reached in practice. Instead, when the gel reaches the Maxwell line, two domains, a swollen one and a shrunken one are formed. Unlike the gas-liquid transition, it is more convenient to discuss the swelling curves for the gels which describes the gel volume at which the total osmotic pressure is zero. It, thus, defines the intercepts of all isotherms on zero pressure axis. It is apparent that when the transition temperature is greater than the critical temperature, the volume change is continuous. When it becomes equal to the critical temperature an inflection point is reached. As the transition temperature is lowered further, the length of the Maxwell line increases and swelling curve exhibits discontinuous transition.

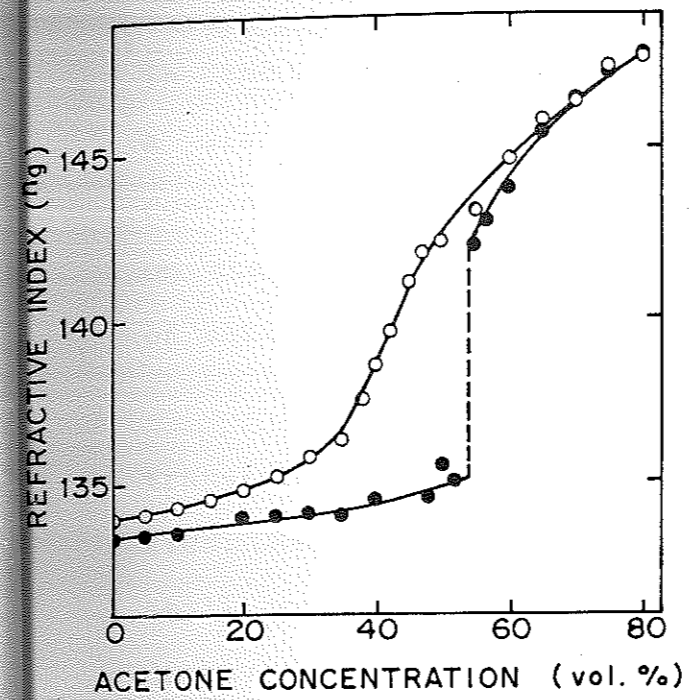
In the case of unionized gels the ionic pressure component of the total osmotic pressure is absent. As the temperature decreases, the force due to polymer-polymer affinity overcomes the force due to rubber elasticity at temperature higher than the critical temperature and the gel collapse takes place in a continuous manner.

As the degree of ionization of the network increases, the hydrogen ion pressure also contributes to the total osmotic pressure. As a result, at any given temperature or solvent composition the swelling ratio (q) is higher than it would have been in the case of the unionized gel. The negative pressure due to polymer-polymer affinity can then overcome the total positive pressure at temperature below the critical temperature. The transition therefore is not only discontinuous but the initial gel volume too is higher, as a result the swelling ratio at the transition increases with increasing ionization.

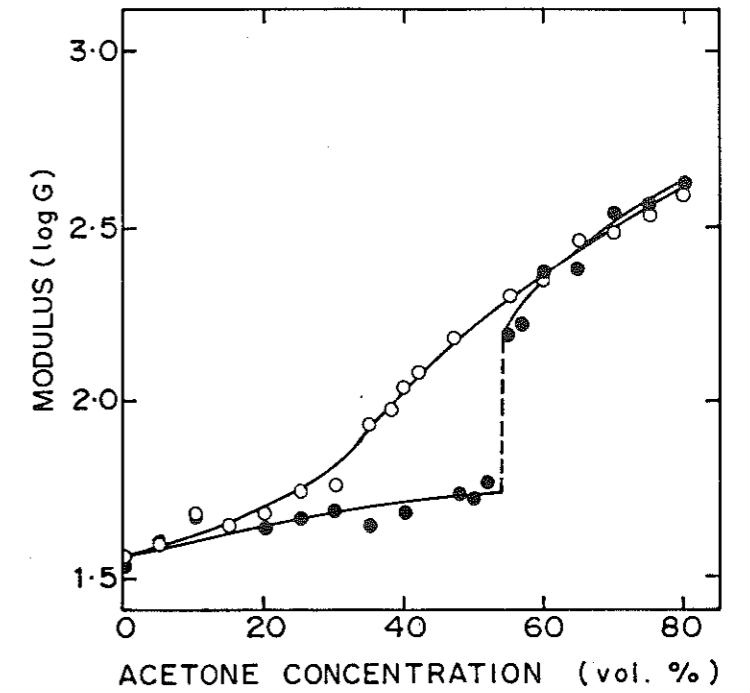
Manifestations of volume phase transitions

Volume phase transition is the most extensively studied manifestation of the structural changes taking place in the polymer network. These transitions are also manifested in other properties. For example, Hrouz and Ilvasky (27) showed that the trends in the plots of swelling ratio versus solvent compositions are also reflected in the refractive index behaviour. In the case of polyacrylamide homopolymers, both swelling ratio and the refractive index varied continuously with solvent composition. In contrast, in the case of hydrolysed polyacrylamide both swelling ratio and the refractive index exhibited a distinct transition at 54% acetone concentration. (See Fig. 1.3). Similar behaviour is observed in other properties of gels such as, modulus, deformational-optical coefficient and stress-optical coefficient. This suggests that the mechanical behaviour is governed by the network volume. This behaviour is also observed in the dielectric properties of the polyacrylamide and hydrolysed polyacrylamide gels.

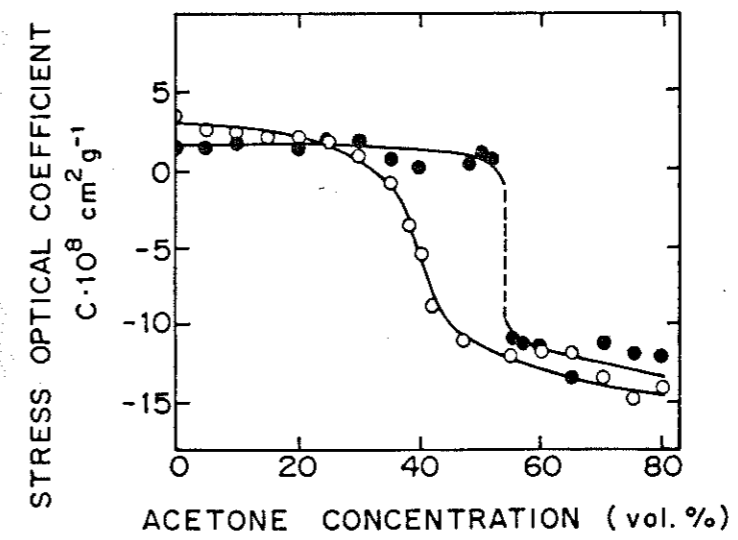
Recently, Liptak et al (28) have reported the permittivity of the hydrolysed and unhydrolysed polyacrylamide gels swollen in different compositions of acetone-water mixtures. It was observed that the permittivity of the unhydrolysed polyacrylamide decreases monotonically with increasing acetone concentration whereas



(a)



(b)



(c)

FIGURE 1-3 : VOLUME PHASE TRANSITION IN HPAM GEL EVIDENCED BY (a) REFRACTIVE INDEX (b) MODULUS AND (c) STRESS OPTICAL COEFFICIENT

in the case of hydrolysed polyacrylamide there exists a distinct transition in permittivity when the acetone concentration varied progressively. This was explained on the basis of charge concentrations due to dissociation of water and ionizable polymer network.

It must be noted however, that the volume phase transitions are not always reflected in all the gel properties. Recently Plestil et al. (29) have investigated the small angle neutron scattering (SANS) behaviour of poly(N,N-diethyl acrylamide) and poly(N,N-diethylacrylamide-sodium methacrylate) solutions as well as gels which exhibited temperature dependent volume phase transition. At low temperature when the polymer is in the Gaussian coil conformation the parameter $d\epsilon/d\Omega$, which denotes the effective scattering cross-section is proportional to q^{-2} ($q = \frac{4\pi}{\lambda}$, where λ denotes the radiation wavelength). At elevated temperature when the chains collapse one can expect the behaviour for a compact particle i.e. $(d\epsilon/d\Omega) \propto q^{-4}$. While such a dependence is observed in the case of both poly(N,N-diethyl acrylamide) homopolymer and copolymer solutions as well as gels, the transition from the coiled conformation to a more compact structure is a continuous one although the volume phase transition is abrupt one. This is probably due to the fact that the gel has not reached the equilibrium.

Criteria for volume phase transition in gels.

In the preceding discussion it has been shown that a wide range of ionic, nonionic, synthetic as well as natural polymers can exhibit either continuous or discontinuous volume phase transitions. Further, the transitions could be induced by temperature, solvent composition, pH, salt concentration and electric field. This behaviour has been qualitatively explained on the basis of the contributions of the various forces to osmotic pressure. A semiquantitative approach to elucidate the volume phase transitions in polymers has been put forth by Tanaka (19). This is based on the equation of state of gels which is an extension of Flory's theory of swelling.

In the case of the nonionic polymeric gel, the osmotic pressure comprises contributions from the rubber elasticity and the polymer-polymer affinity.

Tanaka (30) showed that the equation of state for a nonionic gel can be derived from Flory's equation as follows,

$$\Pi = - \frac{N_A}{kT} \left\{ \underbrace{\ln(1-\phi) + \phi + \frac{\Delta F}{kT} \phi^2}_I + \underbrace{\frac{v_0}{NV} \left[(\phi/\phi_0)^{1/3} - (\phi/2\phi_0) \right]}_{II} \right\} \quad (1.6)$$

where N_A is Avogadro's number, k is the Boltzmann's constant, ΔF is the free energy associated with the contact between

the polymer-polymer segment, N is the number of segments in a polymer chain between two cross-links, ϕ_0 is the volume fraction of the network in the absence of interaction amongst polymer segments. The term (I) arises from polymer solvent interaction. The term (II) arises due to rubber elasticity. The equation on expanding the term $\ln(1-\phi)$ yields,

$$\pi = N_A kT \phi_0^3 \left[S(\varphi/2 - \varphi^{1/3}) + (A/2\phi_0)(1 - \frac{\theta}{T})\varphi^2 + \varphi^3/3 \right] \quad (1.7)$$

where,

$$\varphi = \phi/\phi_0, \quad S = v_0/vN\phi_0^3, \quad A = (1 + \frac{\Delta S}{k}) \quad \text{and} \quad \theta = (\Delta H)/(\Delta S + k)$$

Tanaka (19) argued that the elastic term is not a function of ϕ alone as assumed by Flory but of ϕ/ϕ_0 . ϕ_0 has to be small compared to unity for any transition to be observed. The shape of the isotherm then depends on the values of ϕ_0 , v_0 and S . The value of 'S' determines the relative contribution of the rubber elasticity and free energy of mixing to osmotic pressure. It can be shown that,

$$S \approx v_0 (N)^{1/2} (a^4/b^7) (1 + \phi_f/\phi_e)^3 \quad (1.8)$$

where ϕ_e and ϕ_f represent the volume concentration of polymer chains whose both the ends are attached to the cross-link junctions and only one end is attached to the cross-link junction respectively. The parameter 'a' denotes the radius of the freely jointed chain segment

and 'b' denotes the length. The isotherms plotted for $S = 600$, $\Phi_0 = 0.01$, $A = 1$ and $\Theta = 400$ are shown in fig. 1.4. The coexistence curve, the spinodal line and the volume curves plotted from the isotherms are shown in fig. 1.5. It is interesting to note that the collapse can be observed for $S > S_e$ and the magnitude of collapse increases with S . The critical point terminates at $S = S_e$ for which $\phi = \phi_e$ and $A(1 - \frac{\Theta}{T}) = (\frac{34}{15}) \phi_c$. This point is the critical end point (See fig. 1.6). It was shown that for polyacrylamide gel having $S \approx 1000$ the transition was discontinuous, whereas for the same gel when $S = 55$ the transition is continuous (fig. 1.7).

It may be recalled that in the initial experiments when the discontinuous volume phase transition was first observed, the width of the transition region increased with the increasing degree of hydrolysis of the polyacrylamide samples. The equation of state for the gels, therefore ought to include the effect of the degree of ionization of the gel i.e. the contribution from hydrogen ion (H^+) pressure too. The osmotic pressure of the ionic gel is then given by

$$\Pi = \underbrace{\frac{-N_A k T}{\nu} \left[\phi + \ln(1-\phi) + \frac{\Delta F}{2kT} \phi^2 \right]}_I + \underbrace{\nu k T \left[\frac{1}{2} \phi/\phi_0 - (\phi/\phi_0)^{1/3} \right]}_II + \underbrace{\nu f k T (\phi/\phi_0)}_III \quad (1.9)$$

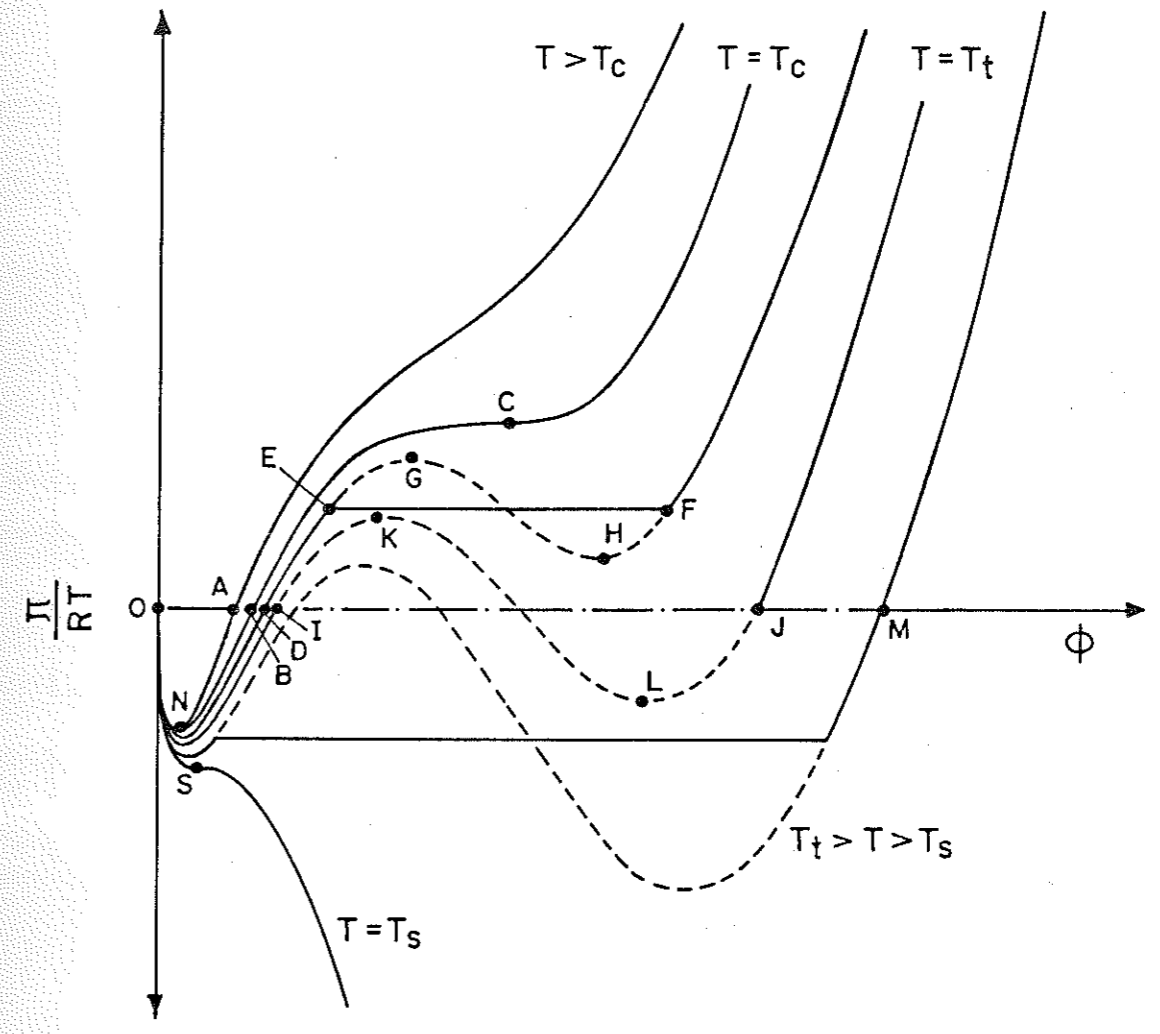


FIGURE 1-4: OSMOTIC PRESSURE-VOLUME ISOTHERMS FOR GELS AT VARIOUS TEMPERATURES

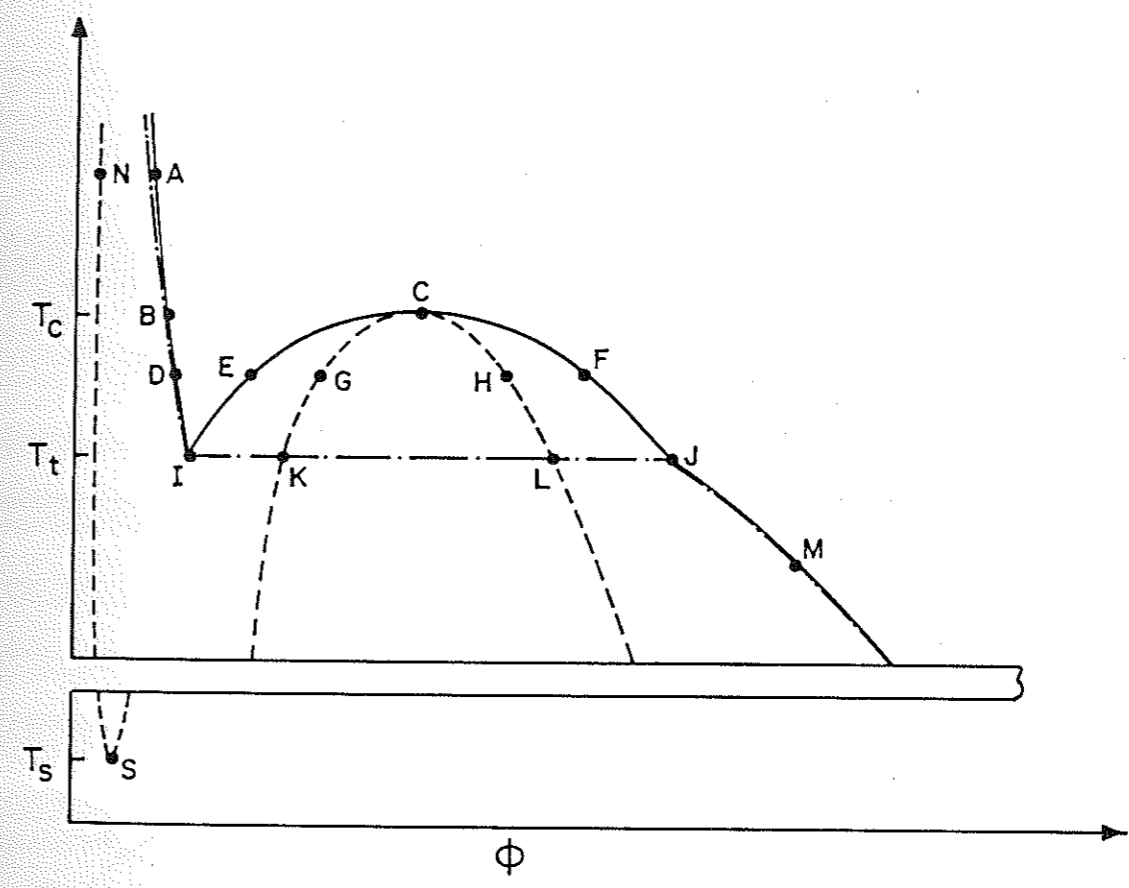


FIGURE 1-5 : TRANSITIONS IN GELS (—) COEXISTENCE CURVE (----) SPINODAL CURVE (---) SWELLING VOLUME CURVE

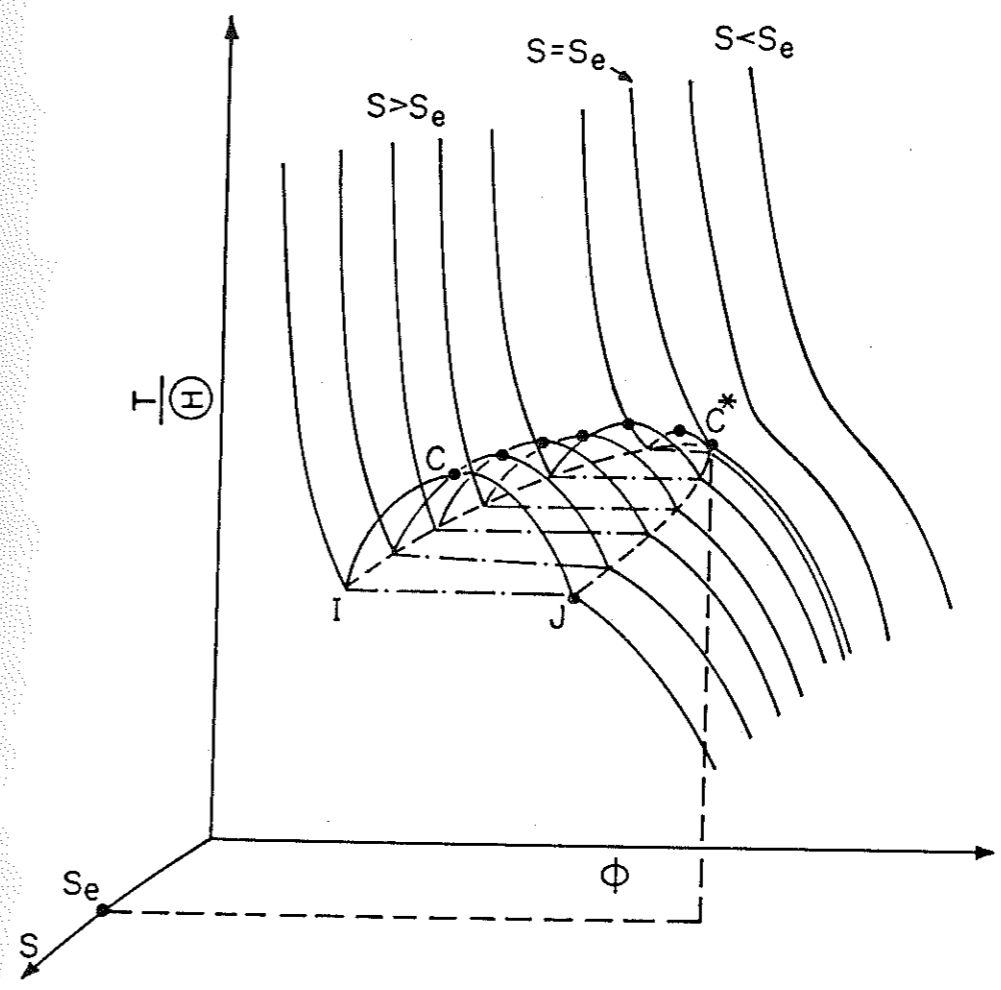


FIGURE 1-6: PHASE DIAGRAMS OF GELS AT VARIOUS VALUES OF S

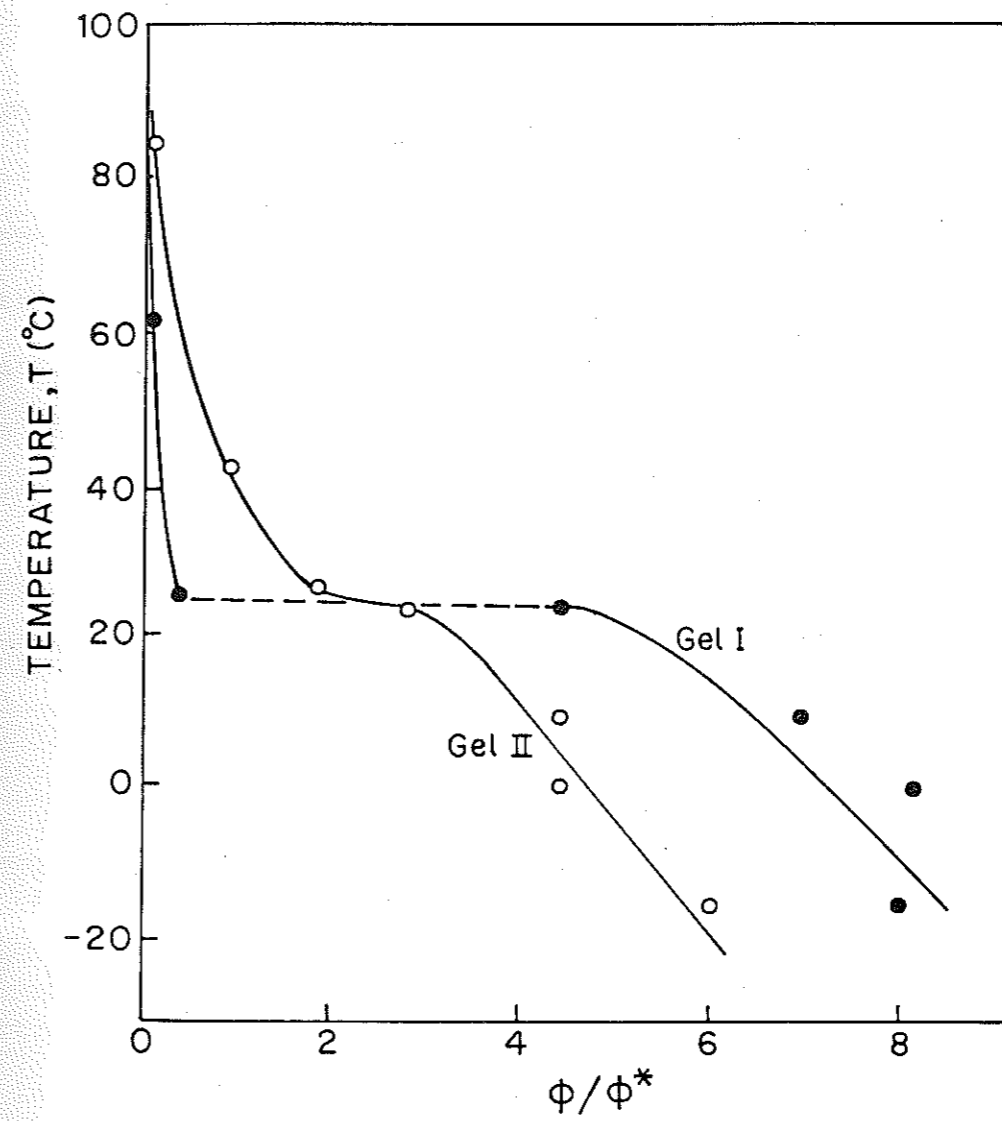


FIGURE 1-7: EFFECT OF CURING TIME ON THE PHASE TRANSITION OF GELS

It is evident that the value of the parameter S which governs the magnitude of collapse increases rapidly with the degree of ionization as compared to that for the unionized gel for which $S = S_0$. This can be seen from the effect of pH on swelling ratio at constant temperature and solvent composition. For reduced temperature greater than -0.338 , (ϕ/ϕ_0) increases continuously with 'f' whereas below this value the swelling ratio changes discretely. The effect of ionization on the phase transition was further verified by studying the swelling ratio for the copolymers of acrylamide and N-acryloxysuccinimide as a function of degree of hydrolysis.

It is thus clear that whether the given polymeric gel would undergo continuous or discrete volume phase transition would in the first instance depend upon the magnitude of S which denotes the relative contribution of rubber elasticity and the free energy of mixing to the osmotic pressure. The presence of ionized groups further increases the value of S with increasing degree of ionization.

Thus in the case of the Poly (N-isopropylacrylamide) a discontinuous transition is observed because of the stiffness of the chain segments ($b/a = 5.3, S \approx 300$), while for hydrolysed polyacrylamide the main contribution to S comes from the term $(2f+1)^4$ where 'f' denotes the number of ionizable groups per chain.

The only additional terms in equation (1.9) is (III) which accounts for the contribution of the hydrogen ion pressure. Here 'f' denotes the number of dissociated hydrogen ions (H^+) per effective chain.

For a gel at equilibrium swelling, $\pi = 0$. Hence,

$$\tau = (1 - \Delta F/kT) = -\frac{\nu\nu}{N\phi^2} \left[(2f+1)(\phi/\phi_0) - 2(\phi/\phi_0)^{1/3} \right] + 1 + \frac{2}{\phi} + \frac{2 \ln(1-\phi)}{\phi^2} \quad (1.10)$$

where τ denotes the reduced temperature (19). Through its dependence on ΔF and T , τ changes with temperature and composition. A plot of reduced temperature versus swelling ratio is shown in fig. 1.8 for various degrees of hydrolysis. For certain values of the reduced temperature the above equation is satisfied by three values of ϕ corresponding to two minima and one maximum of the free energy. The value of ϕ corresponding to the lower minimum represents the equilibrium value. When two free energy minima have the same value, a discrete volume phase transition is observed.

The expansion of the term $\ln(1-\phi)$ results in

$$t = S (\vartheta^{-5/3} - 1/2 \vartheta) - 1/3 \vartheta \quad (1.11)$$

where,

$$t = \frac{(1 - \Delta F/kT)(2f+1)^{3/2}}{2\phi_0}$$

$$S = \frac{\nu\nu}{N\phi^3} (2f+1)^4 = S_0 (2f+1)^4$$

$$\vartheta = (\phi/\phi_0)(2f+1)^{3/2}$$

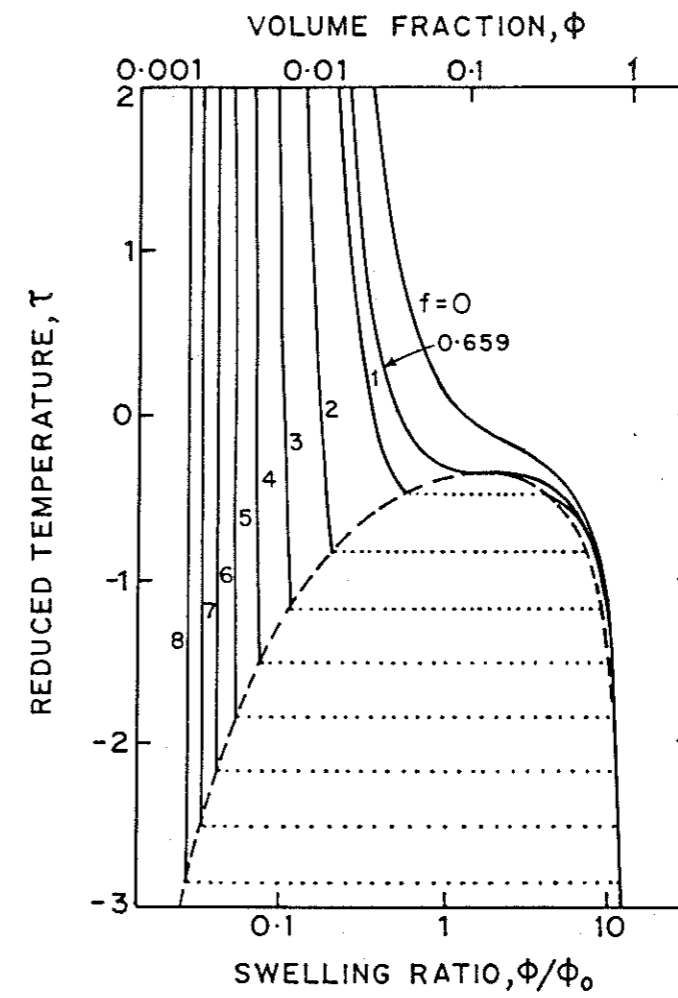


FIGURE 1-8: EFFECT OF IONIZATION ON PHASE TRANSITION

Tanaka's interpretation of the swelling and deswelling of unionized and ionized polyacrylamide gels and the elucidation of the effects of various parameters particularly, the value of 'S' on the phase transition, is however, not without limitations and in some cases is not substantiated by experimental evidence e.g. the difference in the swelling behaviour of the gels I and II shown in figure 1.7 were attributed by Tanaka (19) to the fact that for gel II the time available for cross-linking (3 days) was too short. As a result the value of the parameter 'S' is lower ($S \approx 55$) as compared to that for the gel I ($S \approx 1000$) from which TEMED was washed away after 30 days. Janas et al (31) experimentally verified that curing time had little effect on the cross-link density of the gels. These authors also described the discrepancies between the observed swelling characteristics of the gels and the predictions of the Tanaka's approach.

Infact, the analogy between the collapse of the single polymer chain as the solvent quality becomes poorer and the liquefaction of gases has been recognised for quite some time (32). Dusek and Patterson (33) showed that the concept could be extended to the swollen polymer networks. However, the theory predicted phase transitions for networks at very high cross-link densities. Post

It only
hydrolyses
the chain
(fibrinogen)

and Zimm (34) showed that the internal condensation of DNA molecule from an extended random coil to globular state could be predicted on the basis of extension of the Flory-Huggin's theory when a third virial coefficient is incorporated in free energy equation.

Hsu and Cohen (35) extended the approach proposed by Sanchez (36) for the collapse of the single chain to incorporate higher order terms in Flory's equation for the cross-linked network systems and noted that the swelling ratios observed experimentally would coincide with the theoretical predictions only when the ionic interactions dominate the swelling behaviour.

It was shown that the experimental swelling data of the gels could be satisfactorily correlated on the basis of Herman's equation using a constant value for the cross-link density and an apparent interaction parameter χ_{app} for the gel. However, χ_{app} has to be constant for a given solvent - nonsolvent combination.

The values of χ_{app} so calculated varied with the solvent composition as well as curing time. Although variation of χ_{app} with the duration of curing could be justified on the basis of variation of structure with curing time, it is important that the parameter be independent of the solvent composition. Hence the concept of inhomogeneous gel structure, was adopted. The

existence of inhomogeneties in cross-linked PAM gels was independently proposed by Weiss and Silberberg earlier (37) based on their study of permeation of water through polyacrylamide gels. Using the swelling data Janas et al calculated the model parameters β^* , ϕ_1^* and ϕ_2^* as a function of the time of curing. The parameters ϕ_1^* and ϕ_2^* are referred to as volume fraction of phase - 1 and phase - 2 respectively. The success of this approach lies in that χ_{app} remaining constant for each solvent - nonsolvent combination, the swelling data predicted from the model agreed fairly well with the experimental values in the swollen as well as collapsed regions. It would be further interesting to compare the values of the parameters β^* , ϕ_1^* and ϕ_2^* estimated from the swelling measurements with the values obtained from permeability measurements for the same gel.

Thus the approach proposed by Dusek and Patterson predicts transitions in gels at unreasonably high levels of cross-link densities. The approach suggested by Tanaka lacks experimental validation in respect of the dependence of cross-link density with the duration of curing. The inhomogeneous structure approach proposed by Janas although in qualitative agreement with the findings of Weiss and Silberberg necessitates further confirmation of the parameters.

Ilavsky (38) showed that the phase transition in polyacrylamide gels can be explained on the basis of the contribution of the electrostatic interactions to the swelling pressure. The swelling pressure was defined as

$$P = P_m + P_{el} + P_{os} + P_{eis} \quad (1.12)$$

The contribution P_{os}^m is described in the Flory Huggins equation. P_{mos} denotes the contribution due to the mixing of gel ions with the solvent. P_{el} denotes the change in the elastic network energy with the degree of swelling and P_{eis} represents the change in the free energy due to the electrostatic interaction with the degree of swelling.

The two phases can coexist when the $P-\phi_2$ relationship (ϕ_2 denotes the volume fraction of polymer in the gel) has a Van der Waals loop. The composition of gel phases is defined by the condition that the chemical potentials of the solvent and the polymer in both phases be identical. The composition of phases is given by

$$\int_{v_2'}^{v_2''} P v_2 dv_2 = 0 \quad (1.13)$$

and for free swelling

$$\int_{v_2'}^{v_2''} (\bar{X} - X_c) dv_2 = 0 \quad (1.14)$$

Where v_2' and v_2'' denote the polymer volume fractions in the two phases and \bar{X} and \bar{X}_c denote the values of the

interaction parameter calculated from equation (1.12) and the critical value of interaction parameter at which the collapse takes place. Using the relevant physico-chemical constants for the system poly(acrylamide-co-sodium methacrylate) for various concentrations of sodium methacrylate it was shown that for the sodium methacrylate content of less than 0.4%. $\bar{\chi}$ increased monotonically with V_2 while at around 0.8% concentration a discontinuous change corresponding to the collapse of the gel was observed. Equation (1.12) was thus found to describe the swelling equilibria of the ionized polyacrylamide gels better than the equation used by Janas et al (31) which resulted in the negative values of χ and the concept of the inhomogeneties in the gel structure. Thus, it is possible to explain the transitions in the polyacrylamide gels I and II in fig. 1.7 on the basis of the hydrolysis of the gel during aging rather than the increase in the cross-link density. The hydrolysis of polyacrylamide solutions during ageing was further proved experimentally by colorimetric and light scattering measurements (39). This approach has a merit that it can satisfactorily explain the collapse behaviour of polymer chains even at low degrees of cross-linking for homogeneous gels.

INVESTIGATION OF GEL STRUCTURE BY NMR

In recent years NMR has been extensively used to investigate the structural and dynamic properties of polymeric gel systems. Most of the attention has been focussed on relating the NMR spectral features to the molecular mobility of cross-linked gels.

Doskocilova and Schneider (40) have studied the high resolution proton NMR of swollen cross-linked gels such as poly(methyl methacrylate), poly(styrene), poly(ethylene oxide). The nature of static and magic angle sample spinning (MASS) line shapes were studied and analysed in terms of molecular mobility of chains. Initially the NMR spectra obtained from polymer solutions and gels were very broad and this was attributed to the restricted motions of polymer segments and their high viscosity. However, it has been now realized that the resolution of proton resonance is independent of the solution concentration and viscosity. This is because although the motions of the chain segments are slow, the local motions of the chain segments are fast and are in the range of nanosecond or picosecond. The development of cross-polarization (CP), high power dipolar decoupling and magic angle sample spinning (MASS) techniques have provided the carbon-13 NMR study of various cross-linked polymers. For example Ford and Balkrishnan(41) have reported the carbon-13 study of cross-linked poly

(styrene) gels. Yokoto et al (42) have investigated the effect of chemical composition, degree of cross-linking and temperature on the molecular mobility of cross-linked hydrogels by carbon-13 NMR. Recently, Baselga et al (43) have studied the kinetics of cross-linking in polyacrylamide gel by high resolution proton NMR. Based on these studies, the reactivity ratios of two monomers in copolymerisation were estimated.

NMR has been extensively used to study the state of water in various polymers and gels by spin-lattice relaxation time measurements (44) and also the tacticity and stereochemistry of vinyl polymers (45).

It has been reported in the literature that the water retention characteristics of the hydrolysed starch graft polyacrylonitriles are substantially enhanced by shear (46). Recently Fanta et al discussed the nature of reactions leading to cross-linking during the grafting of acrylonitrile and subsequent hydrolysis reaction. The enhancement of water retention capacity could then be attributed to the scission of cross-links. This aspect has not been investigated in the literature.

RHEOLOGY OF GELS

Rheology of gels has been investigated extensively in the past (47). However, very little attention has been given to the rheological behaviour of superabsorbent polymers. These gels find extensive applications as thickeners for aqueous system. An understanding of the rheological behaviour of these materials are therefore critical.

Taylor and Bagley (48) investigated the viscosity behaviour of gels of superabsorbent polymers such as hydrolysed-starch-g-polyacrylonitrile and carbopol 941. Gels of superabsorbent polymers are thixotropic in nature and also exhibit yield stress. Cheng (49) has derived a constitutive equation which takes into account the time dependent structure formation/breakdown to describe the thixotropic behaviour of materials such as sewage sludges. However, the rheological behaviour of superabsorbent polymer differs from the rheological behaviour of gels, since a part of the structure is never recovered. As a result these polymers show shear dependent superabsorption. This aspect needs further investigation.

SEPARATION PROCESSES BASED ON GELS

In separation processes, superabsorbents offer potentials for wide applications. They can be used as adsorbents, absorbents and packing materials for chromatographic techniques. Recently novel mechanochemical membranes have been developed which are cross-linked polymeric gels (50). These membranes undergo dilations and contractions due to the conformational changes in the network brought about by complexation with polyethylene glycol (PEG). The contractions and dilations influence the pore structure of the membranes which functions like a chemical valve and brings about the size selective separation. Extensive work has been done by Osada and coworkers (51) on the use of these devices in the separation of number of proteins and enzymes from aqueous systems.

Synthetic polymeric gels are being increasingly used as polymeric adsorbents in the removal of organic species from an aqueous media. For example gels based on poly(methyl methacrylate), poly(styrene) and Poly(vinyl pyridine) are used in the adsorption of phenols and derivatives of phenols (e.g. Nitrophenols, Chlorophenols etc.) from waste water (52). These gels are also used in the recovery of metals from various streams (53). It is important to note that the binding energies of

these polymers are lower than those of the conventionally used adsorbents such as activated carbon. As a result the recovery of polymeric adsorbents by regeneration is easier.

A new concept of using cross-linked gels to concentrate solutions of high molecular weight solutes is being explored vigorously (54). Such gels are size selective and concentrate solutes of certain minimum size. Different types of cross-linked gels based on polyacrylamide and polyacrylates have been used for this purpose. From the knowledge of the swelling and deswelling properties of these gels with respect to pH, temperature and ionic strength different regeneration strategies have been developed for the efficient separation processes. The details of these processes and the work done by us on this aspect has been described in chapter VI.

REFERENCES

1. Katchalsky, A., Kunzle, O. and Kuhn, W., *Jl. of Polym. Sci.*, 5, 283 (1950).
2. Katchalsky, A., Lifson, S. and Eisenberg, H., *Jl. of Polym. Sci. Lett.* 571 (1951).
3. Gugliemelli, et al., U.S. Patent 3,425,971 (1969).
4. Tanaka, T., *Sci. American*, 244, 110 (1981).
5. Taylor, N.W. and Bagley, E.B., *Jl. of Appl. Polym. Sci.*, 18, 2747 (1974).
6. Taylor, N.W. and Bagley, E.B., *Jl. of Appl. Polym. Sci.* 21, 113 (1977).
7. Mc Brierty, V.J. *Polymer* 15, 503 (1974).
8. Maquet, J., Theveneau, M., Djabourov, M., Leblond, J. and Papon, P., *Polymer* 27, 1103 (1988).
9. Flory, P.J., *Farad. Discuss of Society*, 7 (1974).
10. Russo, P.S. 'Reversible Polymeric Gels and Related Systems' *ACS Symp. Series* 350, 1 (1987).*
11. Rogovina, L.Z. and Slonimskii, G.L., *Russ. Chem. Rev.* 43 (6) 503 (1974).
12. Carothers, W.H., *Chem. Rev.* 8, 353 (1931).*
13. Flory, P.J. 'Principles of Polymer Chemistry' Cornell Univ. Press Ithaca, NY. (1953)
14. Fanta, G.F., Burr, R.C., Doane, W.M. and Russell C.R., *Starke* 30, 237 (1978).
15. Tanaka, T., Hocker, L.O. and Benedek, G.B., *Jl. of Chem. Phys.* 59, 5151 (1973).*
16. Eldridge, J.E. and Ferry, J.D., *Jl. Phys. Chem.* 58, 992 (1954).
17. Guerrero, S.J., Keller, A., Soni, P.L. and Geil, P.H. *Jl. Macromol. Sci. Phys.* B20, 167 (1981).

18. Kawamishi, K., Komatsu, M. and Inoue, T., *Polymer* 28, 980 (1987).
19. Tanaka, T., *Phys. Rev. Lett.* 40, 820 (1978).
20. Tanaka, T., *Sci. American* 244, 110 (1981).
21. Tanaka, T., *Encycl. Polym. Sci. and Engg.* 7, 514 (1987).
22. Ohmine, I., and Tanaka, T., *Jl. of Chem. Phys.* 77 (11), 5725 (1982).
23. Tanaka, T., Nishio, I., Sun, S.T. and Nishio, S.U., *Science* 218, 467 (1982).
24. Katayama, S. and Ohato A., *Macromolecules* 18, 2781 (1985).
25. Hirokawa, Y. and Tanaka, T., *Jl. of Chem. Phys.* 81 (12), 6379 (1984).
26. Amiya, T. and Tanaka, T., *Macromolecules* 20, 1162 (1987).
27. Hrouz, J. and Ilvasky, M. *Polym. Bull* 12, 515 (1984).
28. Liptak, J., Nedbal, J. and Ilvasky, M., *Polym. Bull.*, 18, 81 (1987).
29. Plestil, J., Ostanevich, Yu. M., Borbely, S., Stejskal, J., and Ilvasky, M., *Polym. Bull.*, 17, 465 (1987).
30. Tanaka, T., *Polymer* 20, 1404 (1979).
31. Janas, V.F., Rodrigues, F. and Cohen, C., *Macromolecules* 13, 977 (1980).
32. Ptitsyn, O.B., Kron, A.K. and Eizner, Yu. E., *Jl. Polym. Sci.*, 16, 3509 (1968).
33. Dusek, K, and Patterson, D., *Jl. Polym. Sci. A-2* 6, 1209 (1968).
34. Post, C.B. and Zimm, B.H., *Biopolymers* 18, 1487 (1979).

35. Hsu, T.P. and Cohen, C., *Jl. Polym. Sci. Lett.*, 23, 445 (1985).
36. Sanchez, I.C., *Macromolecules* 12, 980 (1979).
37. Weiss, N., Vliet, T. Van and Silberberg, A., *Jl. Polym. Sci. A-2* 17, 2229 (1979).
38. Ilvasky, M. *Macromolecules* 15, 782 (1982).
39. Ilvasky, M., Hrouz, J., Stejskal, J. and Bouchal, K., *Macromolecules* 17, 2868 (1984).
40. Duskocilova, D., and Schneider, B., *Pure and Appl. Chem.* 54, 284 (1981).
41. Ford, W.T and Balkrishnan, T, *Macromolecules* 14, 284 (1981)
42. Yokoto, K., Abe, A., Hosaka, S., Sakai, I. and Saito, H., *Macromolecules* 11, 95 (1978).
43. Baselga, J., Llorento, M.A., Nieto, J.L., Fuentes, I.H., and Pierola, I.F., *Eur. Polym. Jl.* 24, 161 (1988).
44. Maquet, J., Theveneau, H., Djabourov, M., Leblond, J. and Papon, P., *Polymer* 27, 1103 (1986).
45. Bovey, F.A., *The Arab. Jl. of Sci. and Engg.* 13, 183 (1988).
46. Fanta, G.F., Burr, R.C., Doane, W.M. and Russell, C.R., *Starke*, 30, 237 (1974).
47. Segeren, A.J.M., Boskamp, J.V. and Tempel, M. Van den., *Farad Disc. Chem. Soc.* 225 (1974).
48. Taylor, N.W. and Bagley, E.B., *Jl. Polym. Sci. Phys.*, 13, 1133 (1975).
49. Cheng, D.C.H., 'Characterization of thixotropic behaviour' Research report No. LR 157 (MH) Stevenage : Warren Spring Laboratory (1971).
50. Osada, Y and Sato , M., *Polymer* 21, 1057 (1980).
51. Osada, Y., and Takeuchi, Y, *Jl. Polym. Sci.* 19, 303 (1981).

52. Komiyama, H and Smith, J.M., AIChE. Jl. 20, 728 (1974).
53. Fox, C.R., Hydrocarbon Processing 57, 269 (1978).
54. Cussler, E.L., Stokar, M.R. and Varberg, J.E. AIChE. Jl. 30, 578 (1984).

NOTATION

a	radius of freely jointed chain segment.
b	Length of freely jointed chain segment.
f	number of ionic groups per effective chain.
i	degree of ionization.
k	Boltzmann's constant.
M_c	average molecular weight between cross-links.
μ_1	chemical potential of the solvent in the network.
μ_0	chemical potential of the solvent outside the network.
q	swelling ratio.
N	number of segments.
ϕ_0	volume fraction of the network in the absence of interactions amongst polymer segments.
T	absolute temperature.
Θ	Theta temperature
N_A	Avogadro's number.
ΔF	free energy
I_0	Ionic strength.
V_m	molar volume of the structural repeat unit.
v_2	Volume fraction of the network.
χ	Polymer - solvent interaction parameter.
v_1	molar volume of the solvent.
π	osmotic pressure.
\bar{v}	specific volume of the polymer.
τ	reduced temperature.



CHAPTER-II

SYNTHESIS AND CHARACTERIZATION OF
SUPERABSORBENT POLYMERS

Introduction

In recent years major attention has been devoted to developing new superabsorbent polymers. A wide range of superabsorbents based on starch-g-copolymers (1), acrylates (2) and polyvinyl alcohol (3) have been discussed in the literature.

Superabsorbents based on sulfonic acid polymers have not been investigated in detail in the past in spite of their high hydrophilicity and strong ionizability, which are essential characteristics for designing effective superabsorbent polymers. However, few indications in the literature do show that sulfonic acid monomer has been used as a comonomer in the graft-copolymers of superabsorbent nature (4).

In this chapter, we will report the synthesis and characterization of superabsorbents based on polystyrene sulfonic acid (PSS) and poly 2-acrylamido-2-methylpropane sulfonic acid (PAMPS). The PSS, gels synthesized were used for separation processes and were called SWELLEX gels. These polymers are specifically chosen because of their good rigidity and easy handlability. This enables us to use them in separation processes which we will describe in Chapter-VI.

Extensive work has been done on polystyrene sulfonic acid gels in the past. These gels were used as packing materials in gel permeation chromatography (GPC) and in ion-exchange applications (5). However, most of the polys-

styrene sulfonic acid gels studied above are highly cross-linked with the cross-linking agent (DVB) content varying from 5-25% on the monomer weight basis. The absorption capacity of these gels is inversely proportional to the percentage cross-linking present, which is very high in the case of gel used so far. They did not therefore show the superabsorption property. From Fig. 2.1 it is observed that, the superabsorption property falls in the range of 0-1% DVB content. Hence the above mentioned polymers were prepared by using suspension, bulk and solution polymerization techniques with DVB content varying from 0-2%. The swelling behaviour of these polymers was studied in detail. Based on swelling ratio measurements, parameters such as volume fraction of the network (v_2), average molecular weight between cross-links (M_c) and effective mesh size (ξ) of the network polymer have been estimated.

The effect of parameters like pH, solvent composition, nature of electrolyte and temperature on superabsorption has been elucidated on the basis of Flory's theory discussed in Chapter-I. It was observed that, polystyrene sulfonic acid gel not only absorbs water but also absorbs and retains organic solvents to a large extent and these absorption characteristics have been correlated in terms of the solubility parameter of ^{the}polymer and ^{the}solvent.

EXPERIMENTAL

Materials

All the common chemicals used were CP grade and

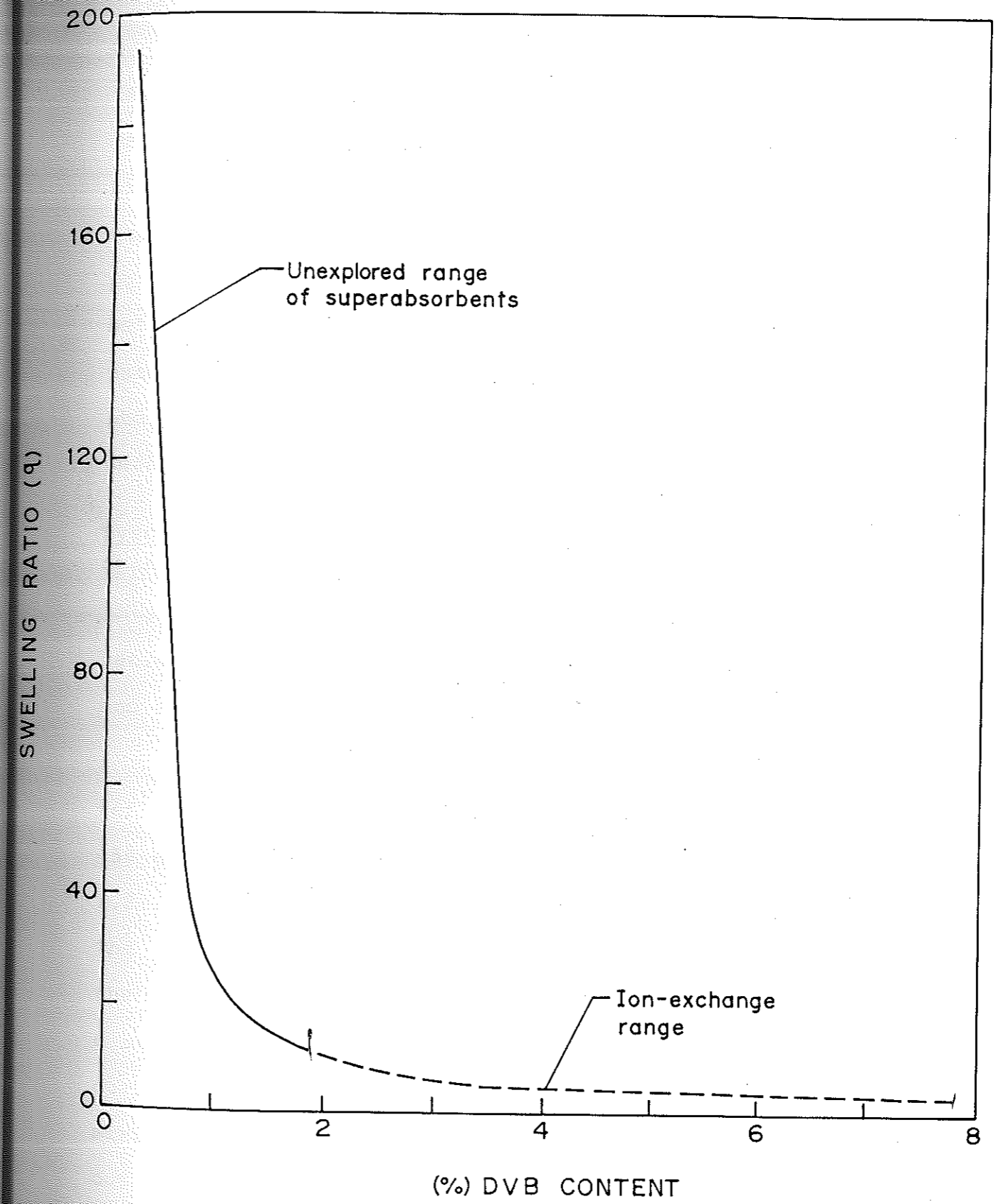


FIGURE 2-1: A RIGID SWELLEX SUPERABSORBENT

were obtained from the sources indicated in the parenthesis. Styrene (SD Chemicals Pvt. Ltd., Bombay, India) was purified by the standard purification method (6); Divinyl benzene (DVB) in 50% ethyl benzene [Fluka, AG Chemische Fabriks CH-9470 Busch] was used as such. Benzoyl peroxide (B.D.H. Chemicals, England) was recrystallized before use. Polyvinyl alcohol (Dow Chemicals, USA) was used as such; Sulfuric acid (98%) [Ranbaxy Laboratories Ltd., Bombay, India] and Silver sulfate (Loba Chem. India) were used as such.

Synthesis of Polystyrene Sulfonic Acid Gels by Suspension Polymerization

These gels were prepared by suspension copolymerization of styrene in presence of small quantity of DVB and subsequent sulfonation.

A 250 ml three necked flask equipped with a stirrer, reflux condenser and a nitrogen bubbler was charged with 150 g of water and 250 mg of polyvinyl alcohol (PVA) (Fig. 2.2). Polyvinyl alcohol was used as a protective colloid. The reaction mixture was stirred continuously till all the PVA was dissolved. Then the solution containing 22.7 g styrene, 0.25 g benzoyl peroxide (Bz_2O_2) and the required quantity of DVB was added. The temperature of the reaction mixture was increased to 90°C. The reaction was carried out for 8 hrs with continuous bubbling of nitrogen gas. The polymer precipitated out during the course of the reaction. The separated polymer was extracted with toluene,

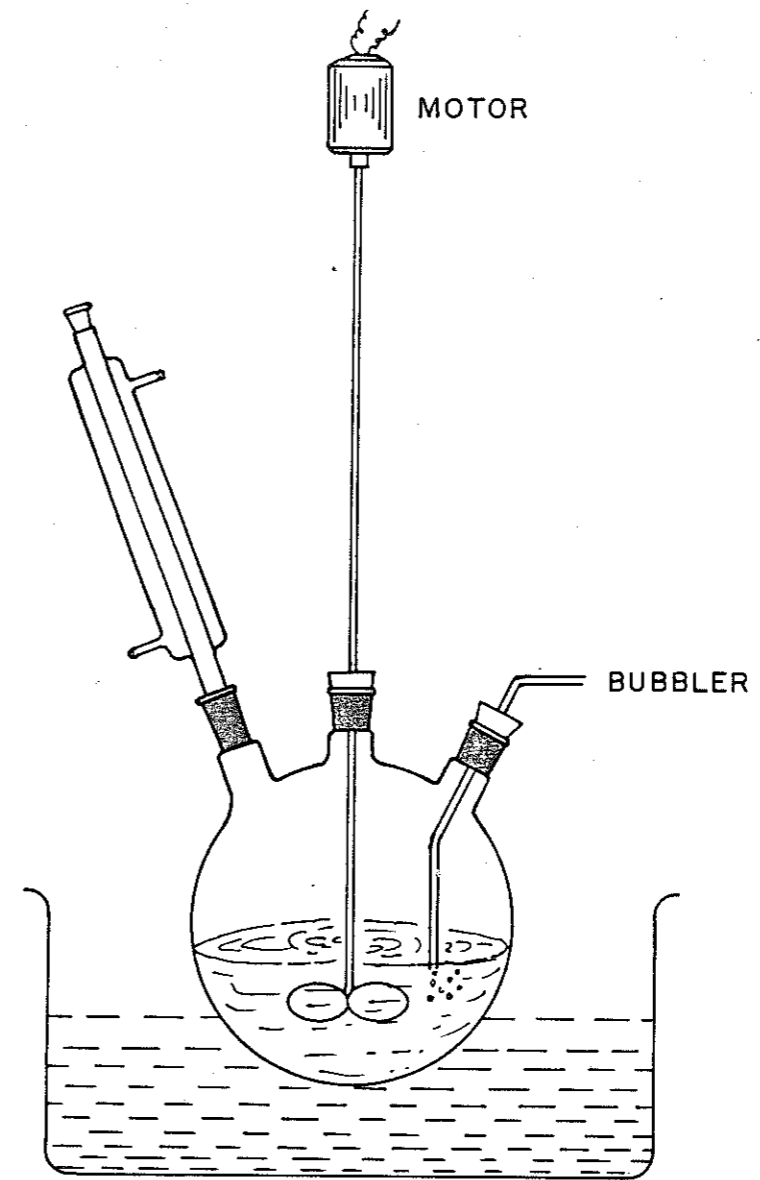


FIGURE 2-2 EXPERIMENTAL SETUP FOR SYNTHESIZING SUPERABSORBENT POLYMERS

washed with water and precipitated in distilled methanol. The isolated polystyrene-DVB polymer was dried in oven at 50°C. Similarly polystyrene without DVB and with various percentages of DVB (0.3 to 2.0%) were synthesized.

Synthesis of Polystyrene Sulfonic Acid Gels by Bulk Polymerization

The gels were prepared by bulk polymerization of styrene with very low content of DVB ($< 0.5\%$) followed by sulfonation under controlled conditions.

The polymerization reaction was carried out in a glass-tube at 60°C under nitrogen atmosphere for 20 hrs. The copolymer was flushed with pure toluene and precipitated by using distilled methanol. The product was filtered and then dried in oven at 60°C for 24 hrs and the sulfonation was carried out by following the procedure described below. These bulk polymerized gels were used to study the swelling behaviour in non-aqueous systems.

Sulfonation of Polystyrene-DVB Copolymers

Sulfonation was carried out in a round bottomed three-necked flask fitted with variable stirrer, thermometer and a calcium chloride guard-tube. The flask was charged with 100 ml concentrated sulfuric acid and 40 mg of silver sulfate. To this mixture, 10 g of polystyrene-DVB (PS-DVB) copolymer was added in 10 intervals. The addition of PS-DVB raised the temperature spontaneously to 100-105°C. The reaction mixture was maintained at 100°C for 3 hrs after which it was cooled to room tempera-

ture. Then it was poured onto 500 ml of 50% sulfuric acid, filtered and washed with acetone-water mixture till the polymer was free from free acid. Finally it was dried in oven at 60°C under vacuum.

Estimation of Degree of Sulfonation

The degree of sulfonation was determined by titrating 1 gm of sulfonated polymer in excess water against 0.1 N sodium hydroxide standard solution. From the amount of alkali consumed by the polymer, the degree of sulfonation was estimated and expressed as number of sulfonic acid groups per 100 styrene units. The elemental analysis was also carried out to confirm the above results.

Swelling Ratio Measurements

The swelling ratio measurements were carried out as follows. A weighed amount of the dry polymer was placed in a glass cell provided with a stopper. The solvent chosen as swelling medium was poured in the cell and allowed to stand in closed condition to reach equilibrium. The excess solvent was drained out and the total weight of the swollen polymer was determined. From the difference in the weight, the swelling ratio (q) was estimated. Ultimate care was taken in carrying out the measurements so as to minimize the losses due to evaporation, drain out, etc.

RESULTS AND DISCUSSION

Effect of Degree of Cross-linking and Degree of Sulfonation on Swelling Ratio

The results of the swelling ratio measurements are summarized in Table-2.1 and Fig. 2.3. It is observed that the swelling ratio goes on decreasing as the DVB content increases and reaches an ultimate value beyond which the swelling becomes independent of degree of cross-linking corresponding to a critical cross-link density. The decrease in swelling is attributed to the extensive network formation due to increase in cross-linking. Extensive work has been done by Errede (7) to correlate the swelling ratio of polystyrene-DVB gels in various solvents to the mole fractions of divinyl benzene. A linear relationship was observed when the swelling ratios (q) were plotted against $f^{-1/3}$, where $f = (r/1+r)$, r being the mole fraction of divinyl benzene. The trends in our results (Fig. 2.4) were also in good agreement with Errede's findings.

On sulfonation, the cross-linked PS-DVB copolymers containing low degree of DVB became highly hydrophilic and exhibited superabsorption property. The swelling ratios obtained ranged from 20 to 150 depending on the degree of cross-linking and degree of sulfonation. However, it was observed from Fig. 2.5 that beyond a specific degree of sulfonation (69.63 SO_3H groups/100 styrene units) the swelling ratio becomes independent of sulfonation leading

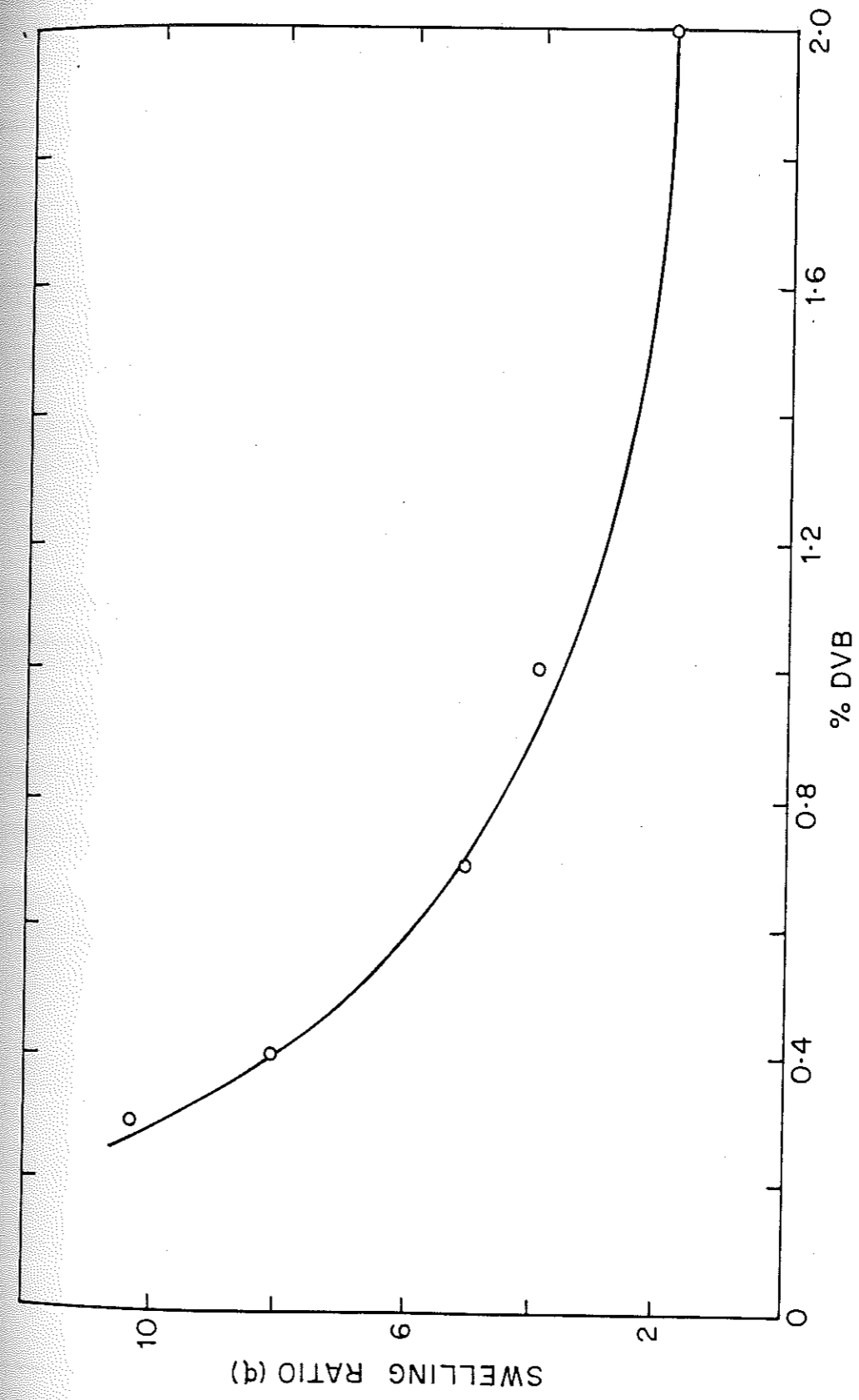


FIGURE 2.3: EFFECT OF PERCENTAGE DVB ON SWELLING RATIO (q)

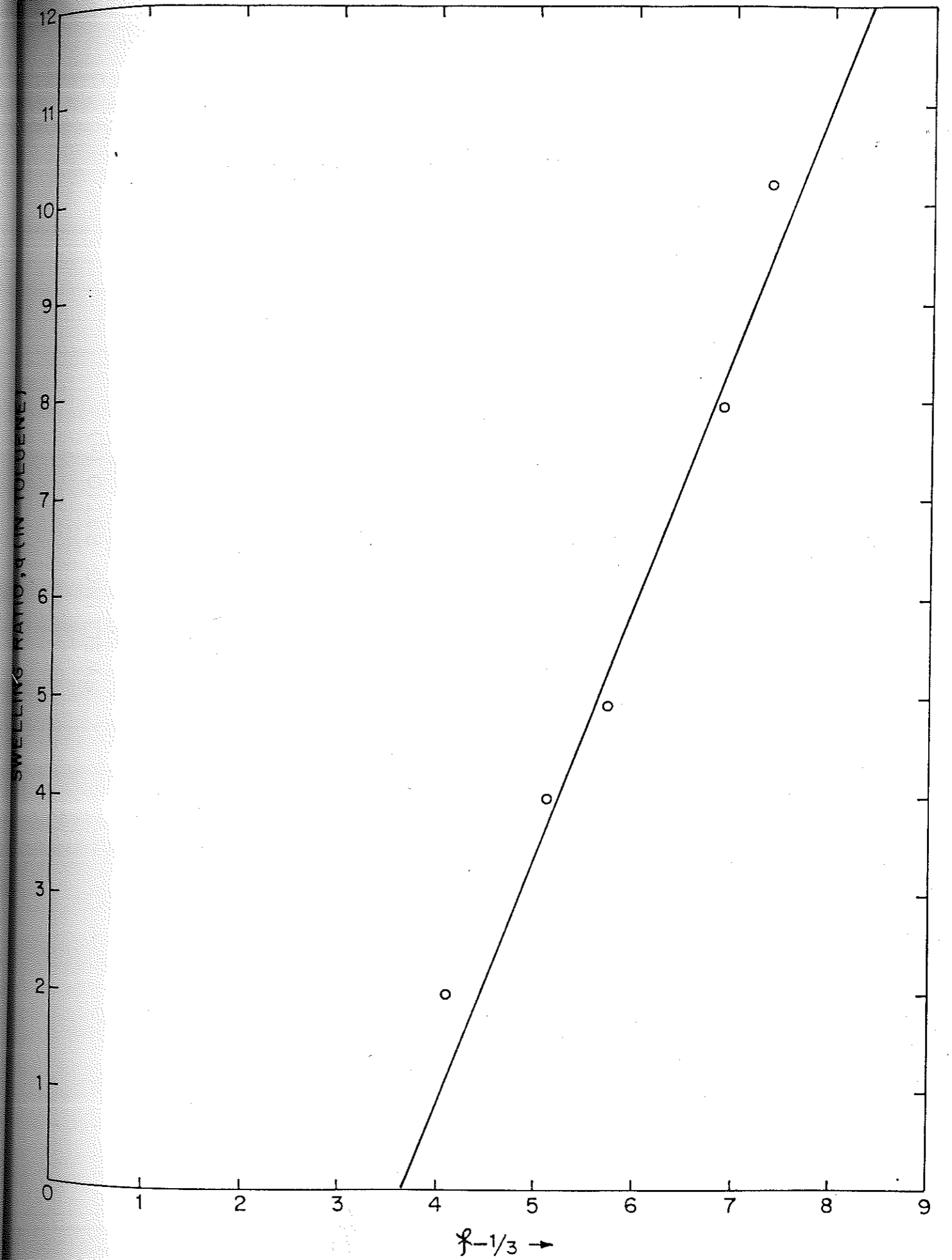


FIGURE 2.4: DEPENDENCE OF SWELLING RATIO ON MOLE FRACTION OF PVP

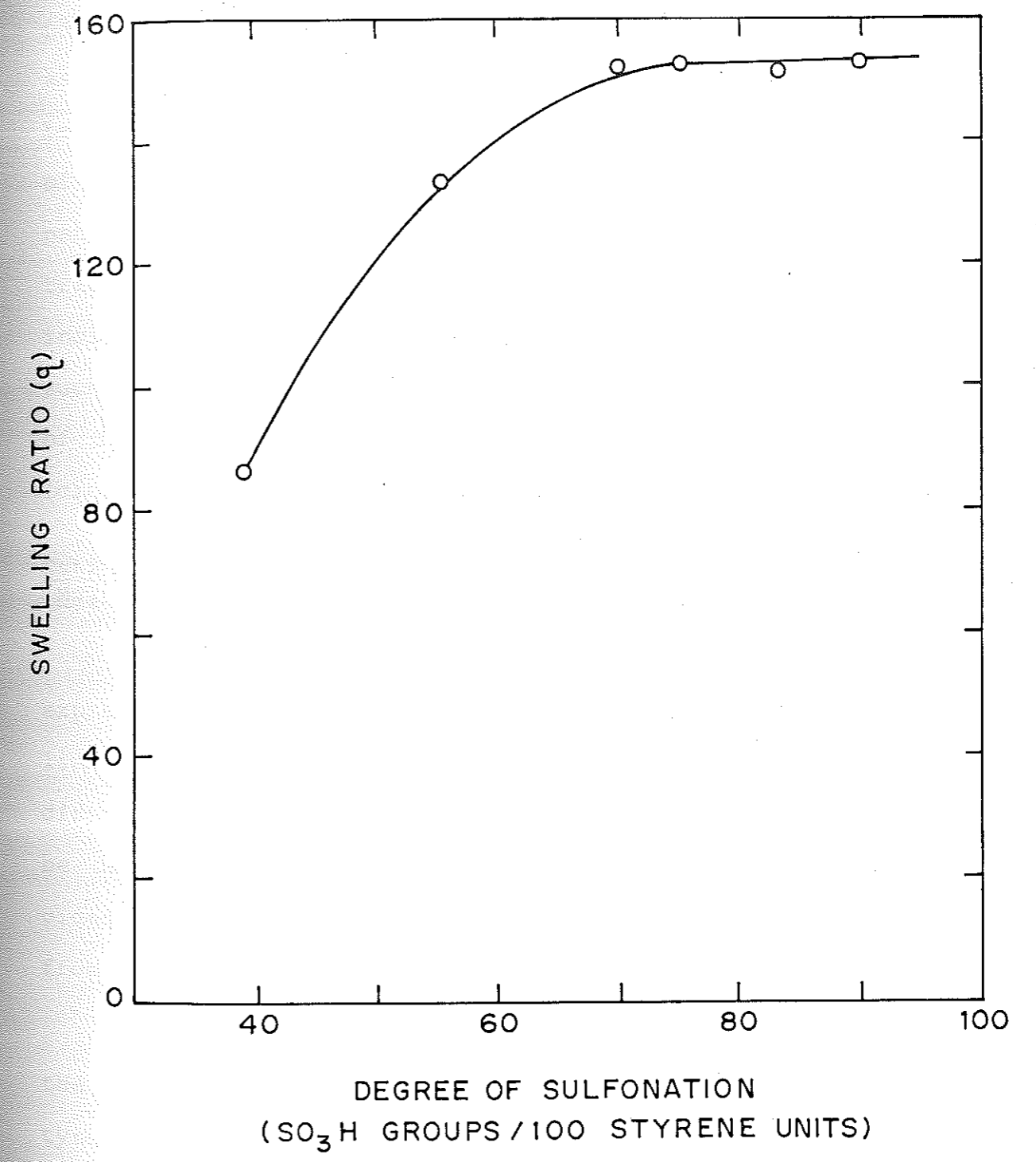


FIGURE 2.5: EFFECT OF SULFONATION ON SWELLING RATIO

to a maximum limit for the charge concentration on the polyelectrolyte chain. The degree of sulfonation can be as high as 80-85% beyond which the sulfonation process becomes sluggish due to steric hindrance. The sulfonation of polystyrene can be carried out by using various sulfonating agents, e.g. H_2SO_4 , chlorosulfonic acid or sulfur trioxide. There are various catalysts suggested which include silver sulfate or even phase transfer catalysts such as quaternary ammonium salts. However, the combination of H_2SO_4 and silver sulfate gives the least side reactions (cross-linking) and more efficient sulfonation.

Estimation of Average Molecular Weight Between Cross-links (M_c)

The degree of cross-linking of a network can be expressed by the average molecular weight between cross-links (M_c). The parameters, swelling ratio (q) and M_c are directly proportional to each other. The value of M_c can be determined by using Flory's equation of swelling, provided the volume fraction of the network (v_2) is known from swelling ratio measurements.

Recently, Barr-Howell and Peppas (8) have reported the dynamic and equilibrium swelling behaviour of polystyrene gels in methylethyl ketone and cyclohexane. The ' M_c ' values varied from 8500-1000 with respect to DVB content of 2-25% and ' M_c ' values became almost constant after 10% DVB content. It was observed from the results that, the value of ' M_c ' strongly depends on the degree of cross-linking as well as number average molecular weight

(Mn) of the uncross-linked polystyrene. It would be appropriate to determine the value of 'Mn' experimentally. The above mentioned authors have assumed the value of Mn to be 50,000 based on their theoretical calculation (9). In our studies the value of Mn for uncross-linked polystyrene was determined by measuring intrinsic viscosity $[\eta]$ in toluene at 30°C. From the relationship,

$$[\eta] = K M_n^\alpha$$

with $K = 9.2 \times 10^{-5}$ dl/g and $\alpha = 0.75$ (10) the value of Mn obtained was 6.17×10^4 g/mole.

In order to estimate 'Mc' values, the swelling ratios were measured in toluene and the volume fraction of the network were calculated. 'Mc' values were calculated by using Flory's equations, (1.2)-(1.3). (Chapter-I). The values of the some of the parameters used for calculations are as follows. \bar{v} is the specific volume of the polymer (0.9615), V_1 is the molar volume of solvent (toluene) (92), and 'X' is the interaction parameter between polystyrene/toluene (0.43) (10). The results of the 'Mc' values are summarized in Table-2.2. In order to verify these results, the 'Mc' values of same samples were determined by measuring their glass-transition temperatures (T_g). Since both the parameters Mc and T_g depend upon degree of cross-linking they are related by the following equation (11).

$$M_c = \frac{3.9 \times 10^4}{(T_g - T_{g0})} \quad (2.1)$$

where, T_{g0} is the glass-transition temperature of uncross-linked polymer and T_g is the glass-transition temperature of cross-linked polymer. Both these values were determined by using Differential Scanning Calorimeter (DSC-2) [Perkin Elmer]. About 5-10 mg sample was heated at a rate of 40°/min and 20 cc of nitrogen gas/min was flushed through the sample holder to maintain an inert atmosphere. Results of the M_c values calculated by swelling and T_g measurements are summarized in Table-2.3.

It is observed from ^{the} table that the results are quite comparable except in the case of 2 % cross-linked polystyrene.

Determination of Average Mesh Size (ξ) of the Network

The network structures have potential applications in separation processes as packing materials. Therefore estimation of average mesh size of the network is essential for the design of proper packing materials which are used for various chromatographic techniques.

When these networks are in equilibrium swollen state, their average mesh-size is related to the volume fraction of the network as follows,

$$\xi = v_2^{-1/3} r_0 \quad (2.2)$$

where, r_0 denotes the end-to-end distance in the unperturbed state and is given as,

$$r_0 = C_n r_f^2 \quad (2.3)$$

and,

$$r_f = l \sqrt{N} \quad \text{and} \quad N = \frac{\lambda M_c}{M_r}$$

where, ' r_f ' is end-to-end distance in the freely jointed chain, ' l ' is the C-C bond length (1.54\AA), ' C_n ' is the characteristic ratio or rigidity factor for polystyrene (=10)

(12), ' λ ' is the number of links per repeat unit ($\lambda = 2$), M_r is the molecular weight of the repeat unit and ' M_c ' is the molecular weight between cross-links.

Using the above equations the mesh-sizes are calculated and summarized in Table-2.4. Depending on the degree of cross-linking, the ' ξ ' values varied from 21\AA to 200\AA . These polymers were subsequently used in the separation of biological macromolecules from water on the basis of mesh size of the network. This will be discussed in Chapter-VI in detail.

Determination of v_2 , M_c and ξ Values for Bulk Polymerized Polystyrene Gels

The above parameters were estimated for bulk polymerized polystyrene gels of very low DVB content in the same manner as mentioned above. The number average

molecular weight (M_n) was found to be 1.37×10^5 . The results are summarized in Table-2.5.

Effect of Electrolytes and pH on Superabsorption

The polystyrene sulfonic acid superabsorbents contain charges on their chain and during the process of swelling there exists an electrostatic repulsion between the like groups of the chain. However, there exists an optimum cooperative electrostatic effect at which the expansion of the chain is maximum with maximum swelling ratio. The presence of electrolytes screens these electrostatic forces in the network and causes deswelling.

Based on Flory's theory of swelling of ionic networks, the effect of electrolytes on swelling ratio (q) can be evaluated by using equation (1.5) (Chapter-I) and the equation,

$$I_0 = \sum c_i z_i^2 \quad (2.4)$$

where, ' c_i ' is the concentration of the electrolyte, ' χ ' is interaction parameter (0.3) and ' z_i ' is the valency of the cation.

The swelling ratios of polystyrene-sulfonic acid (with $M_n = 1.37 \times 10^5$, $M_c = 51772$) in various concentrations of electrolyte solution (NaCl) were determined and results are plotted in Fig. 2.6. It is observed that the experimental values compare well with the theoretical predictions. However, at higher concentration of electro-

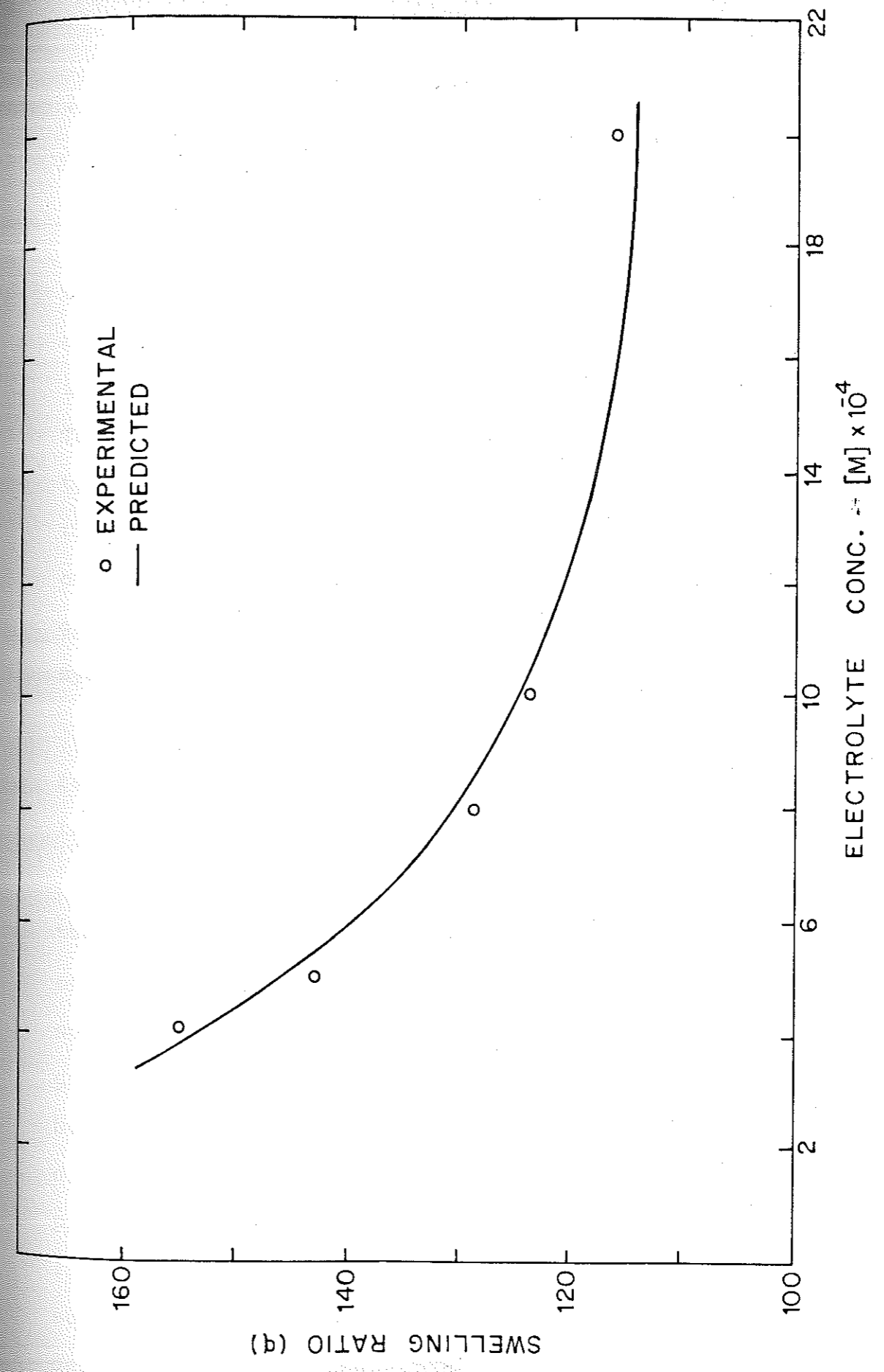


FIGURE 2-6: EFFECT OF ELECTROLYTE CONC. ON SWELLING RATIO (q)

lytes, the experimental values deviate from theoretical values. This may be due to change in the value of ' χ ' with respect to electrolyte concentration. According to Takahashi et al. (13), the interaction parameter ' χ ' depends on the electrolyte concentration. As the electrolyte concentration increases, the interaction parameter also increases and causes deviation in the experimental value. They have calculated the value of χ to be 0.39 for polystyrene sulfonic acid ($M_n = 5 \times 10^5$) in 0.005 M NaCl solution. Therefore for very dilute NaCl solution, the value of χ has been estimated (from the extrapolation of the graph) to be 0.30 for polystyrene sulfonic acid/water system.

In case of multivalent electrolytes the swelling ratio still decreases due to multivalent cross-linking (Fig. 2.7).

When a superabsorbent polymer with a charge on the chain is placed in an ionic solution, an exchange of mobile ion takes place between the network and the solution. However, due to the presence of bound ionic groups to the chain, the mobile ions are unevenly distributed with network having high concentration. This uneven distribution of mobile ions causes variations in osmotic pressure difference which determines the degree of swelling. The effect of pH on swelling ratio of polystyrene sulfonic acid superabsorbent is shown in Fig. 2.8. As described in Chapter-I the polymer exhibits high degree of swelling at low pH and maximum swelling at neutral

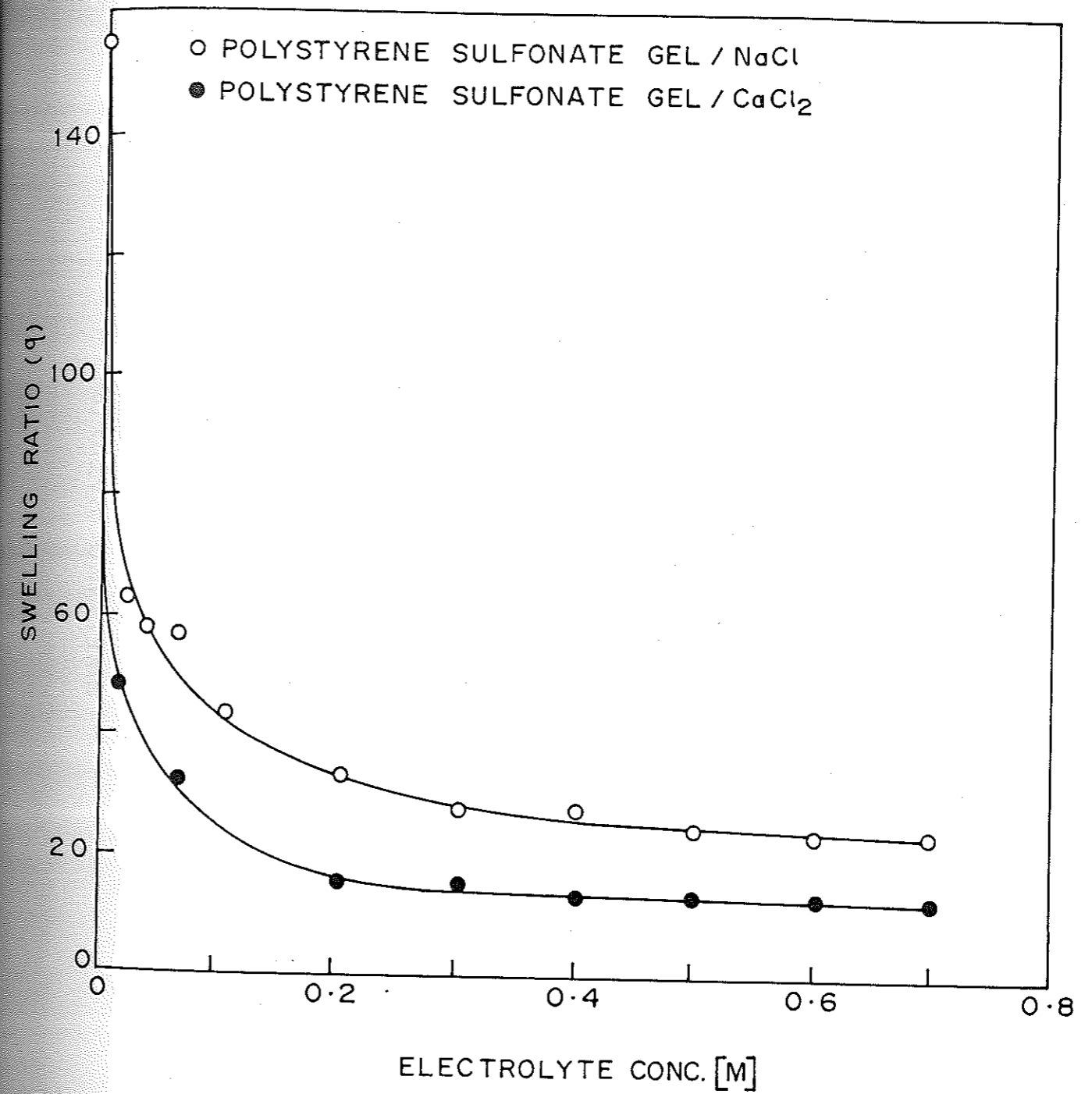


FIGURE 2.7 : EFFECT OF ELECTROLYTE ON SWELLING RATIO

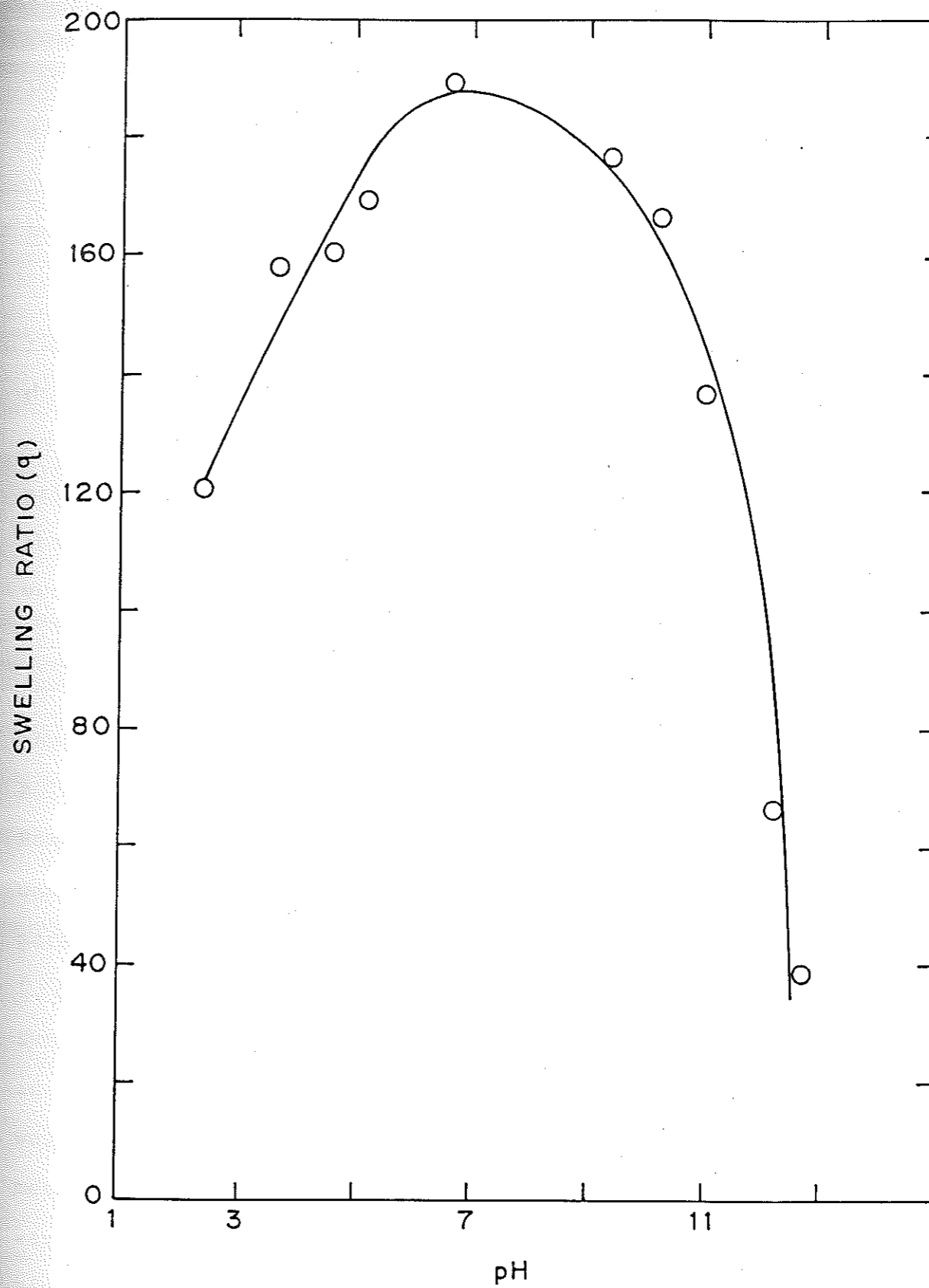


FIGURE 2·8: EFFECT OF pH ON SWELLING RATIO

pH as compared to high pH values. This may be attributed to the strong sulfonic acid groups attached to the polymer.

Swelling Behaviour of Polystyrene Sulfonic Acid Gels in Non-aqueous Media

Superabsorbents and their swelling behaviour have received considerable attention in recent years because of their potential applications in various fields such as biochemistry, chemical engineering and agricultural products. Most of the studies reported earlier on superabsorption have been carried out in aqueous media or solvents mixed with water. Therefore it is interesting to study the swelling behaviour of these ionic networks in non-aqueous system. It is known from the earlier theories that, the electrostatic interaction plays an important role in deciding the equilibrium swelling equation (14). However, their explicit importance is yet to be fully understood. On the other hand, solvent-polymer interaction parameter (χ) which is related to the solubility parameter (δ_p) also appears in the equation, which governs the swelling, therefore it is important to study its role in the swelling behaviour of ionic networks. One of the ways to bring out the relative importance of these parameters is to change the swelling medium in a systematic way. Hence the swelling behaviour of these gels was investigated in a series of solvents such as $R-(CH_2)_n-OH$ with 'n' ranging from 0 to 10 and the results are given in Table-2.6.

It can be readily seen from the table that, for any given cross-link density and degree of sulfonation the swelling ratio is maximum in water and progressively decreases as one goes to higher homologues in the series $R-(CH_2)_n-OH$, i.e. methanol, ethanol, propanol, etc. Such a homologous series was particularly chosen in order to retain the chemical nature of the constituent groups the same while changing only the dielectric constant of the medium. It is observed that, as the dielectric constant of the medium decreases the swelling ratio also decreases. However, the exact functional dependence is yet not fully understood.

There are several theoretical models suggested in the past for explaining the behaviour of polyelectrolytes (such as sulfonated polystyrenes) in solution as well as in gel state. These have been explained by Selegny in depth (15). The swelling behaviour of PS-DVB has been studied in detail by Errede (16). In particular, the swelling of this polymer in different solvents has been analysed in terms of the solubility parameter (δ) and cross-link density (f) which has been defined as $(r/r + 1)$ where 'r' is the mole fraction of DVB in the polymer. It was observed that, the swelling ratio of the copolymer at equilibrium follows the relation,

$$q = c (f^{-1/3} - f_0^{-1/3}) \quad (2.5)$$

where, 'c' is a constant for a liquid and f_0 is the

critical value of cross-link density above which 'q' is equal to zero. The constant 'c' has been found to depend on the solubility parameter as,

$$C = A - 0.60 (\delta_p - \delta_s)^2 \quad (2.6)$$

where, 'A' is constant and the subscripts p and s correspond to polymer and solvent, respectively. The above equation has been found to hold good for a homologous series $\text{Ph}-(\text{CH}_2)_n-\text{H}$ so long as $n < 5$, Ph being the phenyl group.

In order to apply the above analysis to the present case of ionic network polymers, one has to know the exact values of the solubility parameter for the polymer. Our extensive survey of literature however indicates that the values of δ_p have not been reported for this system. Therefore this value has to be estimated indirectly in order to satisfy the above equations. Fig. 2.9 shows the plot of q vs $f^{1/3}$ for the present system of solvents $\text{H}-(\text{CH}_2)_n-\text{OH}$ with 'n' ranging from 0 to 5. It is seen that the graph is more or less linear for $n = 0$ (water), while for $n > 1$ there is a slight deviation from linearity especially at low $f^{-1/3}$ values i.e. high cross-link densities. The inset in the figure shows a plot of the slope of the graph in the linear region as a function of 'n' for the homologous series and it is quite clear from the figure that this relationship is a non-linear one. Errede observed a linear decrease in the swelling parameter C (or the slope of the graph of q vs $f^{-1/3}$) with increasing

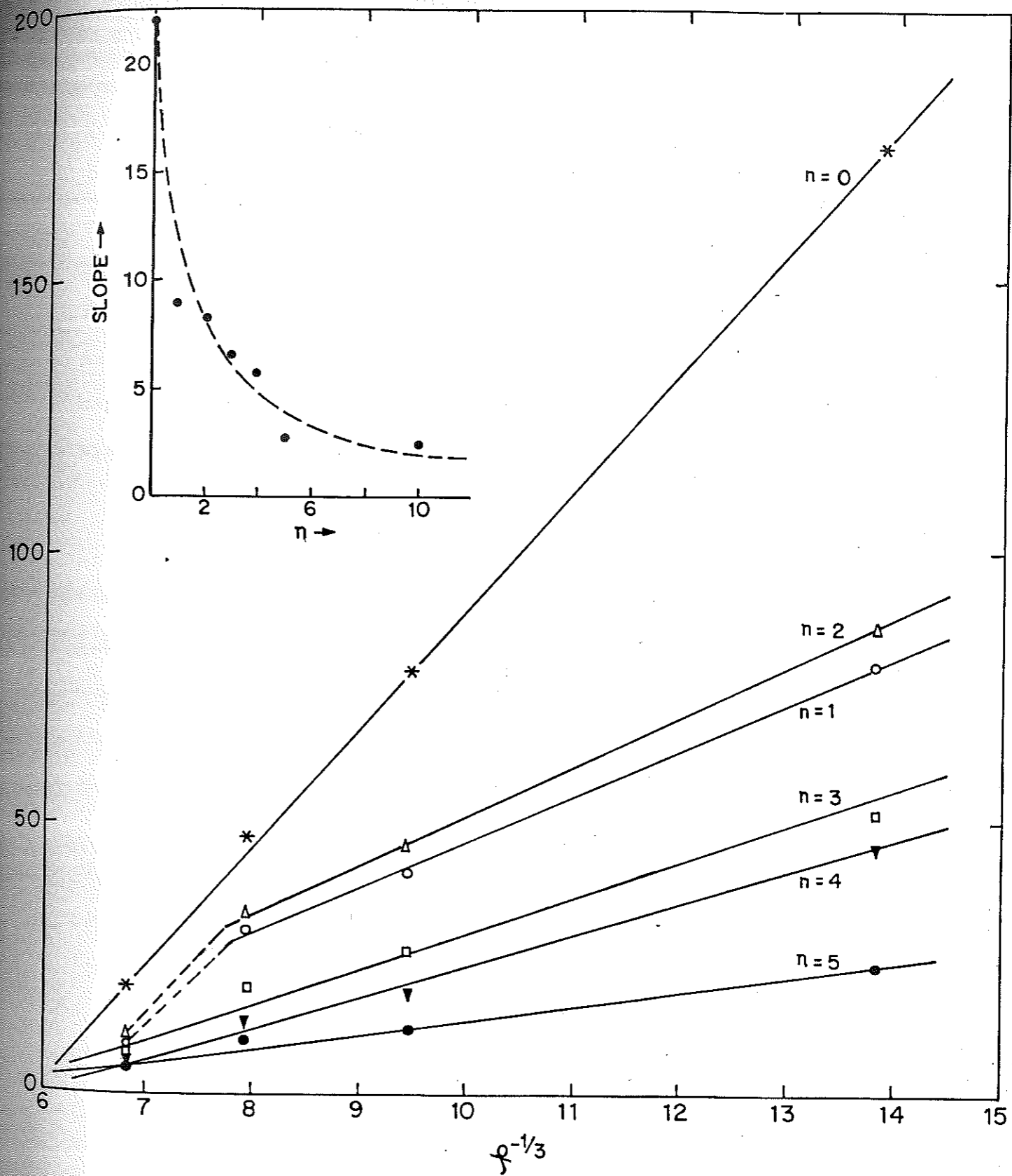


FIGURE 2.9: SWELLING BEHAVIOUR OF PSS GELS IN THE NON-AQUEOUS MEDIA [HOMOLOGOUS SERIES OF THE TYPE $R(CH_2)_n-OH$]

'n' for polystyrene-CO-DVB in various solvents of $\text{Ph}(\text{CH}_2)_n\text{H}$ for atleast upto $n = 6$. The slight deviation for $n > 6$ was explained on the basis of molecular self association between the methylene groups. However, our results seem to suggest that the methylene groups have much greater influence on the affinity of the functional groups such as SO_3H and OH involved in the solvent-power/swelling capacity in the ionic gels than that found in the non-ionic systems.

The above results can be analysed in terms of solubility parameter. By combining the above equations, one finds that the swelling ratio for a given cross-link density should be proportional to $(\delta_p - \delta_s)^2$. Now it is known that the uncross-linked poly(styrene sulfonic acid) is highly soluble in water. From Hildebrand's rule for solubility parameters, it may be deduced that, the δ_p value for this polymer should be within the range ± 2 of that of water ($\delta_s = 23.0$). hence we assumed the δ_p value to be 21.0 and took the available δ_s values from standard literature for making plots of q vs $(\delta_p - \delta_s)^2$. Figure 2.10 shows the graph for four sets of copolymers with different cross-link densities. Curves I to IV corresponds to the M_c values of 2.2×10^4 , 1.9×10^4 , 0.869×10^4 and 0.614×10^4 respectively. it is seen that in all the cases the plot is a linear one, the slope of which depends on the extent of cross-linking. Similar studies were made by keeping the cross-link density

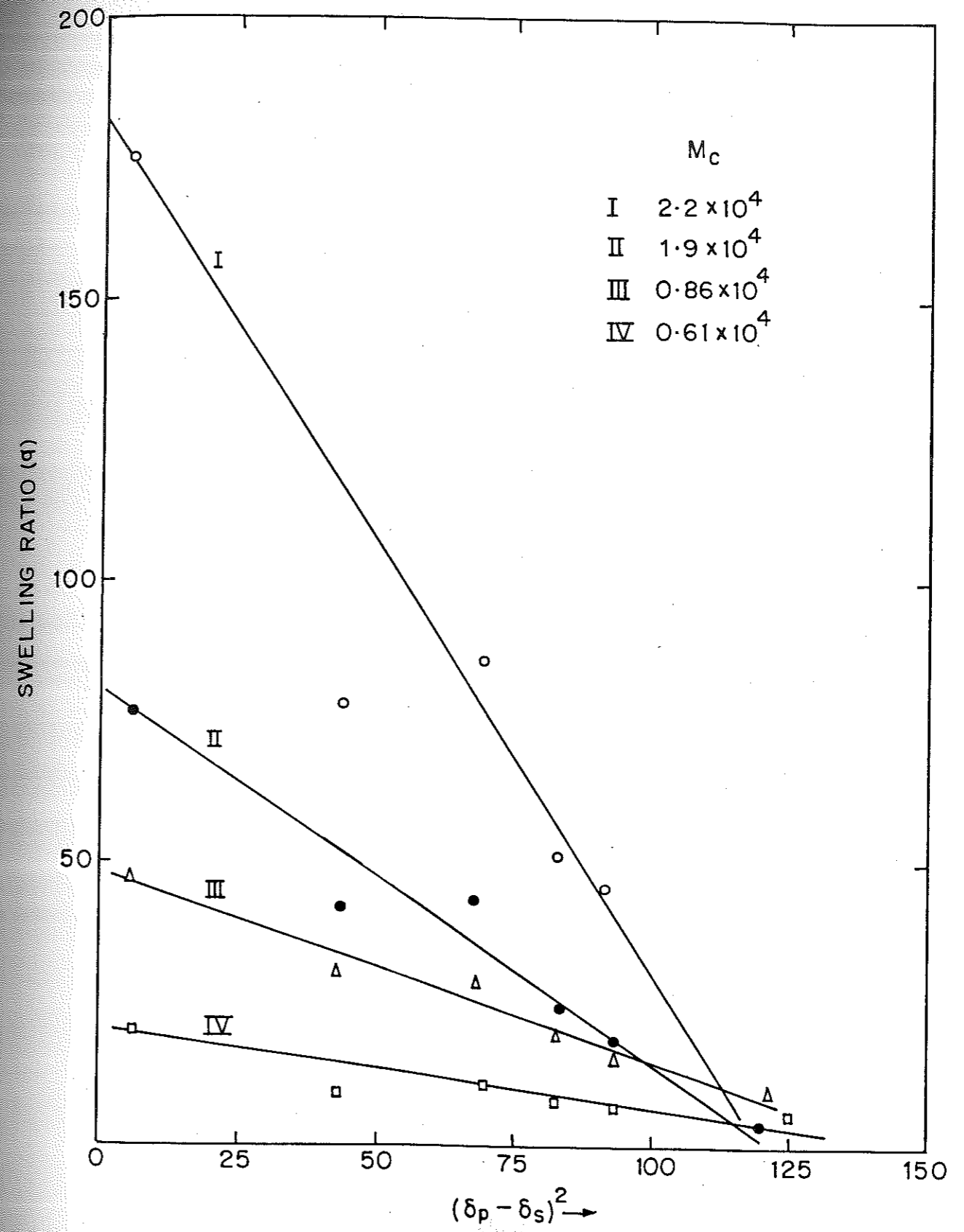


FIGURE 2-10 : DEPENDENCE OF SWELLING RATIO ON SOLUBILITY PARAMETER [I TO IV CORRESPOND TO INCREASING CROSS-LINK DENSITY]

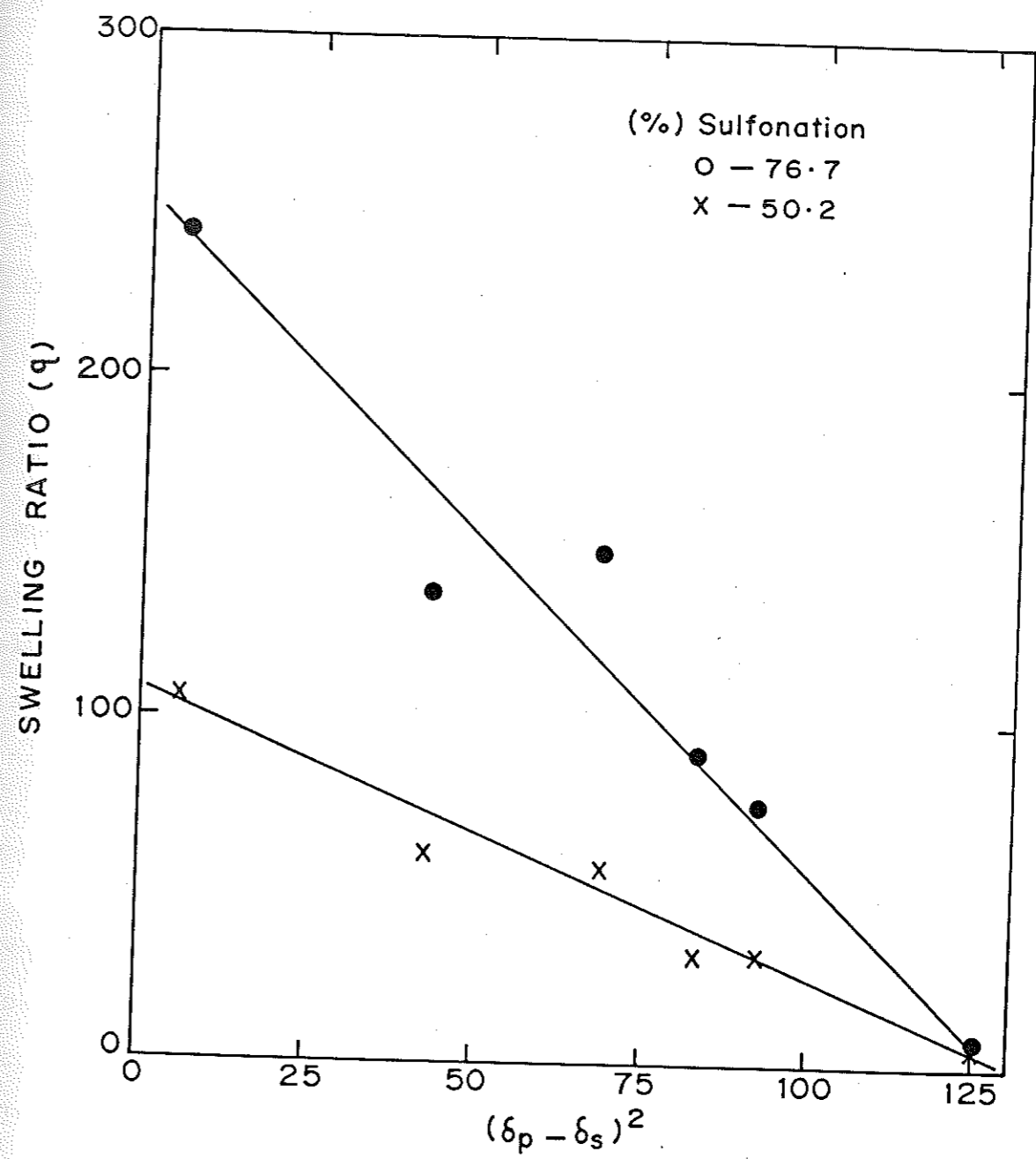


FIGURE 2.11 EFFECT OF DEGREE OF SULFONATION ON THE SWELLING BEHAVIOUR OF PSS GELS

same but varying the degree of sulfonation. Figure 2.11 shows such a plot for two cases, curve-I corresponds to degree of sulfonation of 76% and curve-II to 50%. For both the sets, the graph again is linear, thus lending substance to the above findings. It may be of interest to note that the polymer-solvent interaction parameter (χ) is related to solubility parameter as,

$$\chi = \frac{(\delta_s - \delta_p)^2 v_s}{RT} \quad (2.7)$$

where, 'Vs' is the specific volume of the solvent, 'R' is the gas constant and 'T' the absolute temperature. It thus seems from these studies that, the specific interaction between the solute-solvent molecules plays a dominant role in governing the swelling behaviour of ionic gels.

In order to confirm the reliability of the ' δ_p ' value assumed, the solubility parameter of polystyrene sulfonic acid was calculated indirectly from second virial coefficient (A_2) which is reported in the literature (13). It may be noted that,

$$A_2 = \frac{\rho_s}{M_s \rho_p^2} (1/2 - \chi) \quad (2.8)$$

where, ρ_s and ρ_p are densities of solvent and polymer, respectively and M_s is the molecular weight of the solvent. Using the value of A_2 as 4.0×10^{-5} in water with very

low concentration of sodium chloride ($< 5 \times 10^{-3}$ M) and the above equations. The value of δp was estimated to be 18.9. Considering the fact that the polymer contains sodium ions rather than H^+ and the solvent contains small percent of additional electrolyte, this value is in reasonable agreement with the value of 21.0 assumed earlier.

CONCLUSIONS

In the foregoing the synthesis of polystyrene-CO-DVB by suspension and bulk polymerization methods have been discussed. The gels containing 0.1 to 2.0% DVB were characterized for swelling ratio (q), volume fraction of the network (v_2), average molecular weight between cross-links (M_c) and mesh-size (ξ) of the network. It was observed that as the DVB content increased the ' M_c ' and ' ξ ' values decreased.

The swelling behaviour of sulfonated polystyrene-CO-DVB gels have been studied in a homologous series of solvents of the type $H-(CH_2)_n-OH$ with ' n ' ranging from 0 to 10. The solubility parameter has been found to play an important role in governing the swelling capacity of the gel. The solubility parameter for the copolymer seem to be about 21.0, one of the highest reported so far for polymers. This may be due to highly ionic nature of the polymer. The methylene groups appear to have considerable influence on the affinity of the solvent molecules for the functional groups on the polymer involved in the formation of gel. The analysis and correlation of various

parameters as proposed by Errede appears to be valid for highly swollen ionic gels (low cross-link density) but for small swelling ratios (high cross-link density) some deviations are noticed which could be due to electrostatic interactions between the ionic species trapped within the networks.

Superabsorbents Based on Poly-2-Acrylamido-2-Methyl Propane Sulfonic Acid (PAMPS)

Introduction

It has been indicated in the earlier part that sulfonic acid containing polymers represent a class of strong polyelectrolytes which typically have high degree of ionization and extensive coil expansions in aqueous media. Since these are essential properties for making superabsorbent polymers, the poly-2-acrylamido-2-methyl propane sulfonic acid represents itself as potential superabsorbent polymer. Extensive work has been done on this polymer and copolymers (17,18,19) with other monomers like acrylamide, acrylic acid, 4-vinyl pyridine, acrylonitrile and maleic anhydride. Most of these copolymers are water soluble and have wide range of potential applications including in enhanced oil recovery (20). Fischer et al. (21) have studied the chain characteristics of PAMPS polymer by light scattering and intrinsic viscosity methods.

Although much of the work has been done on synthesis and characterization of water soluble polymers based on PAMPS, efforts have not been made to develop superabsorbent

polymers using PAMPS. However there are few reports wherein 2-acrylamido-2-methyl propane sulfonic acid (AMPS) has been used as one of the comonomer in small quantities for graft copolymerization onto starch to prepare superabsorbent polymers. Recently, Osada and Hasebe (22) have reported electrically activated mechanochemical devices using PAMPS gel. In all the above studies the complete characterization of superabsorbent polymer in terms of degree of cross-linking and swelling behaviour is not emphasized. In this part PAMPS gels with different degrees of cross-linking have been prepared and characterized in terms of swelling ratio (q), degree of cross-linking and average molecular weight between cross-links (M_c).

Preparation of PAMPS Superabsorbents

The monomer, 2-acrylamido-2-methyl propane sulfonic acid, is a white, hydrophilic, crystalline solid having melting point of 185°C . It was procured from Lubrizol Corporation, USA and used as received. N-N-methylene bisacrylamide (Bis-A), ammonium persulfate and tetramethyl ethylene diamine (TEMED) were pure grade and used as such.

PAMPS superabsorbents were synthesized by polymerizing sodium salt of AMPS monomer in a glass tube at 30°C . The reaction mass containing monomer (AMPS-Na), solvent (water), initiator (ammonium persulfate) and cross-linking agent was stirred for 10 minutes with nitrogen bubbling. The polymerization was allowed to carry out for 10 hrs, then the polymerized gels were washed with

sufficient quantity of water and precipitated in acetone. The isolated polymers were then dried in oven at 60°C. Thus, 4.8×10^{-2} moles of AMPS monomer was neutralized with sodium hydroxide to a pH of 8.3 and the volume was adjusted to 100 ml with distilled water in a glass tube. The cross-linking agent Bis-A was added and dissolved completely with vigorous shaking along with the nitrogen bubbling. Then 4.3×10^{-4} moles of ammonium persulfate and 8.6×10^{-4} moles of TEMED were added and polymerization was carried out at 30°C in a water bath for 10 hrs. The products were washed with water and isolated by precipitation and drying. In a similar way PAMPS gels with 2-10% cross-linking agents were prepared and their swelling ratios measured by using methods described previously.

The degree of cross-linking in terms of 'Mc' can be estimated by knowing the swelling ratios (q) of PAMPS gels prepared with different quantities of cross-linking agent. The swelling ratio (q) for ionic networks is given as,

$$q^{5/3} = \frac{V_0}{V_e} \left[(0.5 - \chi)V_1 + \frac{i^2}{4 v_m^2 I_0} \right] \quad (2.9)$$

where, V_0 is the volume of unswollen gel and other terms have been defined earlier. The above equation can be rewritten in terms of 'Mc' as follows,

$$q^{5/3} = \frac{M_c}{\rho_p} \left[(0.5 - \chi)V_1 + \frac{i^2}{4 v_m^2 I_0} \right] \quad (2.10)$$

The results of the swelling ratio measurements in water are summarized in Table-2.7. It can be readily seen from the table that the swelling ratio increases from 56.7 to 400 as the percentage cross-linking decreases from 10.0 to 2.0% and below 2% cross-linking the gel becomes very soft and pasty.

It is interesting to note that the swelling ratio measurements reported above for the case cannot be used to estimate the values of 'Mc' because the value of ' χ ' for PAMPS/water system is not known or reported in the literature. However, the second virial coefficients (A_2) of PAMPS polymer in different concentrations of electrolyte solutions has been reported by Fischer et al. With the A_2 values reported above, the ' χ ' values for polymer and electrolyte solution has been calculated by using equations 2.7 and 2.8. From the value of χ for the polymer in very dilute NaCl solution (0.465) we have estimated the δ_p value for PAMPS using eqn. 2.7 and δ_s value of 23.0 for water. It is interesting to note that the δ_p value is 19.07 which is ^{comparable to} the value observed in PSS gel

studied before. The ' χ ' values calculated are given in Table-2.8. The swelling ratios of PAMPS gels were measured in dilute sodium chloride solution and all the other parameters were taken appropriately for calculation of Mc values. The results of the analysis are summarized in Table-2.9. It is observed from the table that these Mc values compare well with theoretical Mc values calcu-

lated from the moles of cross-linker added per mole of monomer.

CONCLUSIONS

We have synthesized superabsorbents based on poly-(2-acrylamido 2-methyl propane sulfonic acid (PAMPS) and characterized in terms of their swelling ratio (q), volume fraction of the network (v_2) and average molecular weights between cross-links (M_c) by using Flory's theory of swelling. These polymers exhibit high equilibrium absorption capacities even at high degree of cross-linking [4-6 (%) cross-linker] as compared to PSS gels. PAMPS polymers are mechanically stable and can be used for variety of applications where removal of water is the main purpose. We have also estimated the solubility parameter of this polymer and compared with the PSS gel.

The solubility parameters in these highly ionic systems, though high are comparable in both PSS and PAMPS and within the Hildebrand limit, where one considers their soluble nature in the aqueous media. Thus the addition of ionizable groups such as ($-SO_3H$) to a polymer is likely to raise its solubility parameter considerably.

REFERENCES

1. Fanta G.F., Burr R.C., Doane W.M. and Russell C.R., Starke, 30, 237 (1978).
2. Buchanan K.J., Hird B. and Letcher T.M., Polym. Bull. 13, 493 (1985).
3. Masuda F., Chem. Economy and Engg. Review, 15, 19 (1983).
4. Fanta G.F., Burr R.C. and Doane W.M., Jl. Appl. Polym. Sci. 24, 2015 (1979).
5. Ion-exchange Technology edited by Naden and Streat, (1984), Ellis Horwood Ltd., England.
6. Perrin D.D., Armarego W.L.F. and Perrin D.R., 'Purification of Laboratory Chemicals', 2nd Ed. Pergamon Press, (1980)
7. Errede L.A., Jl. Appl. Polym. Sci., 31, 1749, (1986).
8. Barr-Howell B.D. and Peppas N.A., Jl. Appl. Polym. Sci., 30, 4583 (1985).
9. Smith M.J. and Peppas N.A., Polymer, 26, 569 (1985).
10. Brandrup J. and Immergut E.H., Polymer Handbook, (1966), Interscience Publishers.
11. Nielsen L.E., Reviews in Macromolecular Chemistry, 4, 69 (1970). Edited by Buttler G.B. and O'Driscoll, K.F.
12. Flory P.J., 'Statistical Mechanics of Chain Molecules', Wiley Interscience, New York (1969).
13. Takahashi A., Kato T. and Nagasawa M., Jl. of Phys. Chem., 71, 2001 (1967).
14. Ilavsky M., Macromolecules, 15, 782 (1982).

.....

15. 'Polyelectrolytes' Vol. 1 (1976), Edited by Selegny E. D. Reidel Publishing Company, Dordrecht Holland.
16. Errede L.A., Macromolecules, 19, 1522 (1986).
17. Salamone J.C., Tsai C.C. and Watterson A.C., JI. Macromol. Sci.-Chem. A 13 (5) 665 (1979).
18. Salamone J.C., Watterson A.C., Hsu T.D., Tsai C.C., Mahmud M.V., Wisnieshi A.W. and Israel S.C., JI. of Polym. Sci. : Polym. Symp. 64, 229 (1978).
19. McCormick C.L. and Chen G.S., JI. Polym. Sci.-Chem. Ed. 20, 817 (1982).
20. Report on 'Recent Movement in EOR Polymer by: NITTO CHEMICAL INDUSTRY CO.LTD. JAPAN (1981).
21. Fisher L.W., Sochor A.R. and Tan J.S., Macromolecules, 10, 949 (1977).
22. Osada Y. and Hasabe M., Chem. Lett. 1285 (1985).

NOTATION

- C_n rigidity factor or characteristic ratio
 I_0 Ionic strength
 l c-c bond length
 M_c average molecular weight between cross-links
 q Swelling ratio
 r mole fraction of DVB
 r_0 end-to-end distance in the unperturbed state
 T_{g0} glass - transition temperature of uncross-linked polymer
 T_g glass transition temperature
 $[\eta]$ Intrinsic viscosity
 r_f end-to-end distance in the freely jointed chain
 v_2 volume fraction or volume concentration of network
 v_1 molar volume of the solvent
 v_s specific volume of the solvent
 v_m molar volume of the structural repeat unit of the polymer
 Z_i Valancy of the cation
 \bar{v} specific volume of the polymer
 ξ average mesh-size of the network
 ϕ $(r/1+r)$
 λ number of links per repeat unit
 δ_p Solubility parameter for polymer
 δ_s solubility parameter for solvent
 ρ_s density of the solvent
 ρ_p density of the polymer
 X polymer - solvent interaction parameter

TABLE-2.1

Dependence of DVB content on swelling ratio:
Sulfonated PS-DVB/H₂O (with same degree of sulfonation)

No.	DVB content (%) ^a	Swelling ratio (q) in water
1	0.3	152.0
2	0.4	100.0
3	0.7	40.0
4	1.0	20.0
5	2.0	12.0

a : % on the basis of weight of the monomer

TABLE-2.2

Effect of divinyl benzene (DVB) content on volume fraction of the network (v_2) and molecular weight between cross-links (Mc)

No.	DVB content (%)	Volume fraction of the network (v_2)	Mc
1	0.3	0.098	18,116
2	0.4	0.125	13,759
3	0.7	0.204	6,137
4	1.0	0.250	3,979
5	2.0	0.487	655

TABLE-2.3

Comparison of 'Mc' values by swelling ratio
and T_g measurements

DVB content (%)	T_g (°C)	Mc values	
		T_g method	Swelling measurements
0.0	100.0*	-	-
0.4	102.5	15,600	13,759
0.7	108.7	4,482	6,137
1.0	111.2	3,444	3,979
2.0	112.5	3,120	655

* T_{go} = 100°C for uncross-linked or
zero % DVB polystyrene

TABLE-2.3

Comparison of 'Mc' values by swelling ratio
and T_g measurements

DVB content (%)	T_g (°C)	Mc values	
		T_g method	Swelling measurements
0.0	100.0*	-	-
0.4	102.5	15,600	13,759
0.7	108.7	4,482	6,137
1.0	111.2	3,444	3,979
2.0	112.5	3,120	655

* T_{g0} = 100°C for uncross-linked or
zero % DVB polystyrene

TABLE-2.4

DVB content changes mesh-sizes (ξ)
of the polystyrene networks

DVB content (%)	Mesh sizes (ξ)(A°)
0.3	196.3
0.4	158.3
0.7	89.3
1.0	67.2
2.0	21.8

TABLE-2.5

Effect of very low DVB content on
volume fraction of the network (v_2), molecular
weight between cross-links (M_c) and mesh sizes (ξ)
of PSS-gels prepared by bulk polymerization technique

DVB content	v_2	M_c	(ξ) (\AA)
0.10	20.75	5.17×10^4	445.0
0.15	10.94	2.28×10^4	226.0
0.25	9.41	1.91×10^4	197.0
0.40	5.70	0.86×10^4	112.0
0.50	4.80	0.61×10^4	89.0

TABLE-2.5

Effect of very low DVB content on
volume fraction of the network (v_2), molecular
weight between cross-links (M_c) and mesh sizes (ξ)
of PSS-gels prepared by bulk polymerization technique

DVB content	v_2	M_c	(ξ) (\AA)
0.10	20.75	5.17×10^4	445.0
0.15	10.94	2.28×10^4	226.0
0.25	9.41	1.91×10^4	197.0
0.40	5.70	0.86×10^4	112.0
0.50	4.80	0.61×10^4	89.0

TABLE-2.6
Swelling ratio for PSS-gels with different degrees of cross-linking in various solvents

Solvents	No. of (CH ₂) n	Dielectric constant (ϵ)	δ_s	Swelling ratio of gels with different cross-link densities			
				0.1% DVB (I)	0.15% DVB(II)	0.25% DVB(III)	0.40% DVB (IV)
Water	0	78.3	23.0	175.0	77.5	48.2	20.2
Methanol	1	33.6	14.5	77.9	41.0	31.0	8.6
Ethanol	2	24.3	12.7	86.5	45.5	33.5	10.4
i-propanol	3	18.3	11.9	51.5	25.3	20.3	7.5
n-butanol	4	17.8	11.4	46.4	19.0	16.2	7.0
i-amylalcohol	5	14.7	10.0	-	11.5	10.0	6.0
Decyl alcohol	10	8.1	9.8	-	10.0	11.3	5.2

TABLE-2.7

Effect of bis-acrylamide on swelling ratio of PAMPS gels

Bis-acrylamide content (%)	Swelling ratio (q)
0.0	-
2.0	400.0
4.0	309.0
6.0	150.9
8.0	80.4
10.0	56.7

TABLE-2.8

Dependence of 'X' on electrolyte (NaCl) concentration

Concentration of NaCl [M]	Second virial coefficient (A_2) mol. cm ³ / g ²	χ
0.01	19×10^{-4}	0.465
0.05	7.2×10^{-4}	0.487
0.10	5.2×10^{-4}	0.490

TABLE-2.9
Comparison of theoretical and experimental Mc values
of PAMPS gels

Bis-acrylamide content (%)	Mc - values	
	Experimental	Theoretical
2.0	-	7,734
4.0	5,200	3,852
6.0	2,472	2,564
8.0	1,786	1,926
10.0	1,101	1,539

CHAPTER-III

NMR STUDIES IN SUPERABSORBENT POLYMERS

In this chapter some aspects of Nuclear Magnetic Resonance of superabsorbent polymers are reported. Although the aspects on thermodynamics of absorption (1), kinetics of absorption (2), and phase transitions (3) of superabsorbent polymers are extensively studied, there is practically no study reported on the structural and dynamical characterization of this class of superabsorbent polymers through NMR techniques. The chapter is divided into four parts. The first part describes the NMR technique and the second part deals with the state of water in superabsorbent polymer as determined by the spin-lattice relaxation time (T_1) studies. In the third part, high resolution solid-state proton (^1H) magnetic resonance study of superabsorbent polymer is reported. The final part reports the effect of cross-linking on the carbon-13 NMR of this class of polymers.

Nuclear Magnetic Resonance (NMR) Phenomena

The Nuclear Magnetic Resonance spectroscopy deals with the magnetic properties of certain atomic nuclei like hydrogen, carbon, nitrogen, etc. The nuclei that exhibit the NMR phenomena are those for which the spin quantum number (I) is greater than zero. These atomic nuclei, possessing the property of spin, absorb electromagnetic radiation at well defined radio frequencies, when placed in an external static magnetic field. This absorption of energy is recorded in the form of a spectrum. The precise frequency absorbed by a given nuclear species

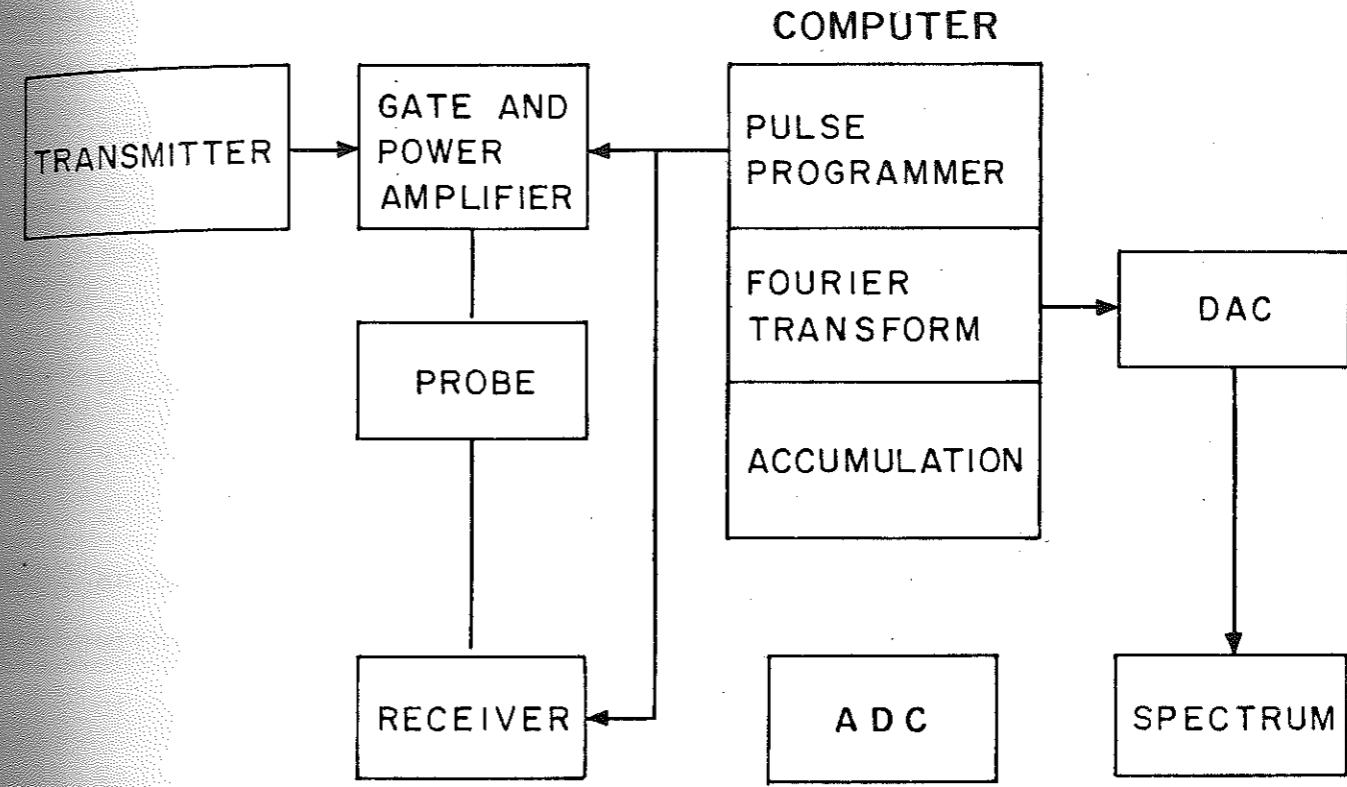
varies depending on the chemical environment of the atom in the molecule. Therefore the NMR spectrum of an organic molecule enables us to record the difference in the magnetic properties of various nuclei present and determines their position in the molecule. The proton NMR is the easiest to observe, whereas nuclei such as ^{11}N , ^{13}C , ^{19}F , ^{29}Si and ^{31}P can be observed as well.

NMR spectroscopy has wide applications in physics, chemistry, biology and medicine. Physicists made use of NMR technique to study the magnetic properties of various nuclei, whereas organic chemists observed that the exact frequency absorbed by a given nuclear species changes with the chemical environment of the atom in the molecule. This effect gives rise to 'chemical shift' and is caused by the interaction of nucleus with the surrounding electron and is quite small (of the order of a few parts per million of the NMR frequency). The chemical shift is made use of to study the molecular structure. The medicinal applications of NMR spectroscopy involves 'in-vivo' studies and spatial localised imaging of anatomical parts of living systems. Various substances in the solid-state have also been studied by NMR methods. Solid-state NMR with cross-polarization (CP) and Magic Angle Sample Spinning (MASS) has provided invaluable structural information about amorphous, polycrystalline and insoluble solids such as coal, oil-shales, polymers, cement, zeolites and other heterogeneous catalysts. In recent years polymers have been

extensively studied by NMR, both in the liquid and the solid states. Most of the polymers contain NMR active nuclei such as ^1H , ^{13}C and ^{15}N . The properties of polymers such as tacticity, chain dynamics and structure can be studied by determining chemical shifts, coupling constants and relaxation parameters of these nuclei.

NMR Spectrometer

The NMR spectrometer consists of a magnet capable of producing a very strong homogeneous field (B_0), a radio frequency (rf) source and a method of detecting absorption of rf energy by the sample (see Fig. 3.1). The static magnetic field (B_0) is provided by a superconducting magnet (7.1 Tesla in our study). The radio frequency is generated precisely in a frequency synthesizer and is gated according to the particular pulse program of the desired experiment. The radio frequency pulse is fed to a power amplifier and then sent into the probe which has the sample in it and is located in the magnet. By a suitable transmitter/receiver isolation scheme, the NMR signal is detected in a pre-amplifier. The signal is further amplified before being presented to a quadrature detector. The detected signal is digitized by the computer and stored in the computer memory. By repeating the experiment, NMR signals can be coadded in the computer memory to attain the desired signal to noise ratio. The block diagram of the FT-NMR is shown in Fig. 3.1, which represents the Bruker MSL-300



ADC - ANALOG TO DIGITAL CONVERTER

DAC - DIGITAL TO ANALOG CONVERTER

FIGURE 3-1: BLOCK DIAGRAM OF FT-NMR SPECTROMETER

system used by us in this work.

Fourier-Transform NMR (FT-NMR)

NMR was originally practised as a continuous wave (CW) technique in which the magnetic field strength (B_0) was held constant and the radio frequency was swept continuously so that various nuclei come in turn into resonance. Now this technique has become obsolete due to the introduction of universally accepted pulsed FT-NMR techniques by Ernst and Anderson (4). Here, the pulse of radio frequency of a given duration contains all frequencies in a certain range. Thus, if a strong pulse is applied to an assembly of spins, all nuclei with resonance frequencies within that range are excited simultaneously. So, instead of sweeping the frequency to obtain the spectrum, one can monitor the decay of the signal induced by the application of the pulse. The free induction decay (FID) signal observed in the 'time domain' [$f(t)$] can be converted into the 'frequency domain' [$F(\omega)$] NMR spectrum by Fourier transformation indicated by,

$$F(\omega) = \int_{-\infty}^{+\infty} f(t) e^{-i\omega t} dt \quad (3.1)$$

Now with the state-of-the-art computer technology and Fast Fourier Transform (FFT) algorithms, the time-to-frequency domain conversion can be made very easily. The advantage of FT-NMR is that the spectra can be obtai-

ned very rapidly with good attendant resolution and very little sample on a number of NMR active nuclei.

State of Water in Superabsorbent Polymers

Introduction

Water in biological systems and polymers is very important since it largely determines the essential properties of the system. However, analysing its behaviour is complicated because of its interaction with other components such as cellular and extracellular matrix. Nuclear Magnetic Resonance (NMR) relaxation is one of the methods that has been used to characterize the dynamics of water in different tissues and polymers (5-8). There are two approaches to study the state of water in polymeric gels by NMR. The first one is a direct method which makes use of the chemical shift resolution of signal itself to distinguish between different states of water. The second approach is based on the study of NMR relaxation processes. The direct approach leads to a technique to examine the possibility that 'ordered' states of water intermediate in rigidity of structure between 'free' water and 'ice' actually exists. Previous studies of proton magnetic resonance of agar gel in water (9,10) indicate that the water proton signal in agar gel differs from that obtained with free water i.e. water proton signal in agar gel is broadened as compared to the free water proton signal. Similar studies were done on various hydrophilic polymers such

as carboxymethyl cellulose, gelatin and starch (11). Based on these studies, it was believed that the water present in the polymer is of two types, namely 'bound' and 'free'. The bound water is held to the macromolecular chain and has a restricted mobility, whereas the free water does not have any restriction on the mobility. In the second approach, the proton nuclear spin-relaxation times, T_1 (spin-lattice) and T_2 (spin-spin), provides information about the dynamics of water molecules and their local environments. The NMR relaxation data are interpreted in terms of the exchange of protons between two or more populations of 'free' and 'bound' water using the traditional fast exchange limit form of the Bloch-McConnell equations or their equivalents. Katayama et al. (12) have reported the spin-lattice relaxation time (T_1) measurement of water in polyacrylamide gel. They observed that, T_1 of water proton in a confined space of polyacrylamide gel is considerably shortened in comparison with that in bulk water. Maquet et al. (13) studied the state of water in gelatin gels by relaxation time measurements and the results were examined in terms of the Zimmermann-Brittin exchange theory (14).

In this part of the chapter, the state of water in superabsorbent polymer, hydrolysed starch-g-polyacrylonitrile, as studied by spin-lattice relaxation time (T_1) measurements is reported. This approach was chosen because the proton magnetic resonance spectra of superabsorbent polymer did not have a chemical shift resolution to disti-

inguish between the bound and free water. The proton nucleus was used to measure T_1 because of its large gyromagnetic ratio and 100 percent abundance.

Relaxation Time Measurements

There are two relaxation times, that one can measure in an NMR experiment. These are the spin-lattice relaxation time (T_1) and spin-spin relaxation time (T_2). T_1 describes the first order rate constant associated with the restoration of longitudinal NMR magnetisation to its equilibrium value after disturbance to a non-equilibrium situation. T_1 is measured by following the return of the magnetisation to its equilibrium value after it has been perturbed by a radio frequency (rf) pulse at the proton resonance frequency. The pulsed NMR methods generally use a $\pi/2 - \tau - \pi/2$ or $\pi - \tau - \pi/2$ two pulse sequences (15) to measure T_1 . The magnetisation in the B_0 field is initially at its equilibrium value M_0 and oriented along the z-axis ($B_0 \parallel z$ -axis). Application of an intense π rf pulse will invert the magnetisation into the negative z-direction while maintaining the magnitude $-M_0$. This is shown in Fig. 3.2 (a). As the magnetisation relaxes back to its equilibrium (inversion recovery) value following the 180° pulse, the value of M_z at any time will be described by the Bloch's equation,

$$\frac{dM_z}{d\tau} = -\frac{(M_z - M_0)}{T_1} \quad (3.2)$$

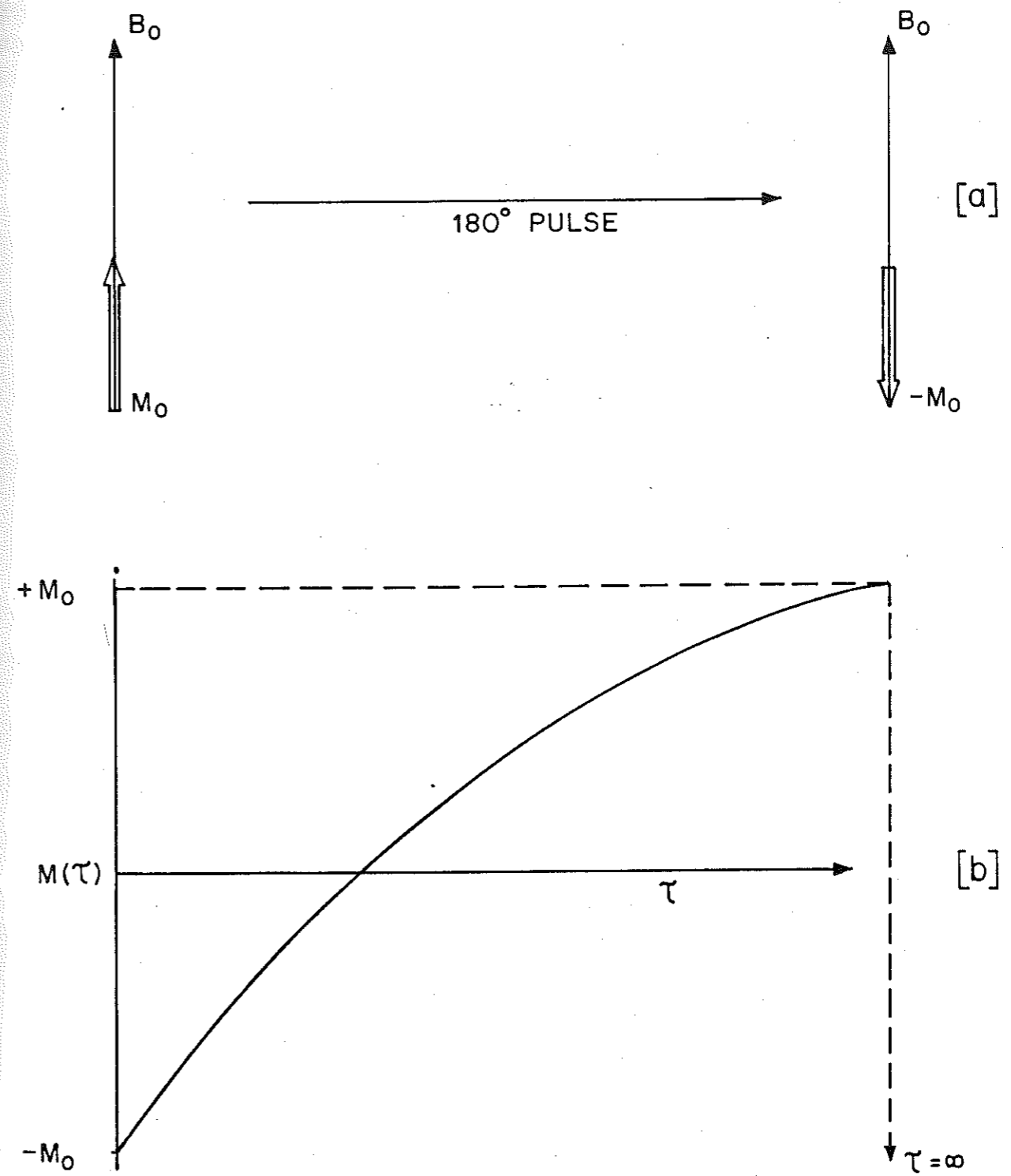


FIGURE 3.2: BEHAVIOUR OF DISTURBED MAGNETISATION AS A FUNCTION OF TIME (τ)

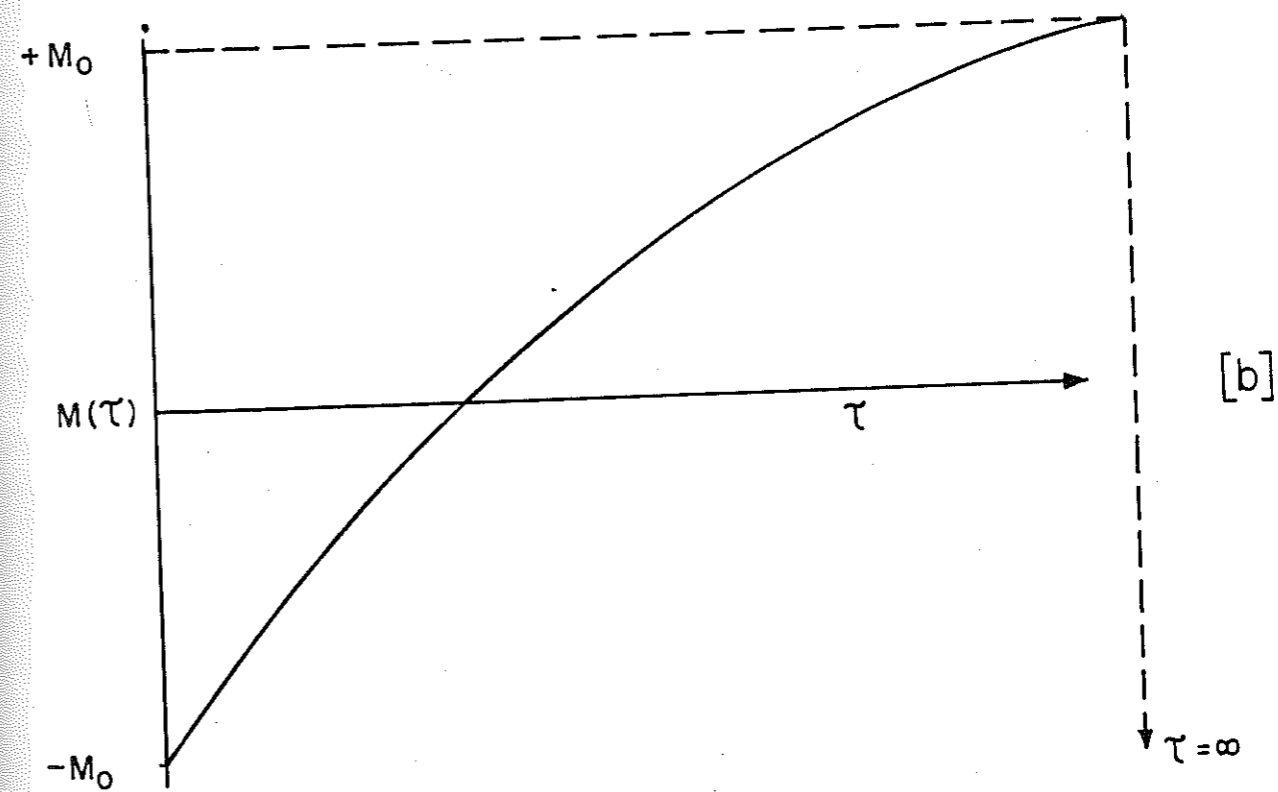
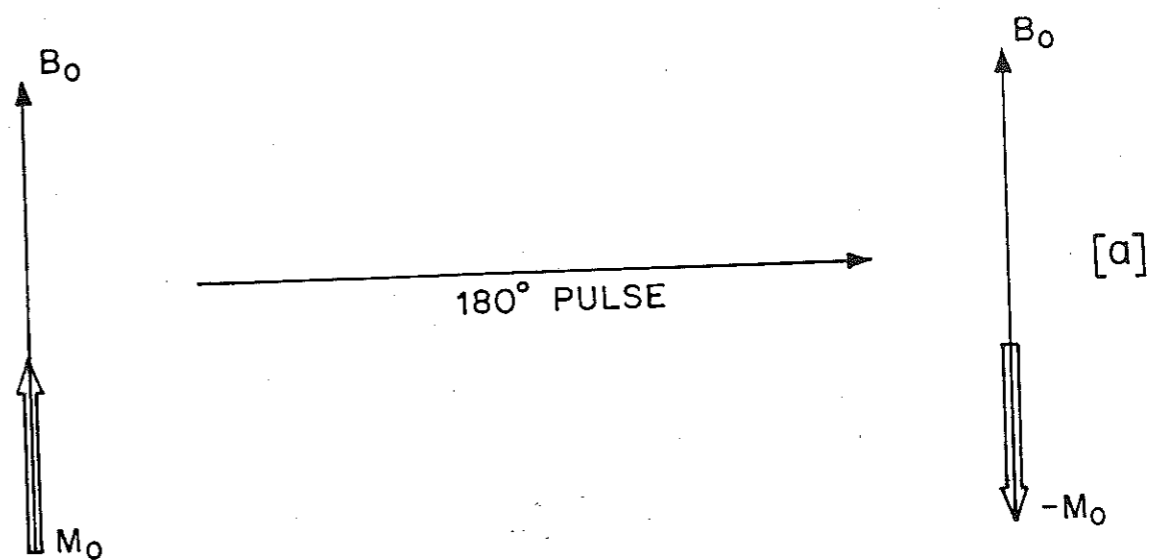


FIGURE 3.2: BEHAVIOUR OF DISTURBED MAGNETISATION AS A FUNCTION OF TIME (τ)

The behaviour of the 'disturbed' magnetisation as a function of time τ is shown in Fig. 3.2 (b). Application of 90° pulse at some time τ after the 180° pulse will cause M_z to be rotated through $\pi/2$ radians so the magnetisation may be detected along 'y' axis. By measuring the magnitude of the free induction decay following the 90° pulse as a function of τ , the time between pulses, T_1 may be determined. The signal amplitude $M_z(\tau)$, following the second pulse describes the relaxation process by the following equation, which may be derived from Bloch's equation.

$$M_z(\tau) = M_0 [1 - \cos \theta] e^{-\tau/T_1} \quad (3.3)$$

where, θ is the angle at which the magnetisation is rotated. In our case θ is equal to 180° , therefore the above equation becomes,

$$M_z(\tau) = (1 - 2 e^{-\tau/T_1}) M_0 \quad (3.4)$$

$$\text{when, } \tau = 0, \quad M_z(\tau) = -M_0$$

$$\tau = \infty, \quad M_z(\tau) = +M_0$$

The above equation can be simplified to yield,

$$\frac{M_0 - M(\tau)}{2M_0} = e^{-\tau/T_1} \quad (3.5)$$

$$\text{or } \ln \frac{M_0 - M(\tau)}{2 M_0} = - \tau/T_1 \quad (3.6)$$

Considering the above equation, a semilog plot of τ vs. $[\frac{M_0 - M(\tau)}{2 M_0}]$ gives a slope which is equal to $(-1/T_1)$. From the slope (Fig. 3.4) one can get T_1 by linear least-squares fit of data.

EXPERIMENTAL

The superabsorbent polymer used in T_1 measurements was hydrolysed starch-g-polyacrylonitrile, which was synthesized by graft copolymerization of acrylonitrile onto gelatinized starch. This graft copolymer was subsequently alkali hydrolysed and isolated in the form of dry powder. It has the equilibrium water absorption capacity of 160 gram per gram of dry polymer. This equilibrium water absorption capacity corresponds to 100 (%) saturation in water. The percentage grafting and the molecular weight of the grafted poly(acrylonitrile) for this polymer were determined to be 48% and 1,20,000, respectively. All the gel samples for T_1 measurements were prepared in deionized, distilled water with polymer concentration varying from 0.2-5.0(%). This range corresponds to 5-100(%) saturation in water. The gel samples were allowed to homogenize for 24 hrs and then taken for T_1 measurements.

All the proton relaxation time experiments were car-

ried out using VARIAN FT-80 NMR spectrometer operating at the proton frequency of 80 MHz. ($B_0 = 1.76$ Tesla). An inversion recovery sequence ($\pi - \tau - \pi/2$) was used for proton T_1 measurements. The π pulse was typically 54 μ seconds. Suitable values of the interpulse delay τ were chosen so that equal sampling of proton magnetisation on the negative and positive sides of the recovery curve was achieved. The probe temperature was carefully monitored and maintained at 32 °C. The proton signal decay was plotted and the T_1 was determined by fitting the data.

RESULTS AND DISCUSSION

The results of T_1 measurements of different concentration of gels are summarized in Table-3.1. It is observed that as the concentration of the polymer decreases or the water content increases the value of T_1 increases from 1.5 seconds to 4.5 seconds. The plot of $(1/T_1)$ versus concentration of the polymer gives a straight line with slope and intercept of 0.068 and 0.2215 respectively. From the intercept, the value of T_1 for zero percent polymer (pure water) is determined to be 4.51 seconds. In order to confirm the accuracy of this analysis, the spin-lattice relaxation time (T_1) of pure water was determined separately under same conditions. The value of T_1 was found to be 4.0 seconds.

Interpretation of T_1 Data

For the analysis of our T_1 measurements a basic model

of polymeric gel is considered which comprises FREE and BOUND water. Both these free and bound water fractions are coupled to the lattice by T_1 and can be denoted as T_{1F} (free) and T_{1B} (bound) as shown in Fig. 3.3.

It is known that the bound water fraction is made up of two types. One is the so-called 'structural water', which stabilizes the structure. For example in gelatin/water system (16) the structural water brings about a specific helical conformation from denatured state. The second type of water binds to the hydrophilic groups of the polymer by hydrogen bonding. In case of superabsorbent polymer studied here, this distinction is not clear, hence these two types of bound water cannot be distinguished.

Now it is to be expected that, the bound water and free water will exchange with a time constant τ_{ex} , one can monitor this exchange process via spin-lattice relaxation time (T_1). When τ_{ex} is slow as compared to T_{1F} or T_{1B} , one should get a biexponential decay of the water NMR signal. In such a case T_{1F} and T_{1B} can be obtained directly. However, when the exchange is rapid, the decay is a single exponential and the observed T_1 contains both T_{1F} and T_{1B} . It may be noted that T_1 of superabsorbent polymer studied here gives only a single exponential decay (Fig. 3.4) for all concentrations, which implies the rapid exchange between free and bound water. Based on the exchange model, when the mean life time of

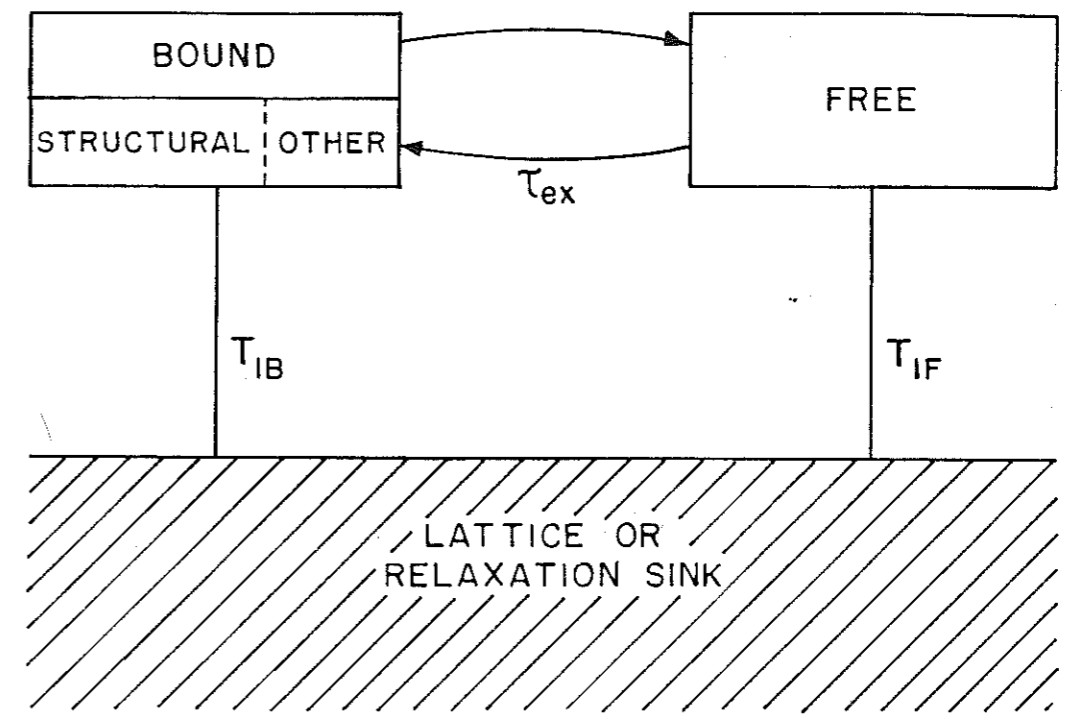


FIGURE 3-3 : EXCHANGE MODEL

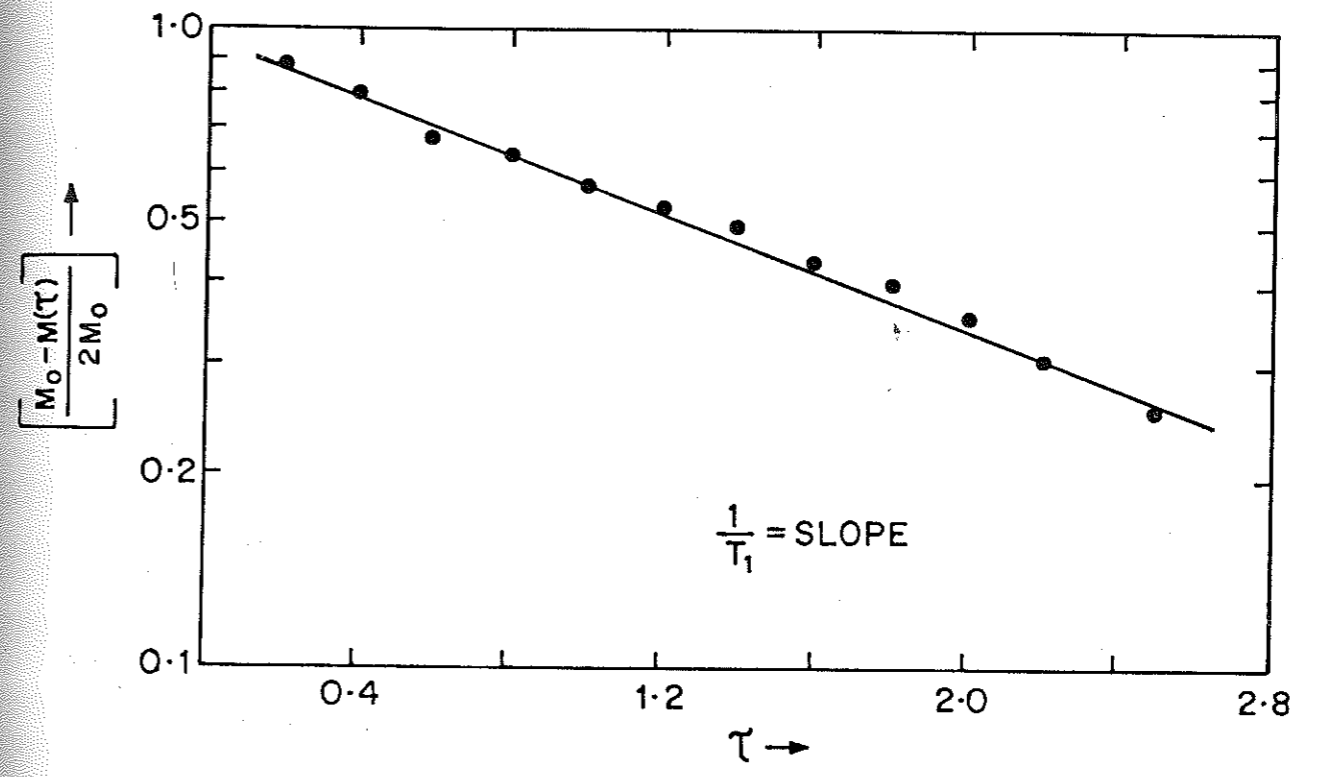


FIGURE 3-4: SINGLE EXPONENTIAL DECAY

proton in each fraction is much shorter than the T_1 of that fraction, the observed spin-lattice relaxation time (T_1) can be given as,

$$\left(\frac{1}{T_1}\right)_{\text{obs}} = \frac{P_F}{T_{1F}} + \frac{P_B}{T_{1B}} \quad (3.7)$$

where, P_B is population of bound water, P_F is population of free water and T_{1F} and T_{1B} are spin-lattice relaxation times of free and bound water.

The hydration constant 'h' which is the grams of bound water per gram of dry polymer can be related to T_1 as follows,

$$\left(\frac{1}{T_1}\right)_{\text{obs}} = \frac{1-hc}{T_{1F}} + \frac{hc}{T_{1B}} \quad (3.8)$$

where, 'c' is the concentration of polymer in grams per 100 gm water. On simplification the above equation yields,

$$\left(\frac{1}{T_1}\right)_{\text{obs}} = h \left[\frac{1}{T_{1B}} - \frac{1}{T_{1F}} \right] c + \frac{1}{T_{1F}} \quad (3.9)$$

It is observed from the above equation that a plot of $(1/T_1)$ versus concentration of the polymer gives a straight line (Fig. 3.5) with slope equal to $h \left[\frac{1}{T_{1B}} - \frac{1}{T_{1F}} \right]$. Now by knowing T_{1F} and T_{1B} , the value of 'h' can be estimated.

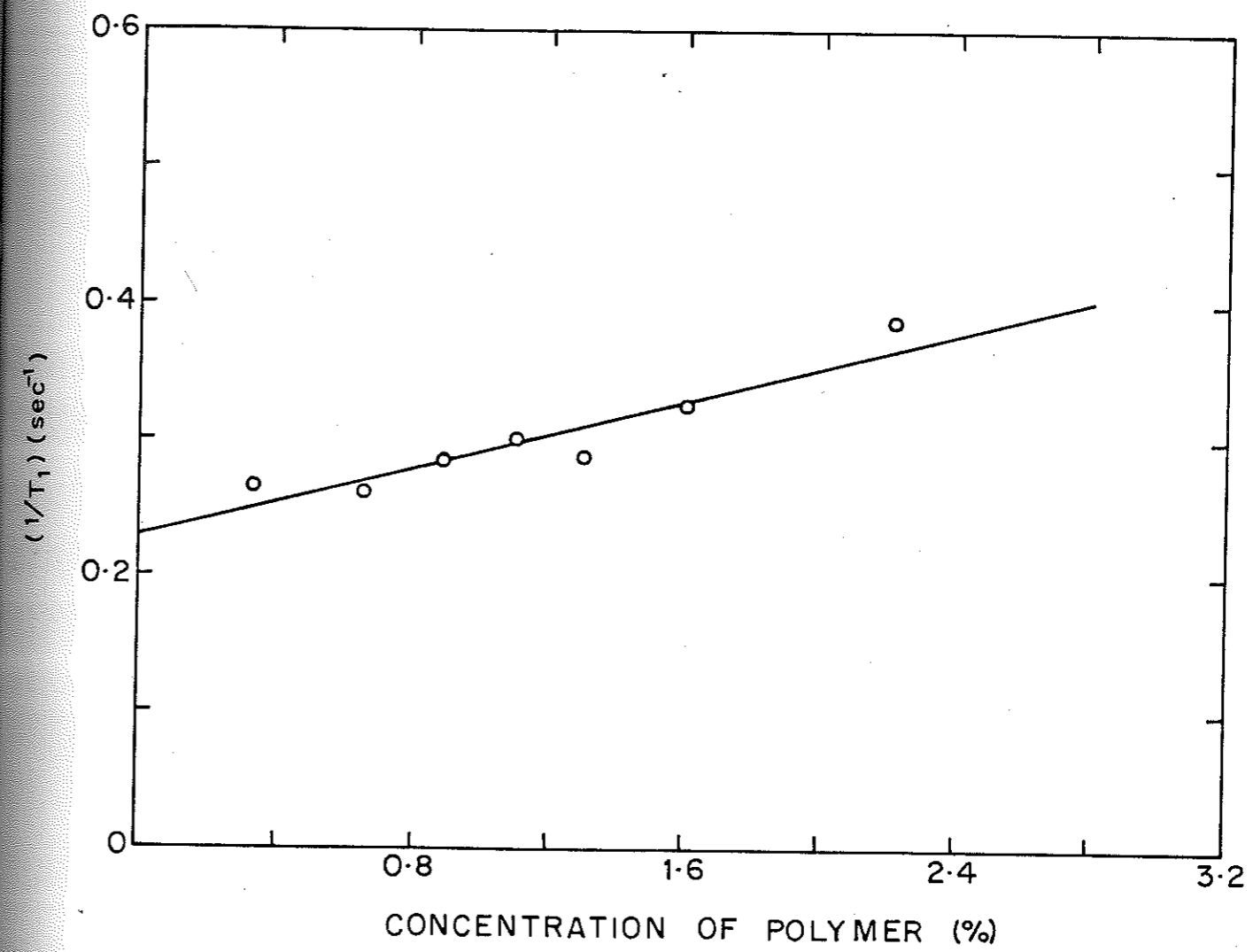


FIGURE 3.5 : CONCENTRATION DEPENDENCE OF RELAXATION RATE

We have determined T_1 of free water (by inversion recovery method) and bound water (by extrapolation of plot of $1/T_1$ against (%) saturation to zero water content (Fig. 3.6) to be equal to 4.0 and 1.0 seconds, respectively. Based on these results and with the help of above model, the hydration constant (h) was estimated to be 0.09 grams of bound water per gram of dry polymer, which corresponds to about 9% of bound water fraction.

CONCLUSIONS

Proton magnetic relaxation has been used to elucidate the state of water in superabsorbent polymers. The proton nuclear spin-lattice relaxation times (T_1) were measured as a function of polymer concentration by using standard pulse sequences. The results of the experiments are interpreted by using a simple exchange model which reveals the existence of two states of water, namely bound and free. Based on the analysis of the model, about 90% of the total water seemed to be present as free water and the remaining as bound water.

The NMR studies reported above are significant in that they show that even when the percentage saturation is 50% or more, most of the water present in the superabsorbent polymer is 'free' and therefore can be released to the surrounding media, as is required when such polymers are used as soil conditioners.

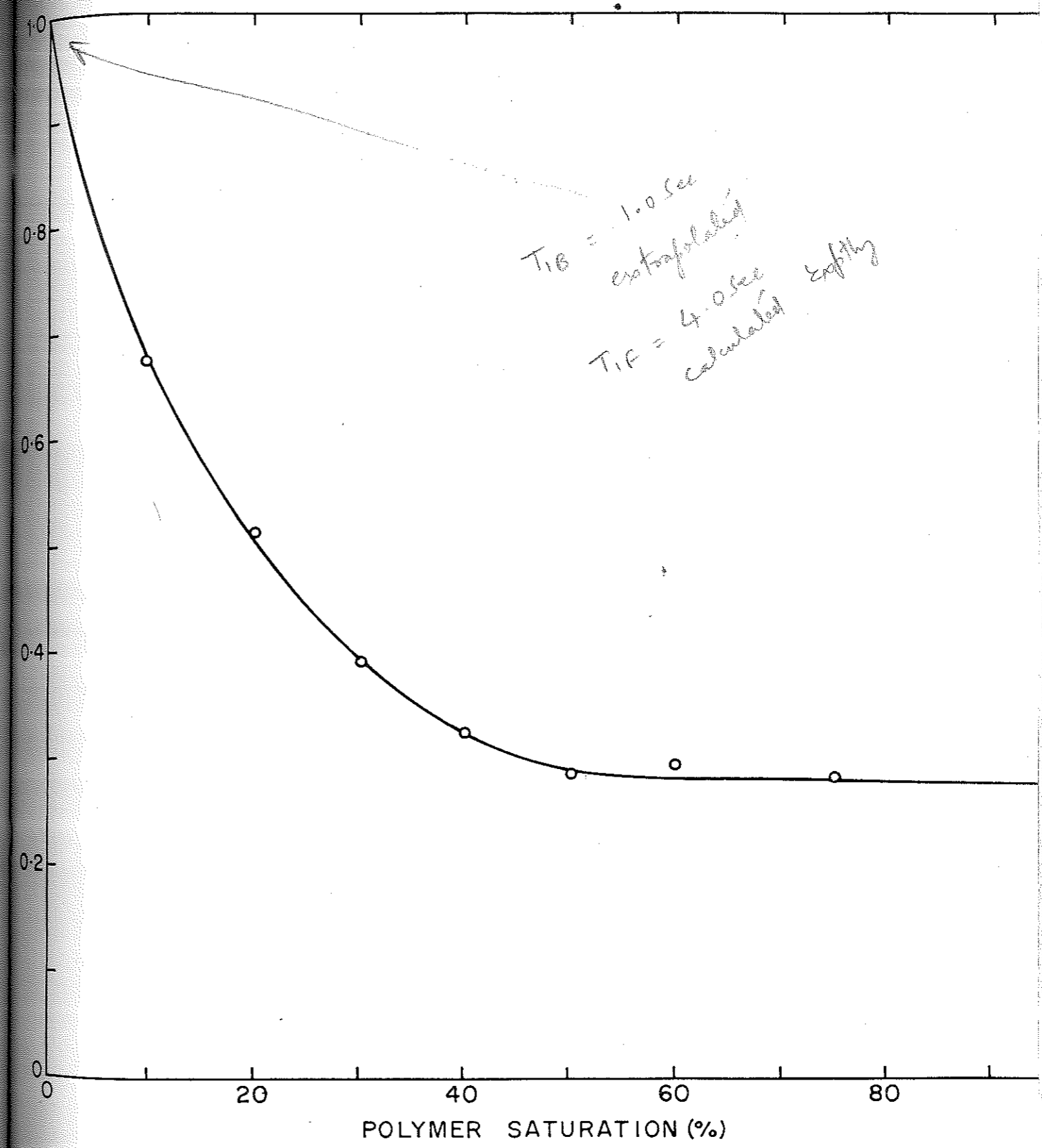


FIGURE 3.6: SATURATION DEPENDENCE OF RELAXATION RATE

High Resolution Solid-State Proton Magic Angle Sample Spinning (MASS) NMR of Superabsorbent Polymers

Introduction

In this part of the chapter, the high resolution solid-state proton NMR spectra of superabsorbent polymer such as hydrolysed starch-g-poly(acrylonitrile) has been investigated using the Magic Angle Sample spinning techniques.

difficult

Polymeric solids are difficult to characterize by conventional proton magnetic resonance owing to the inherently large spectral line broadening, which arises from static dipole-dipole interaction among the abundant proton spins (17,18). As an example, the static proton spectrum of dry hydrolysed starch-g-poly(acrylonitrile) superabsorbent polymer is shown in Fig. 3.7A. The proton spectrum is a featureless broad line with a linewidth of approximately 28 kHz. This severe line broadening is so large that it obscures fine spectral features such as the proton chemical shifts and coupling constants and renders the study of polymeric solids difficult.

Macromolecular mobility can cause a motional averaging of static proton dipolar interactions and reduce the observed proton spectral line width (19,20,21). The extent of proton line narrowing, however, depends on the exact nature of the polymer mobility. Unless the polymer motions are isotropic, or nearly so, the dipolar couplings cannot be averaged to zero, and therefore, fine resolution of

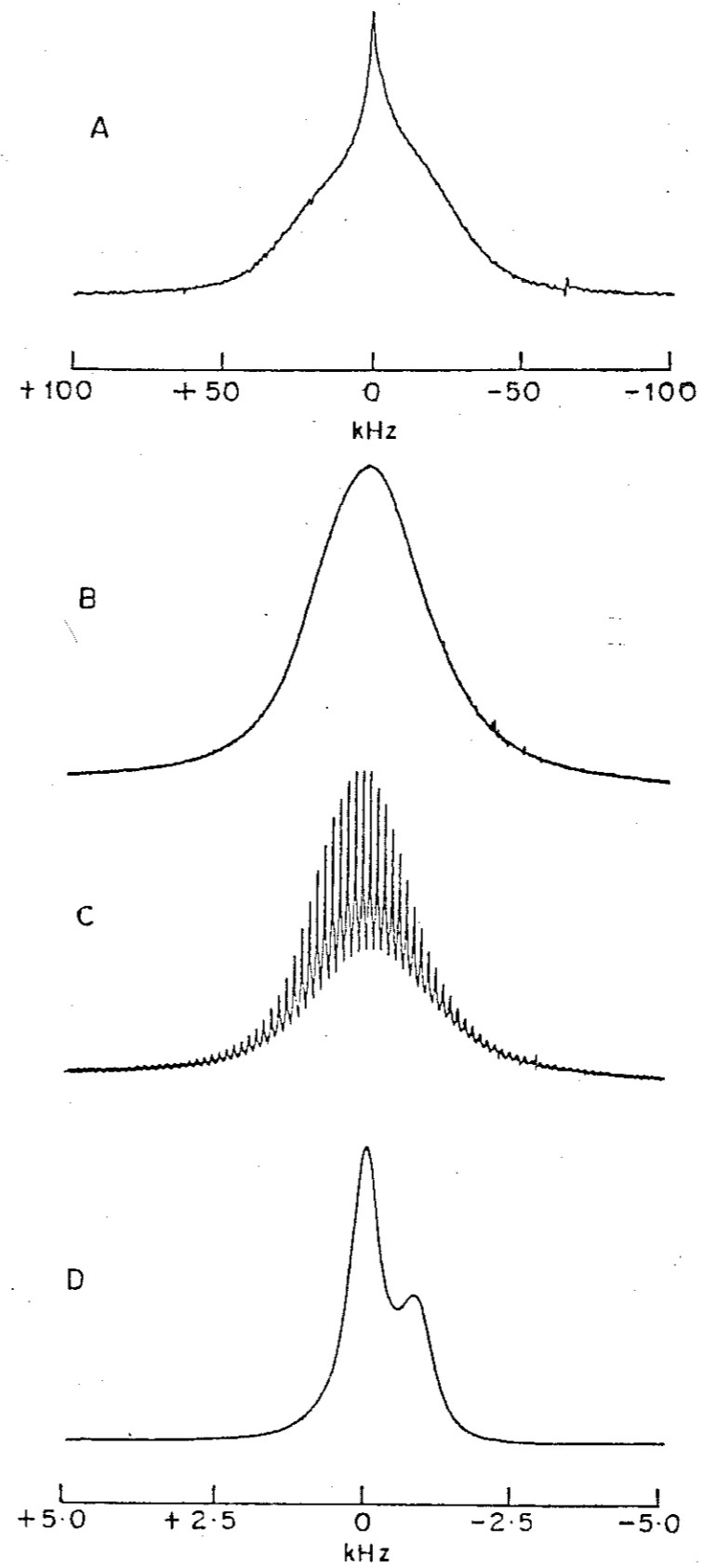


FIGURE 3.7 STATIC PROTON NMR SPECTRA OF HYDROLYSED STARCH-G-POLY(ACRYLONITRILE)
(A) DRY POWDER (B) 0.2% SATURATION (C) SPIN-ECHO SPECTRUM (D) 1.0% SATURATION

polymer structure cannot be revealed. In fact the spectrum of Fig. 3.7A already exhibits some motional averaging at room temperature due to restricted mobility. Here the observed line width is nearly half as compared to a rigid lattice line width for a perfectly rigid polymer. It is well known that the addition of a solvent or plasticizer to a polymer enhances the polymer mobility (22,23). The details of the chain dynamics depend on the specific nature and extent of polymer-solvent interactions and this in essence determines the observed residual proton spectral line width. In case of cross-linked polymers, the degree of cross-linking determines the equilibrium swelling capacity of the polymer in suitable solvents. The extent of chain mobility depends upon the degree of cross-linking and type of the solvent used. This has been shown to cause proton line narrowing in polystyrene-divinyl benzene polymer (24).

EXPERIMENTAL

The details of the superabsorbent polymer used are given in part-I. All the samples for NMR measurements were prepared by adding required amounts of dry polymer to the known volume of D_2O [99.6(%) isotopic purity, obtained from Bhabha Atomic Research Centre at Bombay] for a given percentage saturation. The samples were allowed to homogenize for 3-4 days in sealed vials before transferring them to the MASS rotor.

The experiments were carried out on a BRUKER MSL-300 supercon NMR spectrometer operating at 7.1 Tesla. The proton frequency was 300.13 MHz. The MASS probe was used which gave negligible proton background signal. The probe temperature was 21°C. The proton MASS spectrum was obtained following a single $\pi/2$ pulse. Quadrature phase cycling was used to minimise art facts. Sample dependent recycle times were chosen (2-6 seconds) and MASS speed was varied from 600 Hz to 2.5 kHz.

RESULTS AND DISCUSSIONS

In this superabsorbent polymer, even at a very low concentration of water (0.2% saturation), the polymer proton spectrum at room temperature is quite narrow and exhibits a near Super-Lorentzian line shape (25) due to extensive motional averaging of static proton dipolar interactions. This is shown in Fig. 3.7B, where the residual line width is only 2.1 kHz and can be further narrowed by Magic Angle Sample Spinning (MASS) technique. It is shown in Fig. 3.8 ^{that} the corresponding ^1H MASS spectrum of the polymer gel where the 2.1 kHz line broadening of the static sample has been removed by MASS : gives very high resolution proton NMR spectrum. With this MASS spectral resolution it is possible to resolve the chemical shifts from the different chemical functional groups in the polymer. It may be noticed that on MASS the static spectrum (Fig. 3.7B) breaks into number of center bands,

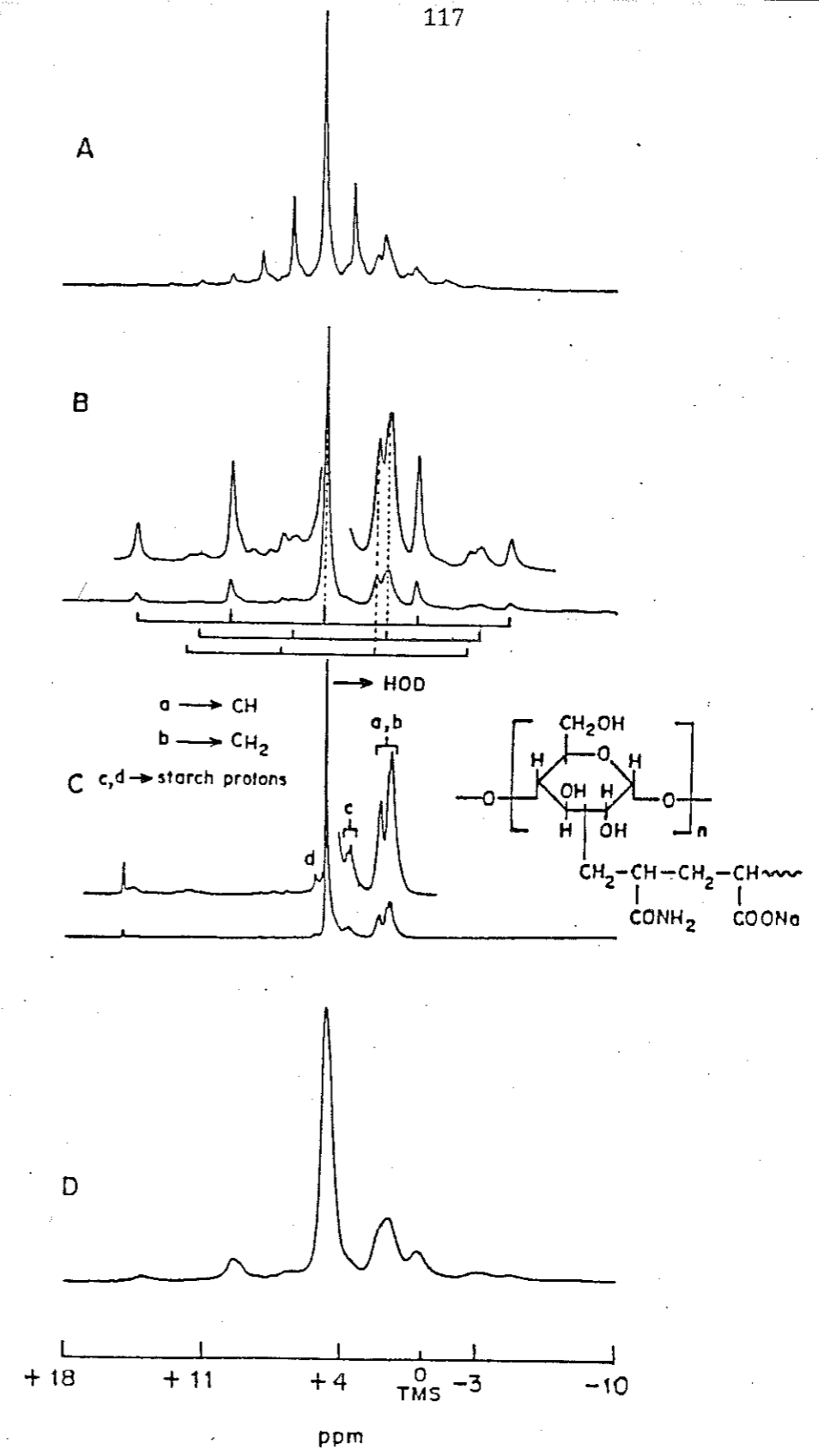


FIGURE 3-8 ¹H MASS SPECTRA OF HYDROLYSED STARCH-G-POLY(ACRYLONITRILE)
 0.2% SATURATION SAMPLE SPINNING AT
 (A) 450 Hz (B) 1.5 kHz (C) 2.0% SATURATION
 SPINNING AT 3.1 kHz (D) SAME AS (B) BUT OFF ANGLE

as well as intense side bands, the envelope of which maps the static proton line shape. The side band pattern is especially very much pronounced at slow spinning speeds (Fig. 3.8A). By comparing MASS spectra taken at different spinning speeds the center bands were identified. The assignments are shown for the different protons in the polymer (see Fig. 3.8).

The success of MASS to yield high resolution proton spectrum in our superabsorbent polymer can be traced to the fact that the proton-proton spin interaction can become inhomogeneous in character (26) and can therefore be further narrowed by MASS at moderately available spinning speeds (2-4 kHz). Inhomogeneous spin-spin interactions can be refocussed in a spin-echo experiment [e.g., CP-MG: $(\pi/2)_x - \tau - (\pi)_y - \tau - \text{Echo}$] pulse sequence [27]. Here the successive application of pulse will refocuss the proton magnetisation repeatedly until the spin-echo has decayed to zero by spin-spin relaxation time (T_2). The Fourier transform of such an echo train gives rise to a spectrum in which the powder pattern of the anisotropic spin interaction is split into a number of peaks separated by the reciprocal of the pulse spacing in the sequence (28,29). Figure 3.7C is a FT-spin-echo spectrum of the 0.2% saturated gel which shows the above effect. The inhomogeneous nature of the proton line broadening in our superabsorbent polymer is demonstrated in this spectrum by the presence of many narrow peaks which, in

a way, map the static proton line shape of Fig. 3.7(B). It may be noted that the maximum external averaging by mechanical rotation of the sample can be accomplished only at the 'magic angle' (30) (spinning axis at 54.7° with respect to B). This is demonstrated in Fig. 3.8D, where a slight missetting of the 'magic angle' leads to loss of resolution of polymer signals and to the broadening of the spinning side bands.

It is also found that in these superabsorbent polymers, the observed spectral breadths of static proton spectra and the final resolution obtainable by mechanical spinning at the magic angle depends strongly on the polymer to solvent (water in this case) ratio. As an example we show in Fig. 3.7D the static proton spectrum of a polymer with 1% saturation. Here the improved separation of the spectral bands corresponding to residual HOD and aliphatic protons is seen. Similarly, ^1H MASS spectrum shows improved chemical shift resolution with an increase in percentage saturation, an example of which is shown in Fig. 3.8C for a polymer with 2% saturation. It appears that at very low concentration of water there is a homogeneous broadening as well, in which case it is likely that it will be necessary to combine MASS with homonuclear multiple pulse techniques (31) for optimum line narrowing. However, addition of more water to the polymer causes an extensive increase in polymer chain mobility and results in increased resolution to be obtained in the final MASS

spectrum.

CONCLUSION

It is shown that in superabsorbent polymeric systems it is possible to obtain a very high resolution proton spectra by MASS technique. Since the polymer proton signals can be resolved, it is possible to undertake studies where specific polymer sites can be probed for obtaining structural and dynamical information. Such studies^{are} facilitated by the extremely high sensitivity of ^1H nucleus. The chemical shift resolution can be increased by operation at high magnetic fields. Since the proton dipolar interactions in these polymeric systems are field independent, the side bands can be eliminated by employing high spinning speeds or side-band suppression techniques (32).

Effect of Cross-Linking on Carbon-13 NMR of Superabsorbent Polymer

Introduction

The property of superabsorption largely depends on the degree of cross-linking present in the structure. This degree of cross-linking can be estimated by measuring the line width at half height of carbon-13 signals in the NMR spectroscopy (33). The degree of cross-linking affects the chain mobility, which in turn reflects on relaxation processes (short relaxation times with restricted mobility) and line width. Various cross-linked polymers have been examined in terms of their structural and

dynamical properties (34). For example, the carbon-13 NMR study of covalently cross-linked gels such as PHEMA, PMMA and poly(vinyl pyrrolidone) indicated that the large line width obtained is due to restricted chain mobility as a result of high degree of cross-linking. Similarly, Ford and Balkrishnan (22) have reported the carbon-13 signal line widths, spin-lattice relaxation times (T_1) and NOE (Nuclear Overhauser Effect) of cross-linked polystyrene-divinylbenzene gels swollen in $CDCl_3$. In the solid-state NMR, the combination of cross-polarization (CP) and Magic angle sample spinning (MASS) with the high power proton decoupling has provided a great deal of carbon-13 NMR information about solid cross-linked polymers such as epoxy, phenolics and polyimides (35, 37, 38).

The carbon-13 NMR spectra of poly(acrylamido-2-methyl propane sulfonate) [PAMPS] superabsorbent polymers with various degrees of cross-linking are reported. Carbon-13 spectra were obtained both on the dry state and swollen state. It was found that spectral changes with changes in cross-link density could be monitored.

EXPERIMENTAL

The synthesis of poly(acrylamido-2-methyl propane sulfonate) superabsorbent polymers with various degrees of cross-linking has been reported in Chapter-II. These polymers were isolated in the form of dry powder and had the equilibrium water absorption capacities of 50-400 g/g depending on the degree of cross-linking.

The proton decoupled ^{13}C spectra were recorded for both dry and swollen samples on MSL-300 FT-NMR spectrometer at 25°C . The samples in the swollen state were prepared by adding the required amount of dry polymer to the known volume of deionized and distilled water. The swollen samples were allowed to homogenize for 3-4 days in sealed vials before transferring them to the probe. The samples were spun at about 1.5-2.0 kHz in a dual-bearing magic angle sample spinning probe. All the spectra were recorded by giving 1 second delay between pulses with acquisition time of 0.082 seconds. About 2000 scans were collected in order to get good signal to noise ratio. All the chemical shifts reported are relative to external tetramethyl silane (TMS).

RESULTS AND DISCUSSION

The carbon-13 spectra of samples with different degrees of cross-linking are shown in Fig. 3.9 and the corresponding assignments of the peaks are summarized in Table-3.2 and Fig. 3.10. The backbone carbon atoms in the polymer chain are directly attached to the cross-linking monomer and give signals in the range of 39-50 ppm. It can be observed from the figure that as the degree of cross-linking increases, the signals lose the resolution and become broader. This broadening may be attributed to the restricted mobility of the chains which are held by cross-linking monomer. This decrease in mobility gives rise to shorter relaxation times and broader lines.

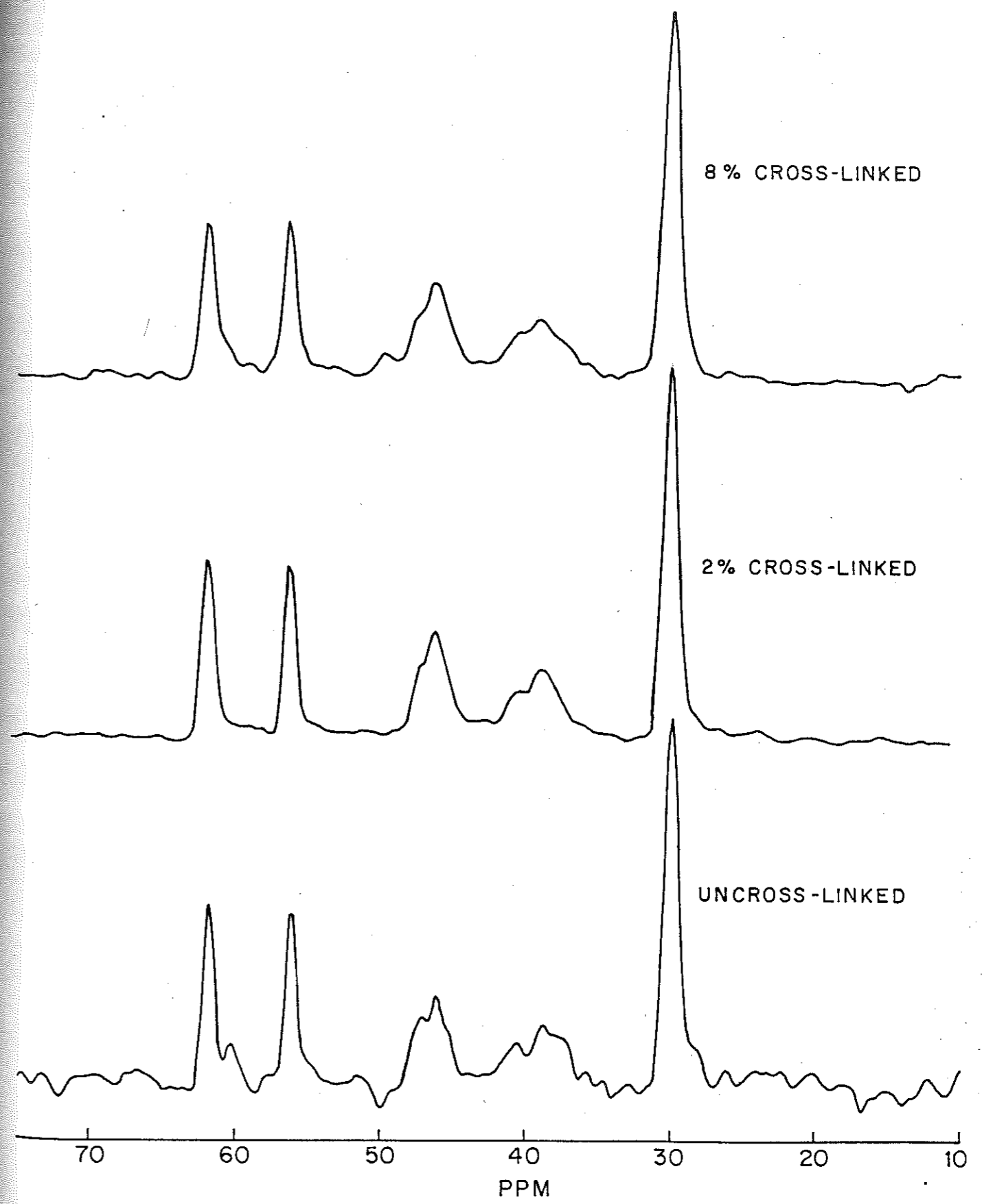


FIGURE 3-9: ^{13}C SPECTRA OF PAMPS POLYMER

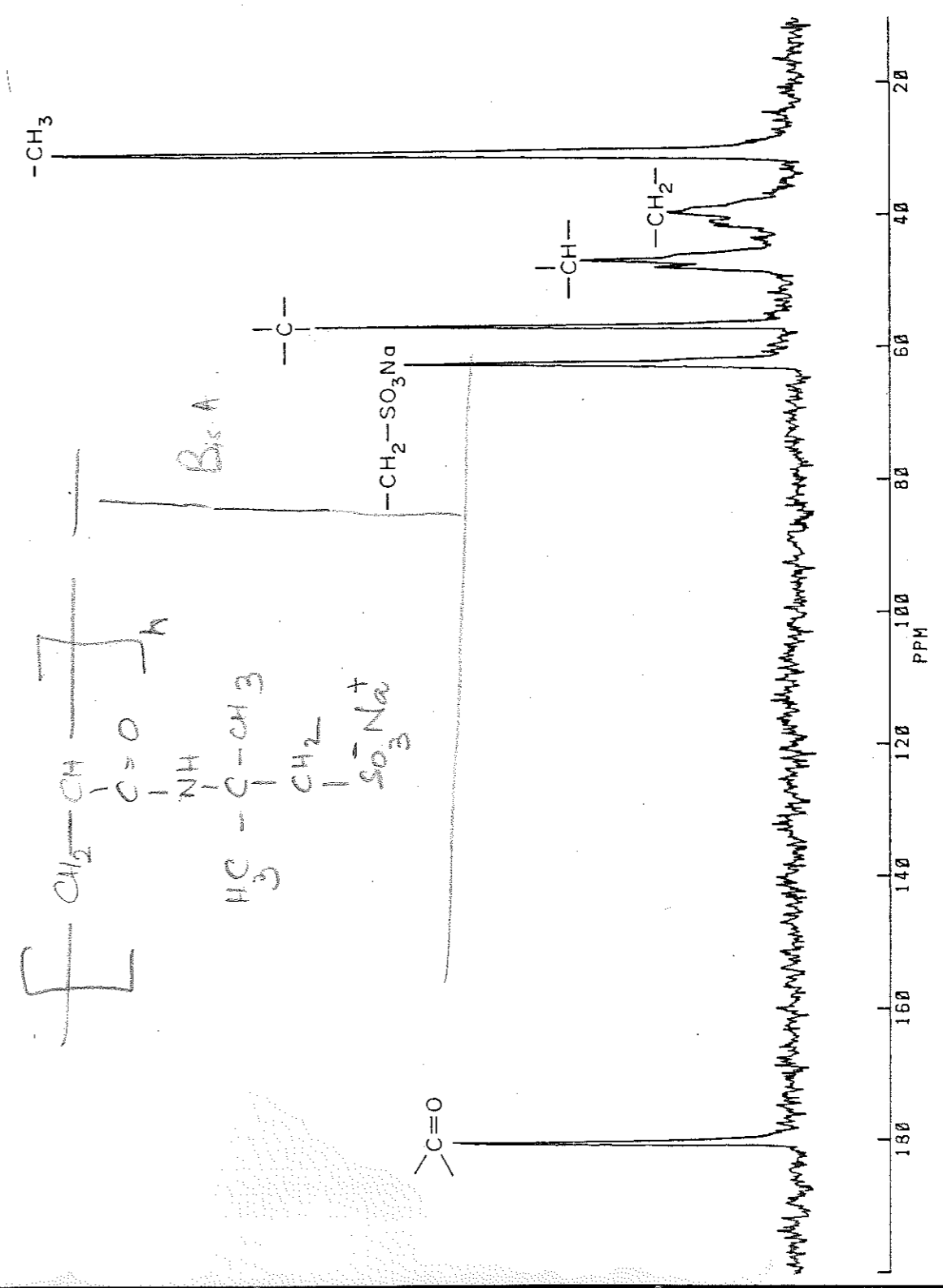


FIGURE 3.10: ¹³C SPECTRUM OF PAMPS SUPERABSORBENT POLYMER

The line broadening of the carbon signals varies depending on their positions in the chain relative to the cross-links. In the past it is reported that the line broadening also depends on the amount of diluent present in the polymer. Therefore in order to remove this ambiguity, the polymer to solvent ratio is maintained constant carefully. It is to be noted that in the PAMPS system studied here, even at the lowest cross-link density employed, the polymer mobility is such as to yield very narrow carbon-13 signals. Therefore, the changes in carbon-13 signal line widths are not spectacular as one might otherwise expect.

REFERENCES

1. Tanaka T., Encyclo. of Polym. Sci. and Engineering, 7, 514 (1987).
See also, Marro A. and Muller I., Rheol. Acta, 27, 44 (1988).
2. Tanaka T. and Fillmore D.J., JI. of Chem. Phys. 70, 1214 (1979).
3. Amiya T. and Tanaka T., Macromolecules, 20, 1162, (1987).
4. Ernst R.R. and Anderson W.A., Rev. Sci. Instrum. 37, 93 (1966).
5. Hazelwood, C.F., Chang E.C., Nichols B.L. and Woessner D.E. Biophysics, 14, 583 (1974).
6. Edzes H.T. and Samulski E.T., JI. of Magn. Resonance, 31, 207 (1978).
7. Escanye J.M., Canet D. and Robert J., JI. of Magn. Resonance, 58, 118 (1984).
8. Wise W.B. and Pfeffer P.E. Macromolecules, 20, 1553 (1987).
9. Hechter O., Wittstruck T., Mc Niven N. and Lester G., Proc. Natl. Acad. Sci. (USA) 46, 783 (1960).
10. Woessner D.E. and Snowden Jr., B.S., JI. of Colloid. Int. Sci. 34, 290 (1970).
11. Sterling C. and Masuzawa M., Makromol. Chem. 116, 140 (1968).
12. Katayama S., Arata Y. and Fujiwara S., Bull. of Chem. Soc. of Japan, 51(5), 1545 (1978).
13. Maquet J., Theveneau M., Djabourov M., Leblond J. and Papon P., Polymer 27, 1103 (1988).

.....

14. Zimmerman J.R. and Brittin W.E., *Jl. of Phys. Chem.* 61, 1328 (1957).
15. Carr H.Y. and Purcell E.M., *Phys. Rev.* 94, 630, (1954).
16. Ref. (13).
17. Abragam A., 'The Principles of Nuclear Magnetism', Clarendon Press, Oxford 98 (1961).
18. McBrierty V.J., *Polymer*, 15, 503 (1974).
19. Mc Gall D.W., *Acc. Chem. Res.* 4, 223 (1971).
20. Ref. (17) page 424.
21. Ganapathy S., Chacko V.P. and Bryant R.G., *Macromolecules*, 19, 1021 (1986).
22. Ford W.T. and Balkrishnan T., *Macromolecules*, 14, 284 (1981).
23. Blum F.D., Dickson J.E. and Muller W.G., *Jl. of Polym. Sci. Polym. Phys. Ed.* 22, 211 (1984).
24. Bahneider D., Doskocilova D. and Dybal J., *Polymer*, 26, 253 (1985).
25. Bloom M., Burnell E.E., Mackay A.L., Nichol C.P., Valic M.I. and Weeks G., *Biochem.* 17, 5750 (1978).
26. Forbes J., Husted C. and Oldfield E., *Jl. of Am. Chem. Soc.* 110, 1059 (1988).
27. Meiboom S. and Gill D., *Rev. Sci. Instrum.* 29, 6881 (1958).
28. Garroway A.N., *Jl. of Magn. Resonance*, 66, 558 (1986).

.....

29. Zilm K.W., Abstracts of FACS, 12th Ann. Meeting Philadelphia, Sept. 29 - Oct. 4, 135 (1985).
30. Andrew E.R., Progress in NMR Spectroscopy, 8, 1, (1972).
31. Waugh J.S., Huber L.M. and Haeberlen U., Phys. Rev. Lett. 20, 180 (1968).
32. Dixon W.T., JI. of Magn. Resonance, 44, 220 (1981).
33. Gutowsky H.S., Saika A., Takeda M. and Woessner D.E. JI. of Chem. Phys. 27, 534 (1957)
34. Harrison D.J.P., Yates W.R. and Johnson J.F. JI. of Macromol Sci. - Rev. Macromol Chem. Phys. C25(4), 481 (1985)
35. Yokoto K., Abe A., Hosaka S., Sakai I. and Saito, H., Macromolecules, 11, 95 (1978).

36. Garroway A.N., Ritchey W.M. and Moniz W.B., Macromolecules, 15, 1051 (1982).
37. Fyfe C.A., Mc Kinnon M.S., Rudin A. and Tchir W.J., Macromolecules, 16, 1216 (1983).
38. Maciel G.E., Chuang I. and Myers G.E., Macromolecules, 15, 1218 (1982).

NOTATION

B_0 magnetic field

C concentration of the polymer

h hydration constant

P_F population of free water

P_B population of bound water

ν radio frequency

T_{1F} spin lattice relaxation time of free water

T_{1B} spin lattice relaxation time of bound water

T_1 spin lattice relaxation time

T_2 spin - spin relaxation time

ω frequency

τ time between two pulses

TABLE-3.1

Spin-lattice relaxation time (T_1) of hydrolysed starch-g-poly(acrylonitrile) superabsorbent polymer at different percentage-saturation of water

Polymer Concentration in water (%)	% Saturation	Spin-lattice relaxation time (T_1) (seconds)
6.2	10.0	1.49
3.3	20.0	1.95
2.2	30.0	2.55
1.6	40.0	3.06
1.3	50.0	3.52
1.1	60.0	3.34
0.88	75.0	3.46
0.66	100.0	3.86
0.33	200.0	3.75

TABLE-3.2

Carbon-13 chemical shifts (relative to TMS) of
poly(acrylamido-2-methyl propane sulfonate) [PAMPS]
superabsorbent polymer swollen in water

Samples	Chemical shifts (ppm)					
	C = O	-CH ₂ -SO ₃ Na	-C-	-CH	-CH ₂ -	-CH ₃
Uncross-linked	180.1	62.6	56.6	46.9	39.6	30.8
2(%) cross-linked*	179.6	62.0	56.4	46.9	40.2	30.2
8(%) cross-linked	180.2	62.5	56.8	46.9	39.7	30.8

* Cross-linked with N-N-methylene bis-acrylamide on the basis of weight of the monomer

CHAPTER-IV

DEFORMATION DEPENDENT SUPERABSORPTION AND
PHASE TRANSITION IN SUPERABSORBENT POLYMERS

Introduction

We have described in the previous chapters the superabsorption phenomenon in gels. In the classical theory of swelling proposed by Flory (1), the free energy of gels at equilibrium swelling can be related to osmotic pressure, which arises due to the imbalance of forces such as elasticity of the network, polymer-polymer, polymer-solvent interactions and counter-ion pressure. The magnitude of these forces depends upon various factors such as nature and degree of cross-linking, temperature, composition and ionic strength of the solvent in which the gel is swelling.

Recently, Tanaka and coworkers (2) have investigated such gels by laser light scattering studies and explained the responses of the gel to the external environment in terms of phase transitions and critical phenomena. Since then significant contributions have been made by many workers in the areas such as thermodynamics of swelling (3,4), kinetics of swelling (5,6), phase transitions (7,8,9), chain dynamics of network structures through NMR (10,11) and macromolecular separations by gels (12,13).

In this chapter, we demonstrate an interesting observation, 'deformation dependent superabsorption and phase transitions'. The superabsorbent polymers consisting of three dimensional network, when subjected to deformation (i.e. mechanical stress) undergoes a structural change

reflecting on the superabsorption characteristics. The results of this finding have been explained on the basis of the permanent and semipermanent cross-links in the network structure. The absorption and retention capacities of superabsorbent polymers is a very strong function of degree of cross-linking (14), which contributes to the elasticity of the network. As we have discussed in the foregoing, cross-linking can be induced chemically by covalent bonds using certain bifunctional monomers as cross-linking agents or in some cases networks are formed by physical cross-linking by weak forces such as hydrogen bonds, van-der-Waal's forces, ionic interactions and entanglement of chains (15,16).

We postulate that the physical cross-linking, which is of a semi-permanent nature, can be altered by subjecting the swollen superabsorbent polymer to a certain stress. This physical cross-linking should contribute to the elasticity of the network and therefore to the elastic retractive force. Due to a decrease in the extent of physical cross-linking, the absorption and retention capacity of the swollen network should be increased. We have undertaken experiments to study the possible increase in superabsorption due to a decrease in degree of cross-linking. Measurements have been performed on hydrolysed starch-g-polyacrylonitrile (HSPAN), poly(2-acrylamido-2-methyl-propane sulfonate) (PAMPS) and hydrolysed polyacrylamide (HPAM) superabsorbent polymers. It was also observed from the above studies that the decrease in degree of cross-linking

is irreversible and there exists a permanent deformation of the structure. The concept of the permanent and semi-permanent cross-links proposed to explain deformation dependent superabsorption has been further corroborated by NMR and rheological measurements.

EXPERIMENTAL

The superabsorbent polymers such as hydrolysed starch-g-polyacrylonitrile, poly(2-acrylamido-2-methyl propane sulfonate) and hydrolysed polyacrylamide were synthesized in the laboratory and isolated in the form of a dry powder having 80 mesh particle size. These polymers had an equilibrium water absorption capacities of 178.0, 256.0 and 175.0 milligrams of water per gram of polymer, respectively.

Two types of experiments were carried out in order to study the effect of deformation due to low and high shear rates. In the first case, in-situ superabsorption under stress was studied at lower shear rates. The apparatus used to study in-situ superabsorption, consists of a jacketed sintered funnel which is connected to the measuring jar. The swollen superabsorbent polymer was sheared in the annular gap between the wall of the sintered funnel and the rotating spindle, which is attached to the coaxial cylinder fixture of viscometer (Rheotest-2) (Fig. 4.1). The temperature was maintained at 25°C by passing water through the jacket using a temperature con-

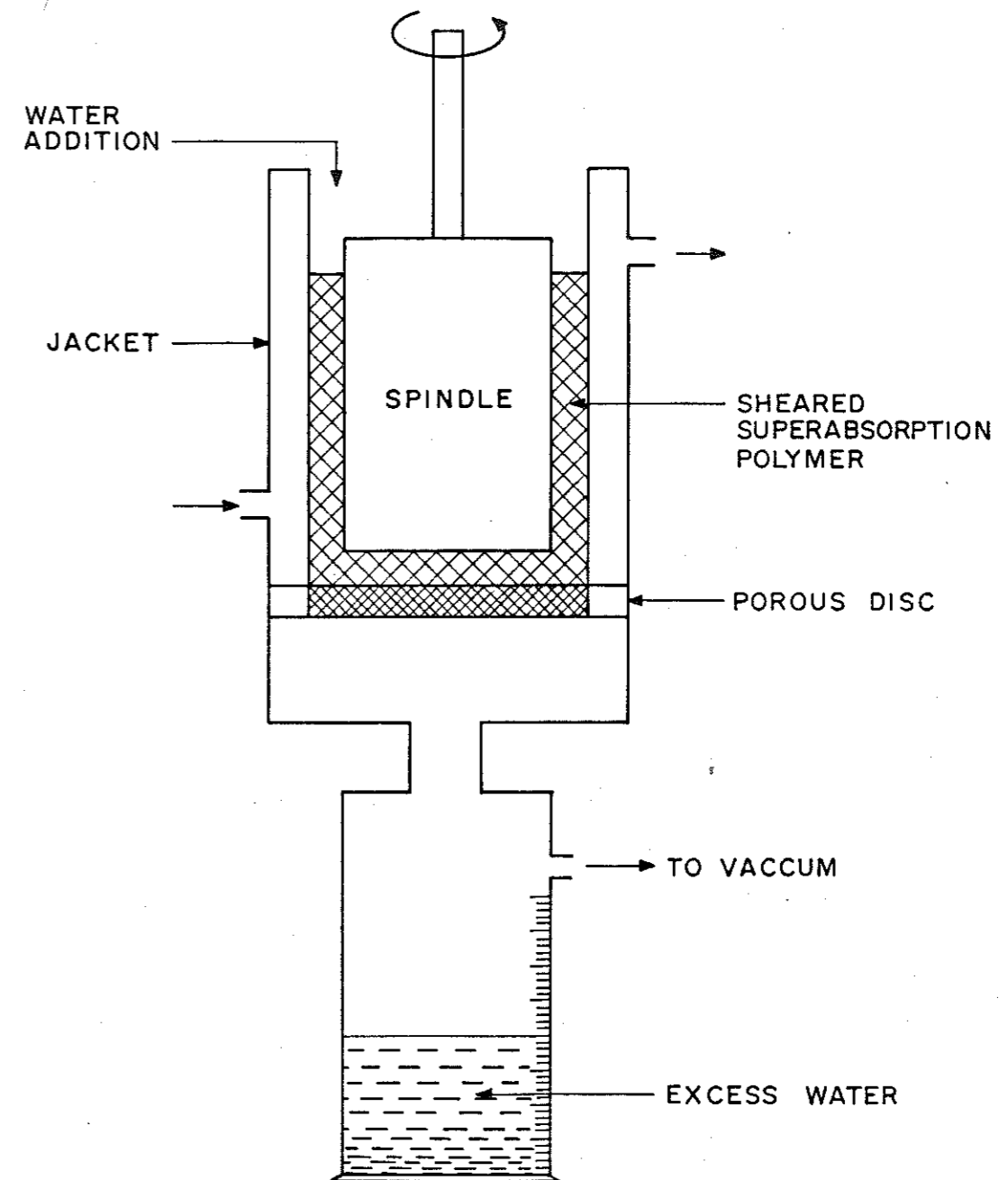


FIGURE 4.1 IN-SITU SUPERABSORPTION UNDER DEFORMATION - EXPERIMENTAL SET UP

trolled bath. The shear rate was varied by changing the speed (in RPM) of the spindle. However, it was not possible to assign any concrete value to the shear rate, since the gel was found to be slipping at the rotating surface and this slip velocity could not be defined quantitatively. During the process of shearing, water was continuously added and the excess water collected in the measuring jar under the application of slight vacuum. From the difference in the added and released water, the equilibrium absorption capacity with respect to time was calculated.

In another set of experiments the effect of very high shear rate applied in a high shear device on super-absorption was studied. The equilibrium swollen polymer was sheared in this high speed device at an approximate shear rate of 2800 sec^{-1} for different periods of time (0-5 minutes). Subsequently the samples were precipitated in ethanol and dried in oven at 60°C . After complete drying the samples were analysed for water absorption capacities.

RESULTS AND DISCUSSIONS

The results of our absorption measurements are summarized in Figs. 4.2, 4.3 and 4.4. It can be readily seen from Fig. 4.2 that the initial absorption capacity of hydrolysed starch-g-polyacrylonitrile has increased from 178 ml/g to 205, 215 and 248 ml/g with an increase in RPM (80 to 245). It is interesting to note that the new equilibrium value attained decreases slightly once

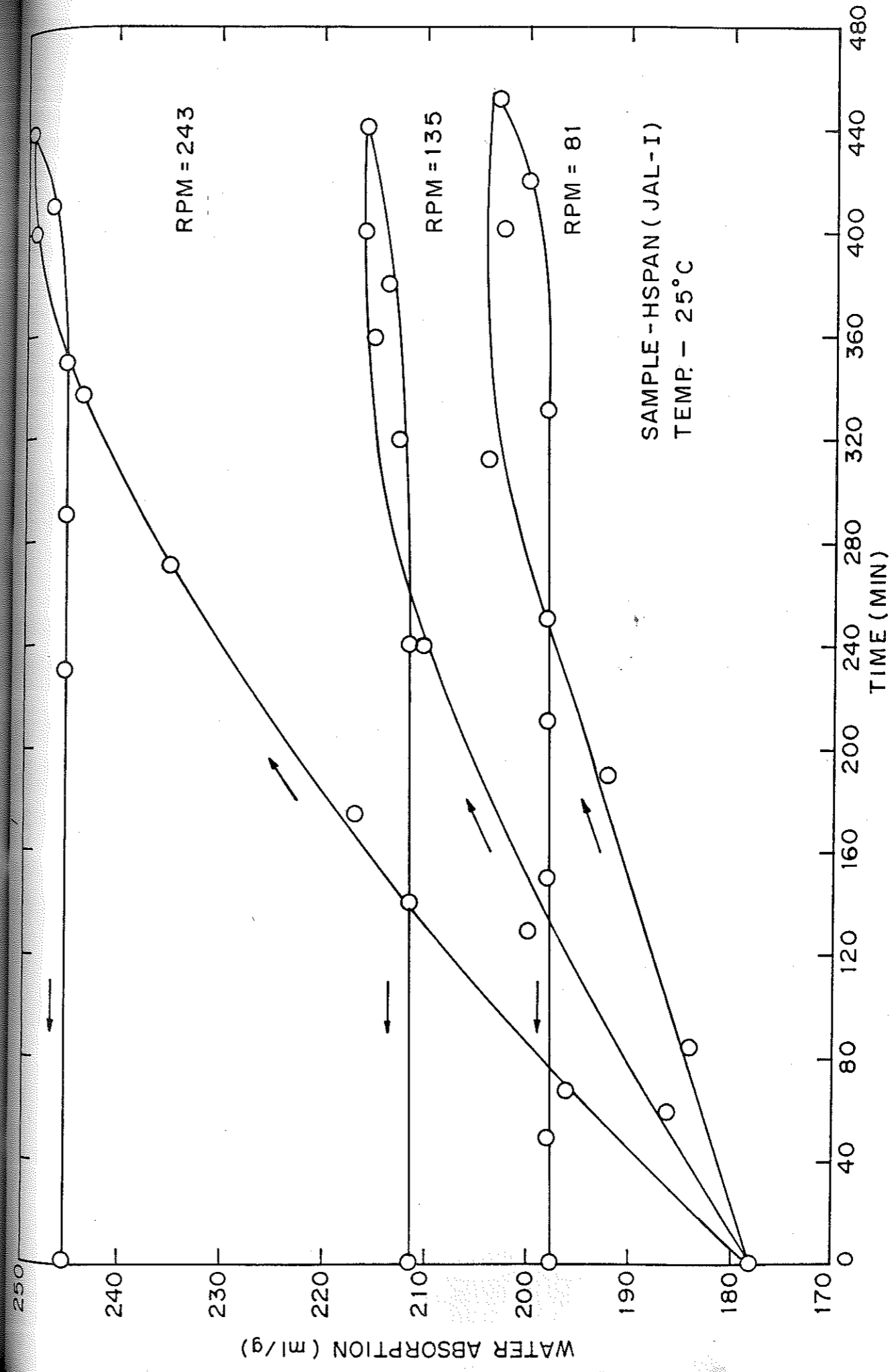


FIGURE 4.2: DEFORMATION DEPENDENT SUPERABSORPTION (IN - SITU METHOD)
HSPAN / WATER SYSTEM

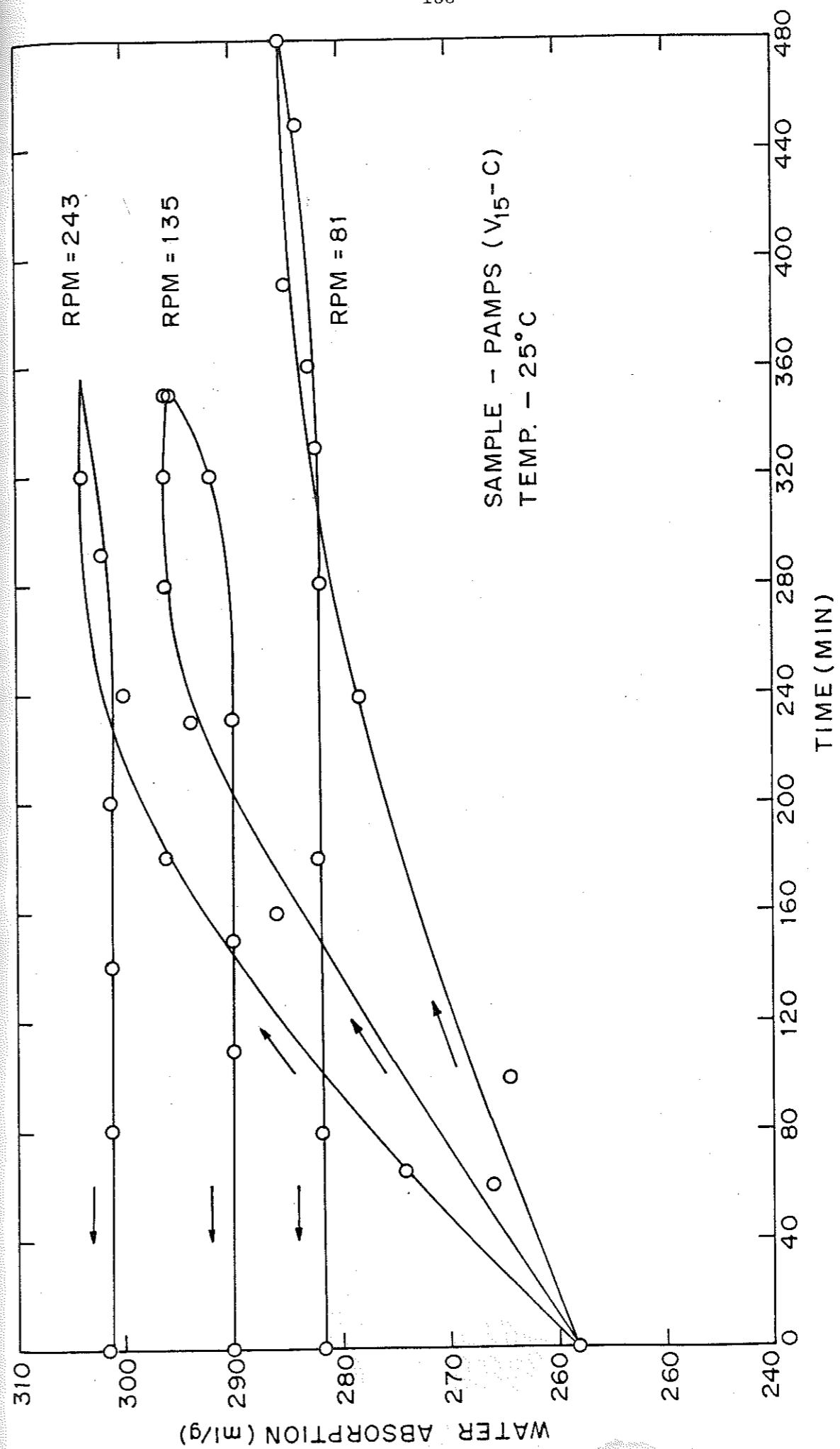


FIGURE 4-3: DEFORMATION DEPENDENT SUPERABSORPTION (IN-SITU METHOD) PAMPS/
WATER SYSTEM

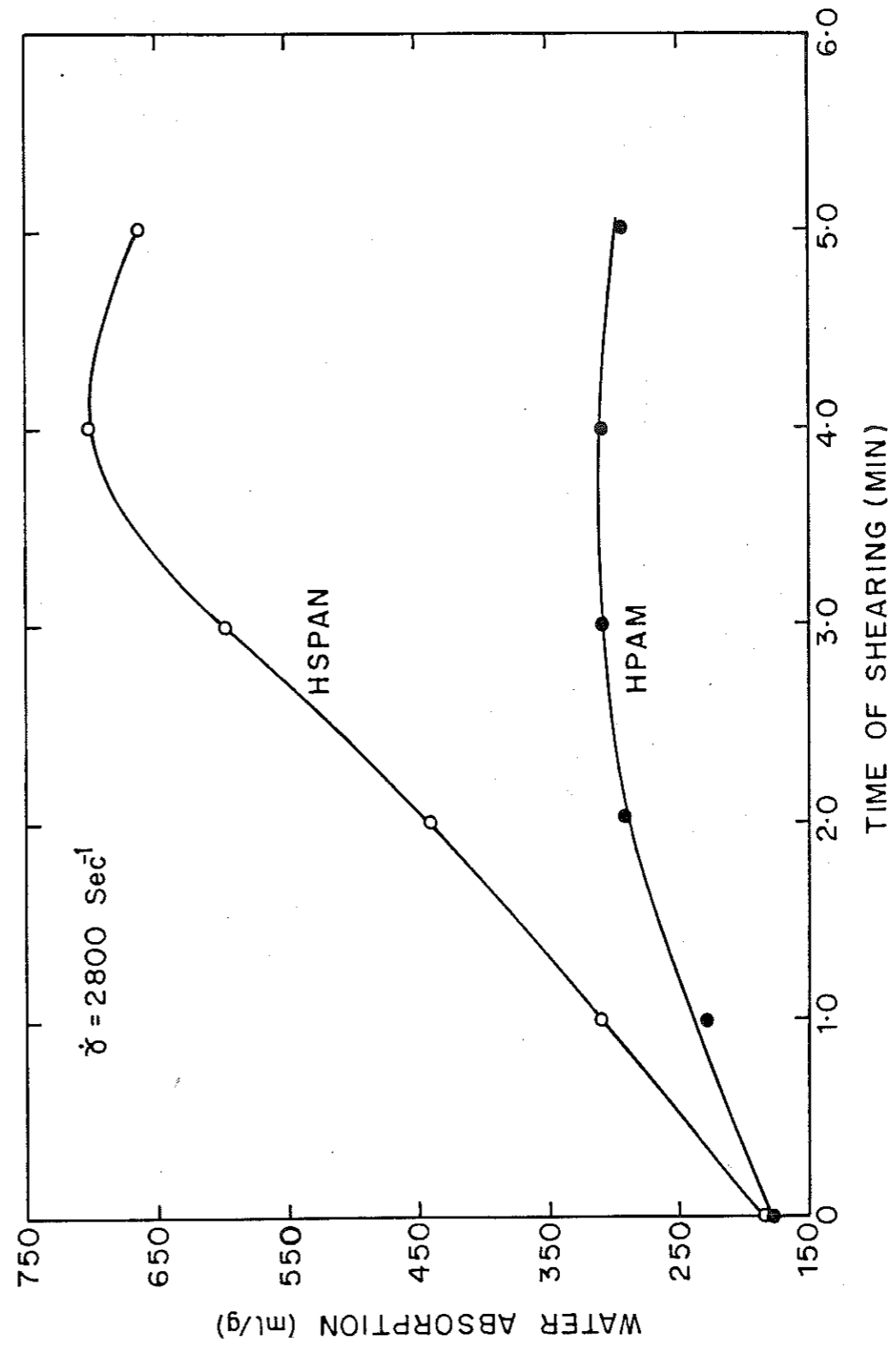


FIGURE 4.4 : DEFORMATION DEPENDENT SUPERABSORPTION IN HIGH SPEED DEVICE

the process of shearing stops. This clearly indicates the partial recovery of the structure. Similar observation was made for other superabsorbent polymer namely PAMPS (Fig. 4.3). However, the increase in superabsorption is less in this case as compared to HSPAN. This may be attributed to the fact that HSPAN is a graft copolymer with starch as a backbone and hydrolysed polyacrylonitrile as pendant chains which form entanglements in the structure and are more sensitive to shearing. It is observed from the results that, as the shear rate increases (increase in RPM) the equilibrium absorption capacity also increases. However, at very high shear rates (in high speed device) imposed for long time, there could be a total degradation of the network which will ultimately behave like a homogeneous solution.

The equilibrium swollen polymers (HSPAN and HPAM) were sheared in a high speed device for 0-5 minutes at an approximate shear rate of 2800 sec^{-1} . It can be seen from Fig. 4.4 that the initial absorption capacities of HSPAN and HPAM increased from 178.0 ml/g to 700.0 and 300.0 ml of water per gram of polymer respectively, when the samples were sheared for 4 minutes. After 4 minutes we observed a slight decrease in the absorption capacity and lower mechanical stability of these superabsorbent polymers.

We believe that the 2-4 fold enhancement in absorption capacity is due to the alteration of the weak secondary structures when deformation is imposed. It is impor-

tant to note that before examining the sheared samples for absorption capacities, they were precipitated in ethanol and dried in oven. In order to find the effect of solvent treatment on superabsorption, we subjected both the sheared and unsheared samples with identical treatment of precipitation and isolation. From the analysis we found that the absorption capacity of sheared and precipitated sample increased from 178.0 ml/g to 700.0 ml/g whereas in the case of unsheared and precipitated sample only marginal enhancement was observed.

NMR and Molecular Basis for Deformation Dependent Superabsorption

We have used Nuclear Magnetic Resonance (NMR) spectroscopy to provide an explanation for the deformation dependent superabsorption on a molecular basis. We believe that breakdown of the physical entanglements due to the application of shear force is reflected in the enhancement of macromolecular mobility of the chains. In a superabsorbent polymer, the addition of a solvent enhances the motion of the polymeric chains (17). NMR has been extensively used on polymeric gel systems and most of the attention has been focussed on relating the NMR spectral features to the degree of cross-linking and the type of the solvent used (18).

In these polymeric systems, the spectral line width shows a discontinuous transition as shown in Fig. 4.5

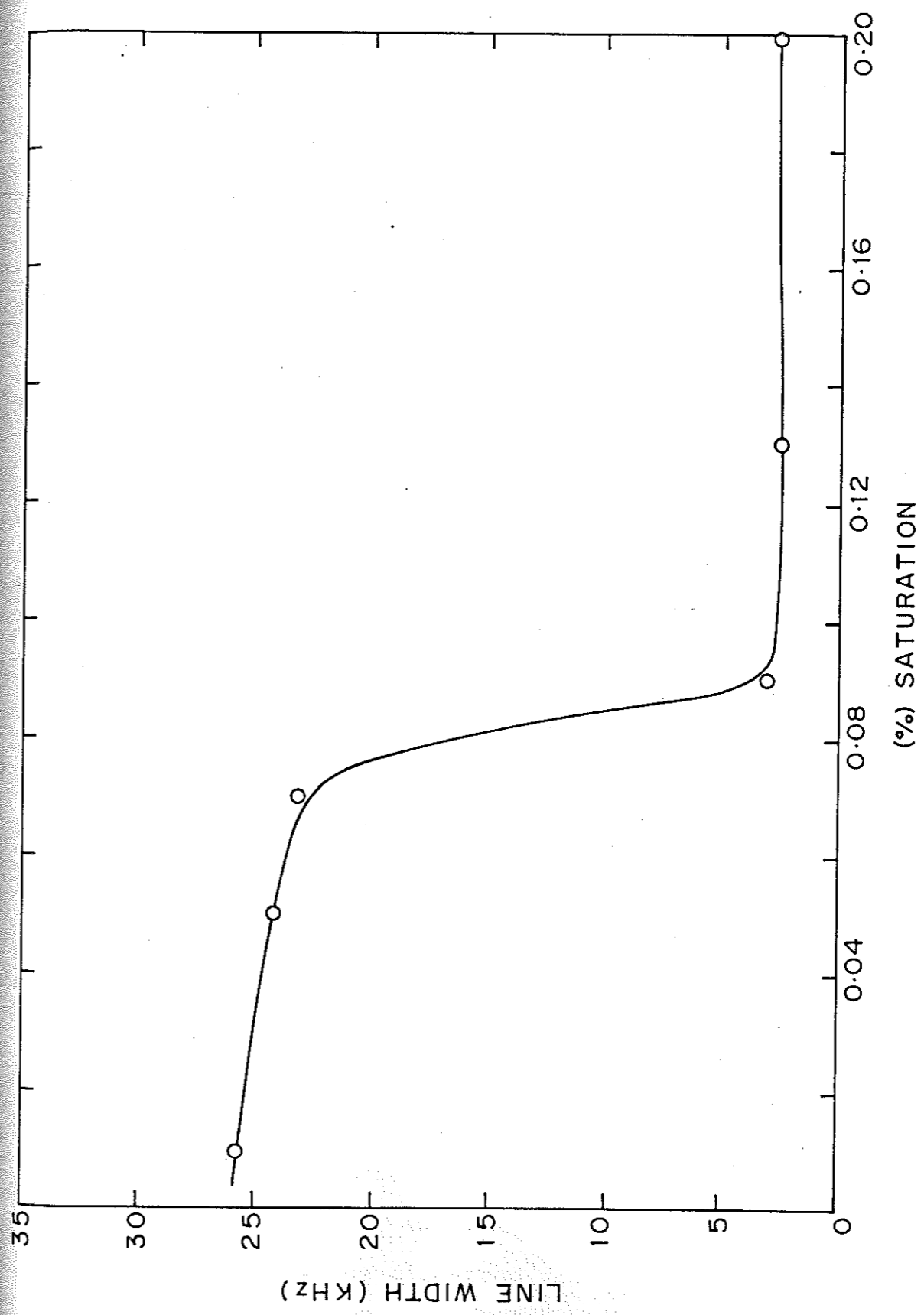


FIGURE 4.5 : LINE WIDTH TRANSITION WITH RESPECT TO (%) SATURATION

with respect to the degree of saturation. Typical fully relaxed state ^{13}C spectra, taken with dipolar decoupling are shown in Fig. 4.6. Even at 1% saturation the ^{13}C spectrum has a sufficiently high resolution emphasizing near-complete averaging of chemical shielding and carbon-proton dipolar interactions. The transition in line width due to solvent effected polymer mobility takes place in the range of 0.08 to 0.25% saturation. If one were operating in this regime, the changes in the chain dynamics due to deformation can be best seen in the NMR spectrum.

Figure 4.7 shows the dipolar decoupled ^{13}C spectra of an unsheared and sheared superabsorbent polymer. Here the (%) saturation was carefully chosen so that we are in the line width transition region as explained above. The spectrum for unsheared sample has overlapping ^{13}C resonances from the carbonyl, glucose and aliphatic regions. Upon shearing, the spectrum shows narrowing of the peak, especially in the low field region (see Figs. 4.7A and 4.7B). In these spectra, since the carbon-proton dipolar coupling is removed by dipolar decoupling, the observed narrowing of the line comes from a better averaging of the chemical shielding anisotropy (CSA), which is expected to be more pronounced for the carbonyl and amide carbons. This is in fact observed. It may be noted that no differences can be discerned from the carbon-13 spectrum obtained for unsheared and sheared samples having a high

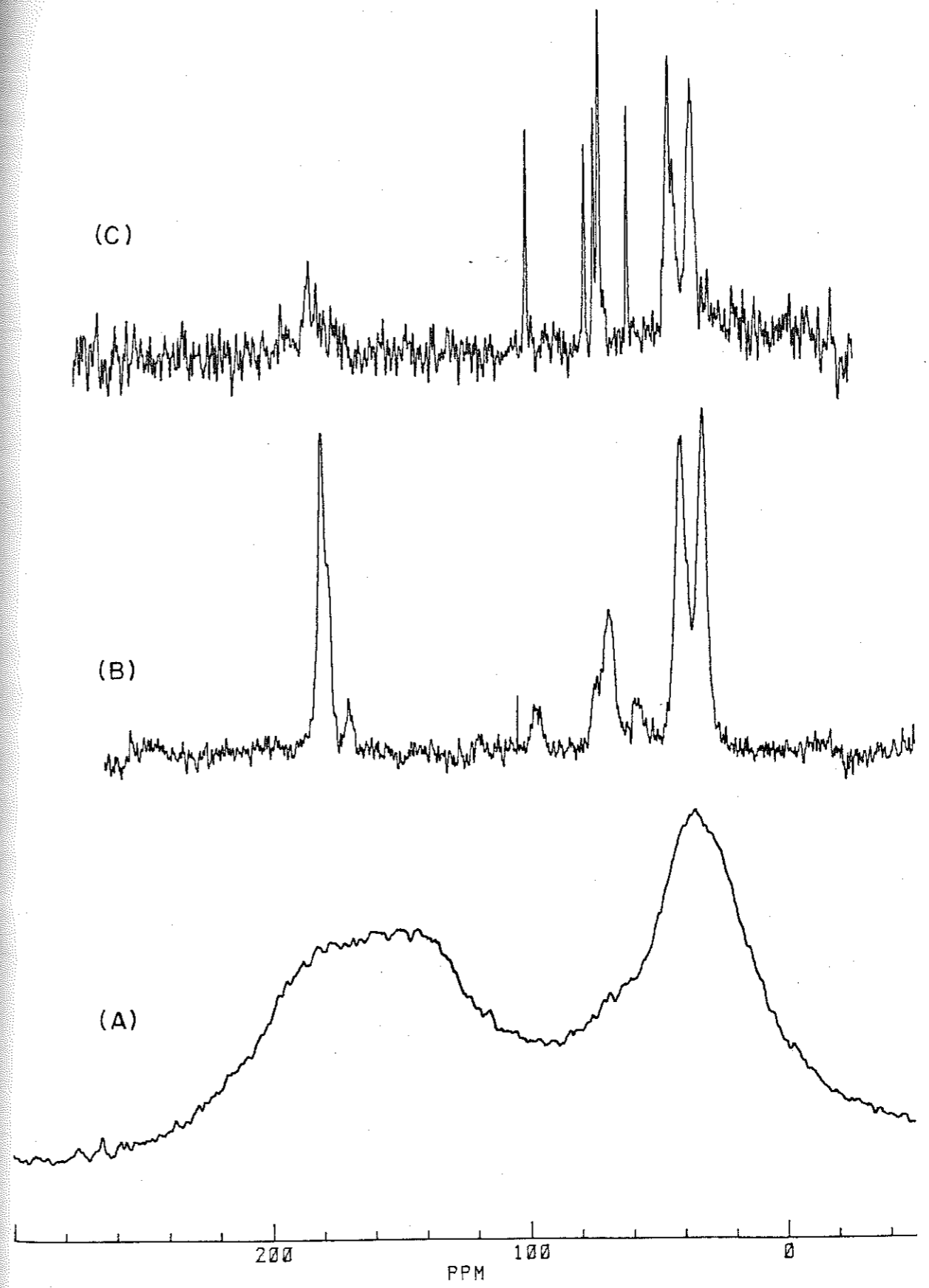


FIGURE 4-6: ¹³C SPECTRA OF HSPAN POLYMER AT DIFFERENT (%) SATURATIONS(Sat). (A) 0.08 % Sat, (B) 0.25 % Sat, (C) 2.0 % Sat.

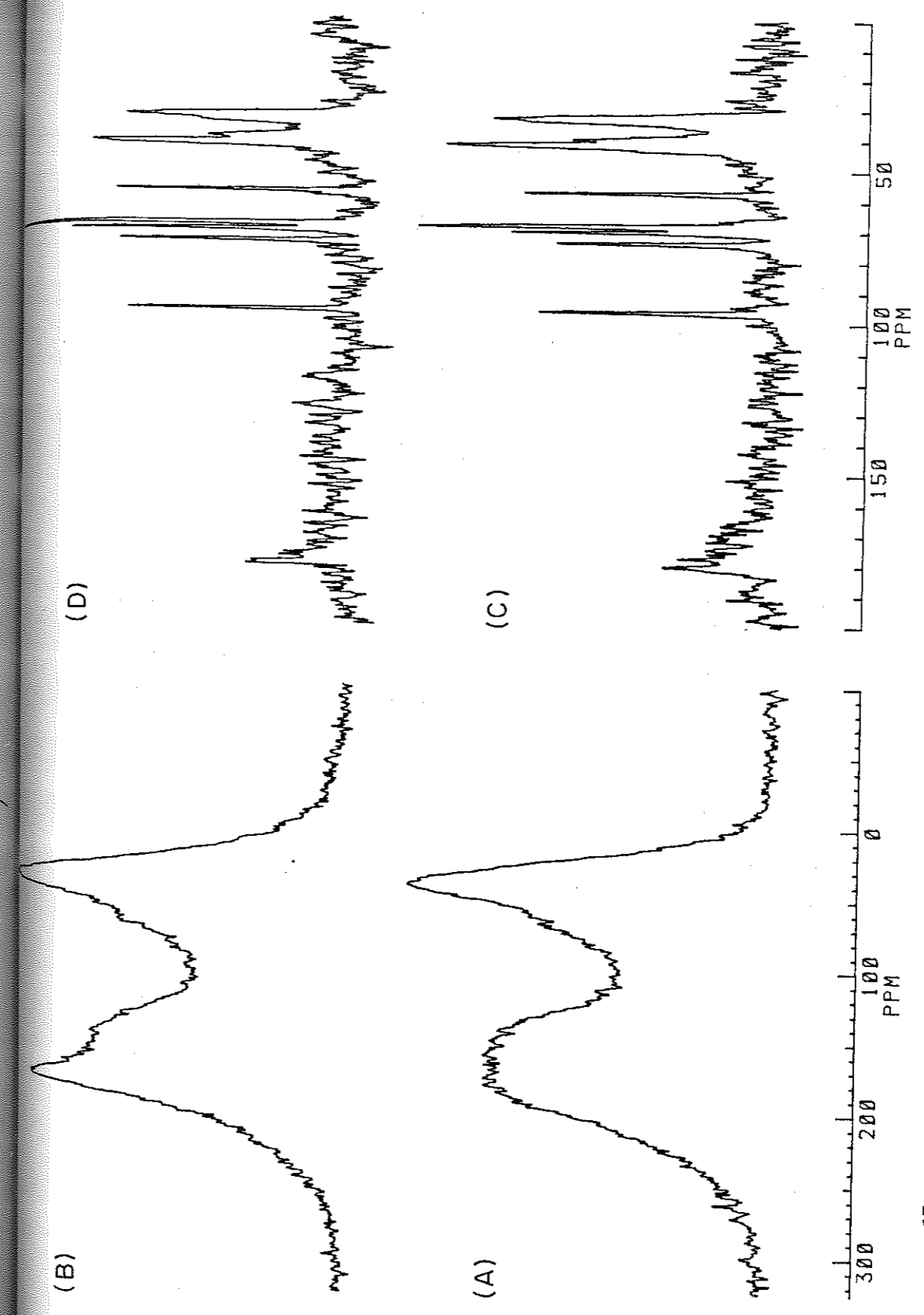


FIGURE 4.7: ¹³C SPECTRA OF HSPAN POLYMER (A) & (B) UNSHEARED AND SHEARED AT LOW % SATURATION. (C) & (D) UNSHEARED AND SHEARED AT HIGH % SATURATION

% saturation, as shown in Figs. 4.7C and 4.7D.

We also obtained the Magic Angle Sample Spinning (MASS) proton NMR spectra of the same samples and the results are summarized in Figs. 4.8A and 4.8B. The corresponding static proton spectra are shown in Figs. 4.8C and 4.8D. Pronounced side band pattern is seen, which originates from an inhomogeneously broadened proton-proton dipolar interactions due to lack of spin-diffusion among protons. The envelope of spinning side bands maps the so called super Lorentzian (^1H) proton line shape. The degree of super Lorentzian character strongly depends upon the mobility of the polymer chains. In the sheared sample, the side band manifold extends twice the spectral range as compared to the unsheared sample, consistent with a near super Lorentzian character in the static proton spectra of sheared sample.

Based on the above results, it is apparent that, subjecting the superabsorbent polymer to a history of deformation results in a decrease in the degree of cross-linking which in turn enhances the molecular mobility and superabsorption of the polymer.

All the NMR experiments were carried out on an FT-NMR spectrometer (Bruker MSL-300) operating at 7.1 Tesla. The ^{13}C spectra were recorded by employing a single $\pi/2$ pulse, followed by acquisition. During acquisition, the protons were decoupled by using ≈ 30 kHz R.F. field.

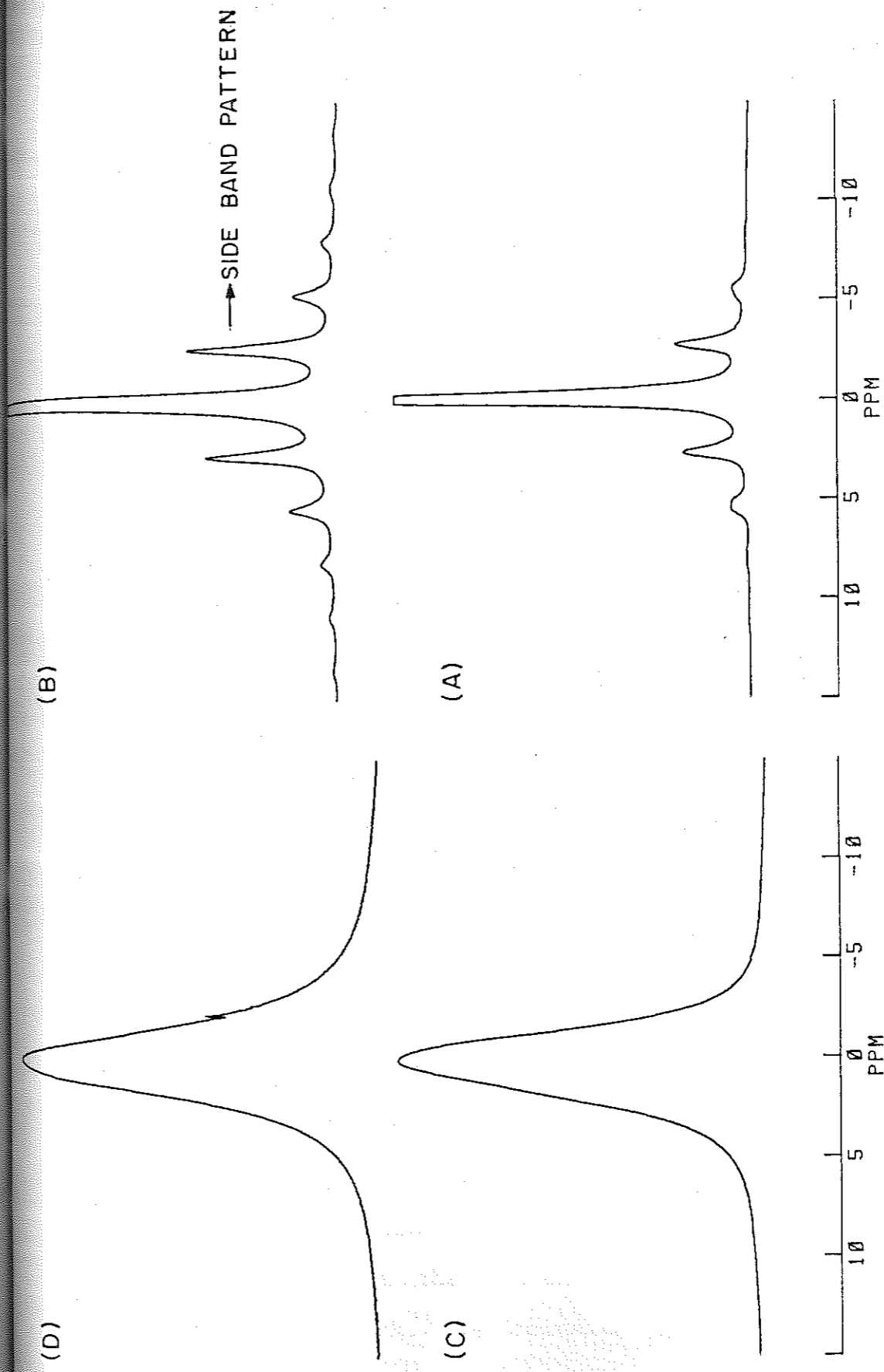


FIGURE 4-8: ^1H SPECTRA OF HSPAN POLYMER (A) & (B) UNSHEARED AND SHEARED (MASS SPECTRA). (C) & (D) UNSHEARED AND SHEARED (STATIC SPECTRA).

Quadrature phase cycling was used throughout to eliminate artefacts in the final spectra. Number of accumulations were typically of the order of 10,000. The number of scans were chosen to give spectra with a good signal to noise (S/N) ratio. Proton MASS spectra were recorded on a MASS probe which gave negligible proton background signal. The proton FID was recorded following a $\pi/2$ pulse and Fourier transformed. The number of accumulations was forty. ^{13}C and ^1H spectra are referred to TMS. All the NMR measurements were carried out at ambient probe temperature (25°C).

Deformation Induced by Centrifugal Action

The deformation can be applied to swollen superabsorbent network in many ways. If a polymeric gel is modelled in the way Silberberg(19) has done, then the mechanical spinning of the swollen network at high speeds in a cylindrical tube may cause a rapid motion of the free (unbound) solvent molecules due to the centrifugal force. This rapid motion of the solvent molecules can impose a mechanical stress to the network chains and thus reduce the degree of physical cross-linking. In this part we have examined the effect of this mechanical stress on absorption capacity of hydrolysed starch-g-polyacrylonitrile superabsorbent polymer. The extent of mechanical stress depends upon the concentration of the solvent present in the network, the spinning speed and the spinning

time. In order to demonstrate these effects, we carried out the spinning experiments in a 10 mm (dia) NMR tube spinning at 30 Hz around its own axis. The gel samples were prepared in water at different percentage saturations ranging from 100-20 (%). The 100 (%) saturation corresponds to the initial equilibrium absorption capacity of the unspun sample (i.e. 160.0 ml of water per gram of dry sample). The samples, after complete homogenization were packed in tube and rotated at 30 Hz for a fixed time of 30 minutes. After spinning, the samples were taken out in a petri dish and dried in oven at 60°C till constant weight was obtained. The equilibrium absorption capacities were determined for these dried samples and the results are summarized in Table-4.1.

It can be seen from the Table-4.1 that the maximum superabsorption was achieved for the sample equilibrated to 40(%) saturation and there was practically no change observed in the case of the solid powder which did not have any water in the system. Further, we examined the effect of spinning time on superabsorption capacity of the sample equilibrated to 40(%) saturation and the results are shown in Table-4.2. It is observed from Table-4.2 that the absorption capacity increases as the spinning time increases.

Deformation Dependent Phase Transitions

We have discussed in the foregoing that the volume

phase transitions can be induced by variation in the external parameters such as, pH, ionic strength, temperature, solvent composition and electric field.

In this section, we report the existence of a new phase transition and reentrant phase transition for the systems HSPAN/diacetone alcohol-water and HSPAN/N-methyl pyrrolidone-water. These transitions are observed by imposing the deformation to the swollen network.

The experiments were carried out in an apparatus described before by using in-situ superabsorption technique. The deformation was effected by shearing the swollen gel in an annular gap of the rotating cylinder and a stationary wall of a sintered disc glass funnel. The shear rate was kept constant by keeping the RPM fixed and the time of shearing was varied from 0 to 60 minutes. The diacetone alcohol concentration in water was varied from 0 to 100% by (v/v) monotonically. The solvent, diacetone alcohol was chosen particularly because of its good miscibility with water and low evaporation rate which provide accurate measurements of equilibrium absorption capacities. The temperature was kept constant at 25°C by using temperature controlled bath. The absorption capacities for sheared samples were measured by using the in-situ absorption technique described previously.

The results of our experiments are shown in Fig. 4.9. It can be seen that we have carried out all our shearing experiments below 40% diacetone alcohol concentration.

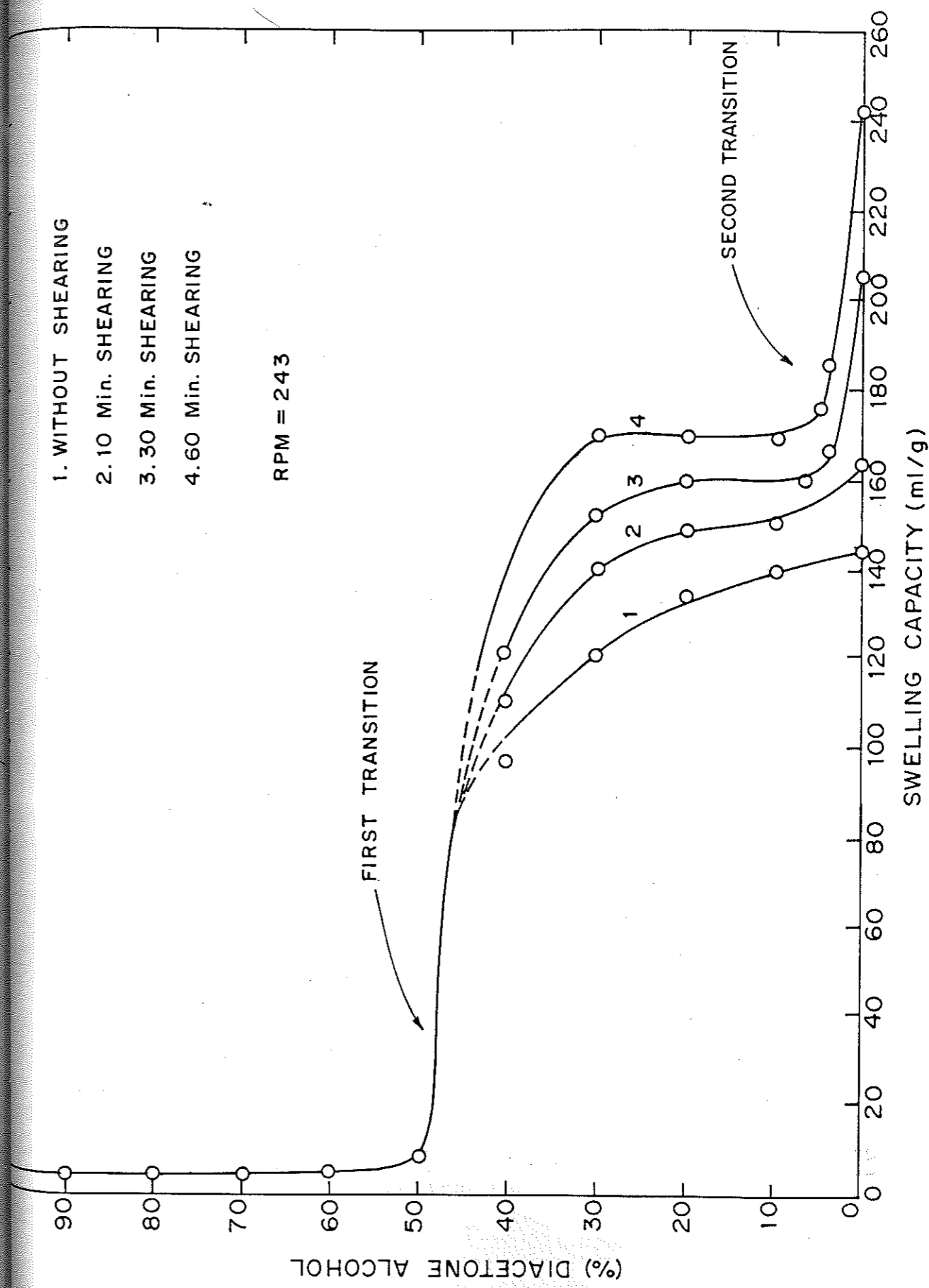


FIGURE 4.9 : DEFORMATION DEPENDENT PHASE TRANSITIONS - OBSERVATION OF SECOND TRANSITION (HSPAN/DIACETONE ALCOHOL WATER SYSTEM)

This is because above this value, the superabsorbent polymer drastically undergoes a volume phase transition and becomes a heterogeneous system for which uniform shear can not be applied.

It is observed from Fig. 4.9 that as the time of shear increases the absorption capacity also increases and at 60 minutes there is a drastic increase in absorption capacity from 140 ml/g to 240 ml/g at about 1% of Diacetone-alcohol concentration.

We believe that this deformation induced volume phase transition at very low diacetone alcohol concentration is observed for the first time. We have also observed a deformation induced reentrant phase transition for the same superabsorbent system when the solvent was changed from diacetone alcohol to N-methyl pyrrolidone. This kind of reentrant phase transition was shown by Katayama et al. (20), for polyacrylamide derivative copolymeric gels in dimethyl sulfoxide-water systems, when the ratio of water to dimethyl sulfoxide was varied monotonically. This phenomenon was explained by assuming a non-linear relationship between the free energy of contact between polymer segments of gel and solvent of different compositions. In our study of phase transition of HSPAN N-methyl pyrrolidone/water system, the reentrant behaviour was observed by subjecting the swollen network to deformation which is shown in Fig. 4.10. It can also be seen that as the time of shear increases the reentrant beha-

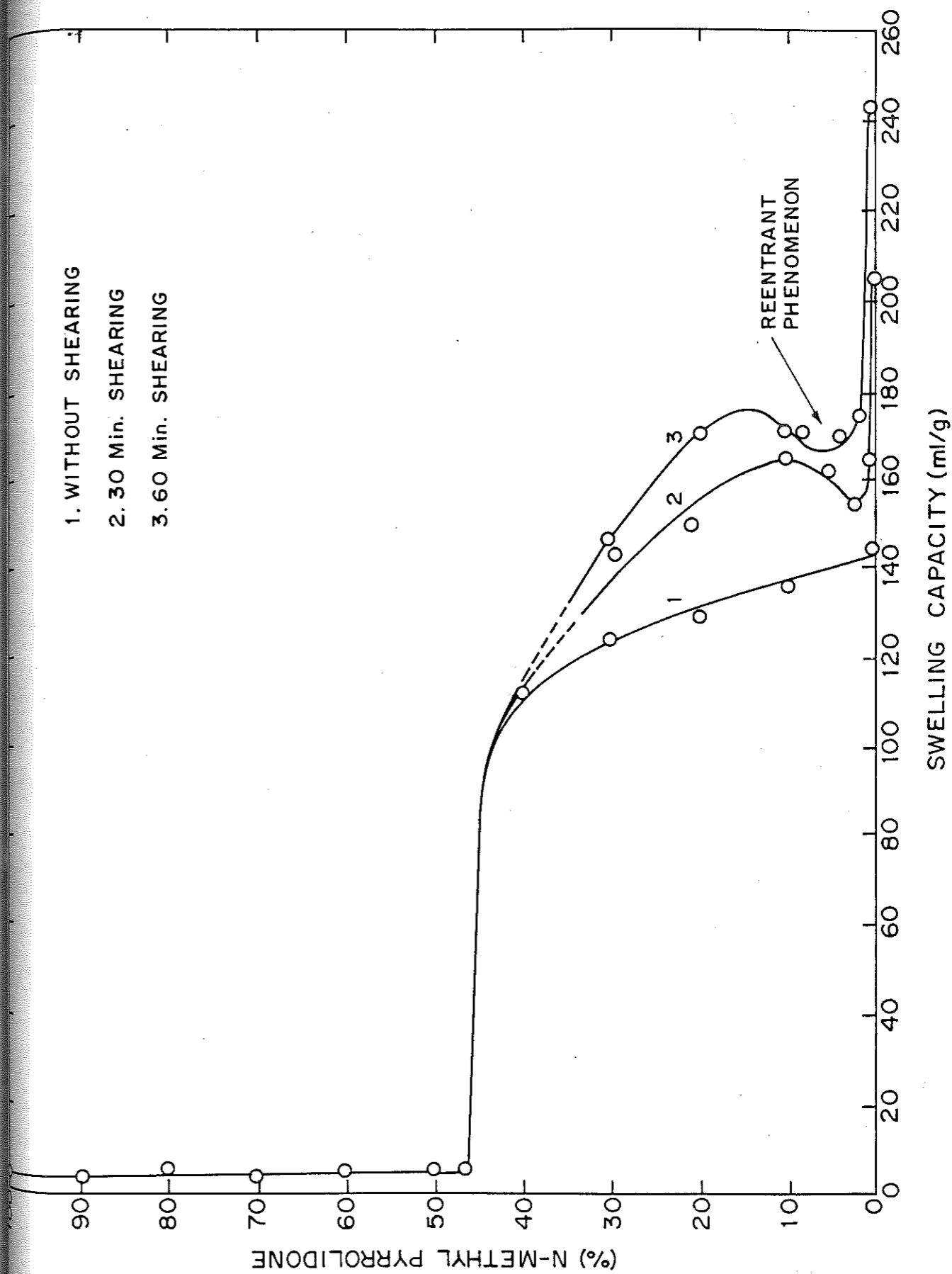


FIGURE 4-10 : DEFORMATION DEPENDENT PHASE TRANSITIONS - OBSERVATION OF REENTRANT PHENOMENON

viour is more pronounced. However, the exact functional dependence of solvent composition and shear on phase transition is yet to be fully understood.

Memory Effects in Superabsorbent Polymers

The superabsorbent polymers seems to have a memory in the sense that the material which was subjected to deformation undergoes a structural change and attains a new equilibrium absorption capacity. Subsequently, when this sample was precipitated in a non-solvent, dried and analysed for absorption capacity, it showed almost the same new value it had before the precipitation. Figure 4.11 shows the memory effect in a superabsorbent polymer such as hydrolysed starch-g-polyacrylonitrile. It can be readily seen that the absorption capacity of the polymer increases from 176 ml/g to about 245 ml/g (determined by in-situ absorption method) by imposing deformation for about 400 minutes.

After attaining the equilibrium value the swollen gel was precipitated in a non-solvent (ethanol) dried and analysed for absorption capacity, which indicated the same value it had before precipitation. Similar observation was also made for this polymer when the deformation was removed before it had reached the equilibrium value.

This is at once novel and intriguing. One would have expected that when the polymer is precipitated into a solid form and the capacity for water absorption measured

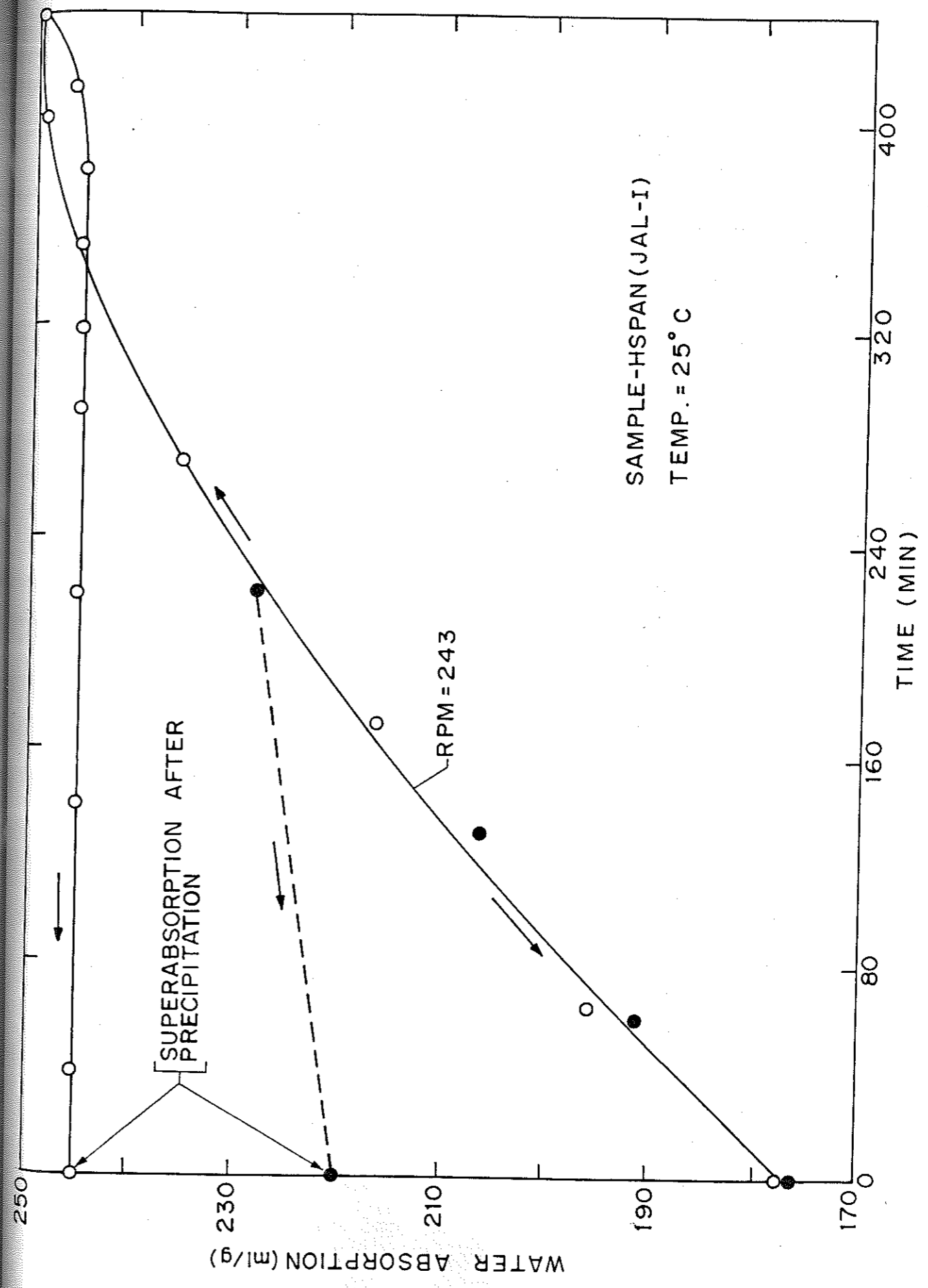


FIGURE 4.11 : MEMORY EFFECTS IN SUPERABSORBENT POLYMERS (HSPAN/WATER SYSTEM)

again, there would be a difference, since new structured attributes would be assigned to the polymer. This memory effect is reminiscent of shape memories (21) in other systems and is reported for the first time.

Implications of the Present Work

The new phenomena reported here have a number of implications. First of all the fact that one could subject a superabsorbent polymer to a mechanical stress and increase its absorption capacity has a pragmatic importance in their manufacture. Secondly, all the previous theories of superabsorption are based on equilibrium conditions. The kind of time dependent phenomenon shown in Fig. 4.2 imply that we need to have new non-equilibrium frameworks to analyse the data.

Thirdly, we have to be careful when studying the transition in superabsorbent polymers. For instance, the work done by Tanaka and his coworkers based on polyacrylamide superabsorbents shows the transition. However, if the deformation or deformation history is going to be critical, then it means we have to consider these systems as metastable.

Finally the memory effects are most intriguing. In spite of the drastic phase changes that the gel undergoes, it remembers the state at which it was before precipitation. This also implies long range order in such systems.

REFERENCES

1. Flory P.J., 'Principles of Polymer Chemistry', Cornell Univ. Press Ithaca, NY. (1953)
2. Tanaka T., Encyclo. of Polym. Sci. and Engineering, 7, 514 (1987).
3. Marro A. and Muller I., Rheol. Acta, 27, 44 (1988).
4. Ilavsky, M., Polymer, 22, 1687 (1981).
5. Tanaka T. and Fillmore D.J., JI. Chem. Phys. 70, 1214 (1979).
6. Schosseler F., Mallo P., Cretenot C. and Candau S. JI. Disp. Sci. and Technol. 8(4), 321 (1987).
7. Tanaka T., Fillmore D.J., Sun S.T., Nishio I., Swislow G. and Shah A., Phys. Rev. Lett. 45, 1636, (1980).
8. Tanaka T., Phys. Rev. Lett. 40, 820 (1978).
9. Tanaka T., Sci. American, 244, 110 (1981).
10. Ford W.T. and Balkrishnan T., Macromolecules, 14, 284 (1981).
11. Ganapathy S., Badiger M.V., Rajamohanam P. and Mashelkar R.A., Macromolecules (communicated).
12. Cussler E.L., Stokar M.R. and Varberg J.E., AIChE J. 30, 578 (1984).
13. Freitas R.F.S. and Cussler E.L., Separation Sci. and Technol. 22, 911 (1987).
14. Buchanan K.J., Hird B. and Letcher T.M., Polym. Bull. 15, 19 (1986).
15. Fanta G.F., Burr R.C. and Doane W.M., ACS Symp. 187, 195 (1982).
16. Rodehed C. and Ranby B., JI. Appl. Polym. Sci. 32, 3323 (1986).

17. Ganapathy S., Chacko V.P. and Bryant R.G., *Macromolecules*, 19, 1021 (1986).
18. Bahneider D., Doskocilova D. and Dybal J., *Polymer*, 26, 253 (1985).
19. Weiss N. and Silberberg A., 'Hydrogels for Medical and Related Applications', *ACS Symp. Ser.* 31 69, (1976).
20. Katayama S., Hirokawa Y. and Tanaka T., *Macromolecules*, 17, 2641 (1984).
21. Takeda K., Akiyama M. and Yamamizu T., *Die. Angew. Makromol. Chemie.* 157, 123 (1988).

TABLE- 4.1

Effect of percentage saturation on superabsorption
by spinning method

(%) Saturation	Absorption capacity (ml/g)
0.0 (dry powder)	158.9
100.0	177.9
60.0	218.0
40.0	245.9
2.0 *	174.7 *

[* (Expt. carried out in MASS rotor spun at 2.0 kHz)]

TABLE- 4.2

Effect of spinning time on superabsorption
(Spinning speed : 30 Hz)

Time of spinning (min)	Absorption capacity (ml/g)
0.0	169.2
10.0	231.3
20.0	241.9
30.0	245.9
40.0	238.5
60.0	239.4

CHAPTER-V

RHEOLOGY OF SUPERABSORBENT POLYMERS

Introduction

Superabsorbent polymeric gels, because of their large swelling power find extensive applications as thickeners for printing pastes, oil drilling systems, etc. An understanding of the rheological behaviour of these materials is therefore critical. The viscosity and mechanical stability of the gels in the swollen state depends on the chemical composition, degree of ionization and degree of cross-linking. The nature of the swollen gel can vary from soft to a hard rubbery mass depending upon the extent of cross-linking. For example the polystyrene-divinyl benzene gels, which are extensively used in ion-exchange technology (1) are hard gels, whereas polyacrylamide gel used in electrophoresis (2) is a soft gel. These gels can be characterized by their equilibrium, dynamic, kinetic and rheological properties.

Behaviour of gel

Gels of superabsorbent polymers are thixotropic in nature and exhibit yield stress. The behaviour of these gels under stress can be studied by models used to study thixotropy. Thixotropy is a time dependent phenomenon. The term was first coined by Peterfi (3) in 1927 to describe the isothermal reversible sol-gel (solid-liquid) transitions due to shear. Later on this phenomenon was redefined by British Standard Institution as 'decrease in viscosity under stress, followed by gradual recovery when the stress is removed.'

The phenomenon of thixotropy is very commonly found in materials like starch pastes, gelatin, drilling muds and latex paints. This time dependent phenomenon is interpreted in terms of the change in the structure of the material which may be reversible or irreversible. Viscosity-time measurements during shear or after shear are generally carried out to explain the time-dependent effects. When the material is subjected to a constant shear, the viscosity drops sharply at first, but the rate of change continually decreases until a constant or nearly constant level is reached. When the shearing action is stopped, the viscosity increases quickly at first, then more slowly and approaches the original value asymptotically. This can be described by a 'Hysteresis Loop'. Efforts have been made in the past to develop a theoretical description for the thixotropic materials. A systematic outline of published model and possible constitutive equations for thixotropic materials is given by Mewis in 1979 (4).

Recently Cheng (5) has derived rate type of constitutive model to describe the thixotropic behaviour of materials such as sewage sludges. It is basically a yield-pseudoplastic constitutive equation in which the yield stress is expressed as a function of time using a 'structural parameter', (λ). Cheng's model predicts the structural breakdown and the recovery of thixotropic fluids. It is postulated that a thixotropic fluid, when subjected

to shear, results in breakdown of the structure of the material with time. The new structure tries to rebuild itself by a process of recovery. Ultimately, the fluid attains an equilibrium structure. When the shear is stopped and the fluid is allowed to rest, the recovery of the structure begins and after enough time, the fluid attains a fully built-up structure.

Viscosity behaviour of superabsorbent polymers

Taylor and Bagley (6,7) investigated the viscosity behaviour of gels of superabsorbent polymers such as hydrolysed starch-polyacrylonitrile (HSPAN) and Carbopol 941. These polymers form highly visco-elastic suspensions in water, even at concentrations that are less than 1% by weight. These suspensions consist of swollen, closely packed deformable gel particles with little or no interstitial solvent. The thickening action of these gels strongly depends on the dilution and the ionic strength of the system.

The rheological behaviour of gels of superabsorbent polymers, especially thixotropic ones has not been reported in the literature. Contrary to the normal thixotropic fluids, these gels behave differently. If this gel is sheared, the structure of the gel breaks down, which is reflected in the viscosity of the gel decreasing with time (Fig. 5.1). After attaining equilibrium, if the gel is allowed to rest, it is found that the structure is not fully recovered.

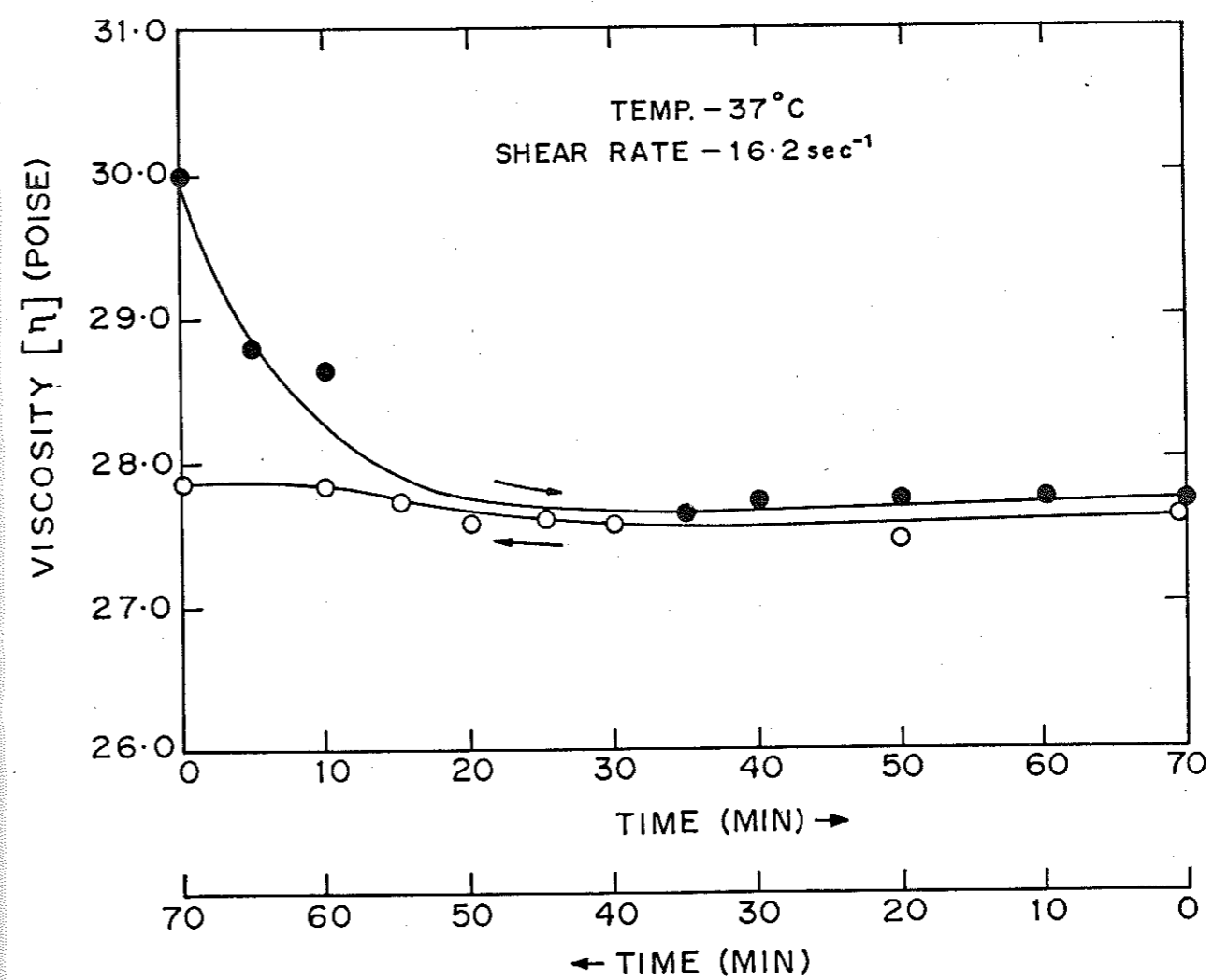


FIGURE 5.1 VISCOSITY vs TIME - HSPAN POLYMER
(100 % SATURATION)

Based on the experimental observations a mathematical model has been developed in this chapter, which takes into account the reversible and irreversible structural changes.

EXPERIMENTAL

Two types of superabsorbent gels were used to study the viscosity behaviour. The first one was hydrolysed starch-g-polyacrylonitrile, (HSPAN) which is semisynthetic and the second one was polyacrylamido-propene sulfonic acid, (PAMPS) which is totally synthetic superabsorbent polymer. The particle size of these gels (in dry state) was around 100 mesh and equilibrium swelling capacities were 175.0 ml/g and 225.0 ml/g respectively. The equilibrium swelling capacity of the gel corresponds to complete saturation.

The samples were prepared in distilled water at different percentage saturation in a closed container and allowed to stand for 24 hrs. The viscosity measurements were carried out with respect to time on a co-axial cylinder viscometer (Rheotest-2 (MLW)). The material was sheared in the annular gap (1.14 mm) of coaxial cylinder system. The temperature was carefully maintained at slightly above the ambient temperature (at 37°C) to prevent any evaporation of the solvent, which may change the concentration of the gel. The viscosity was determined at 10 minutes interval for upto 80-90 minutes. After attaining

the steady value of viscosity (in about 80 minutes) the shear was stopped and again the viscosity was measured at every 10 minutes by rotating the cylinder for a very short time (15 seconds). This rotation for short time was assumed to be insufficient to cause any significant change in the structure.

RESULTS

The results of the viscosity measurements with respect to time are plotted in Figs. 5.1-5.3 corresponding to 100.0, 150.0 and 200.0% saturation of HSPAN gels respectively. It can be seen from Fig. 5.1 that at constant shear ($\dot{\gamma} = 16.2 \text{ sec}^{-1}$) the viscosity decreases from 30.0 poise to 27.6 poise in about 30 minutes and remained constant thereafter upto 70 minutes. When shear is discontinued, the viscosity gradually increases and reaches a constant value of 27.8 poise. This clearly indicates the partial recovery of the structure. Similar observations were made for gels saturated to higher levels (see Figs. 5.2 and 5.3).

MODEL

As discussed in the foregoing, the partial recovery of the gel indicates that it has a 'reversible' as well as 'irreversible' structure. The mathematical description of the above can be given as,

$$\tau = \tau_y + k \dot{\gamma}^n \quad (5.1)$$

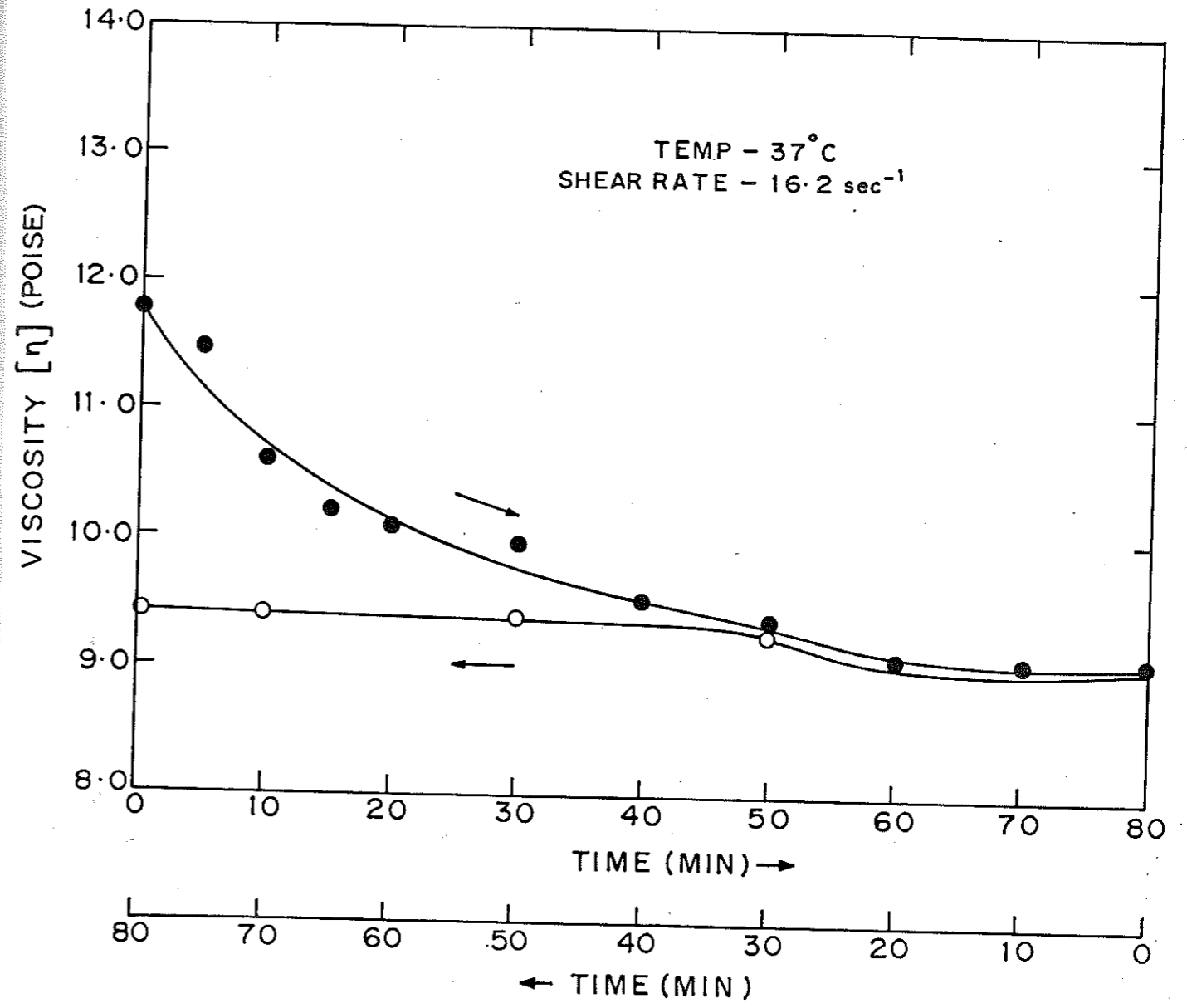


FIGURE 5.2 VISCOSITY vs TIME - HSPAN POLYMER (150 % SATURATION)

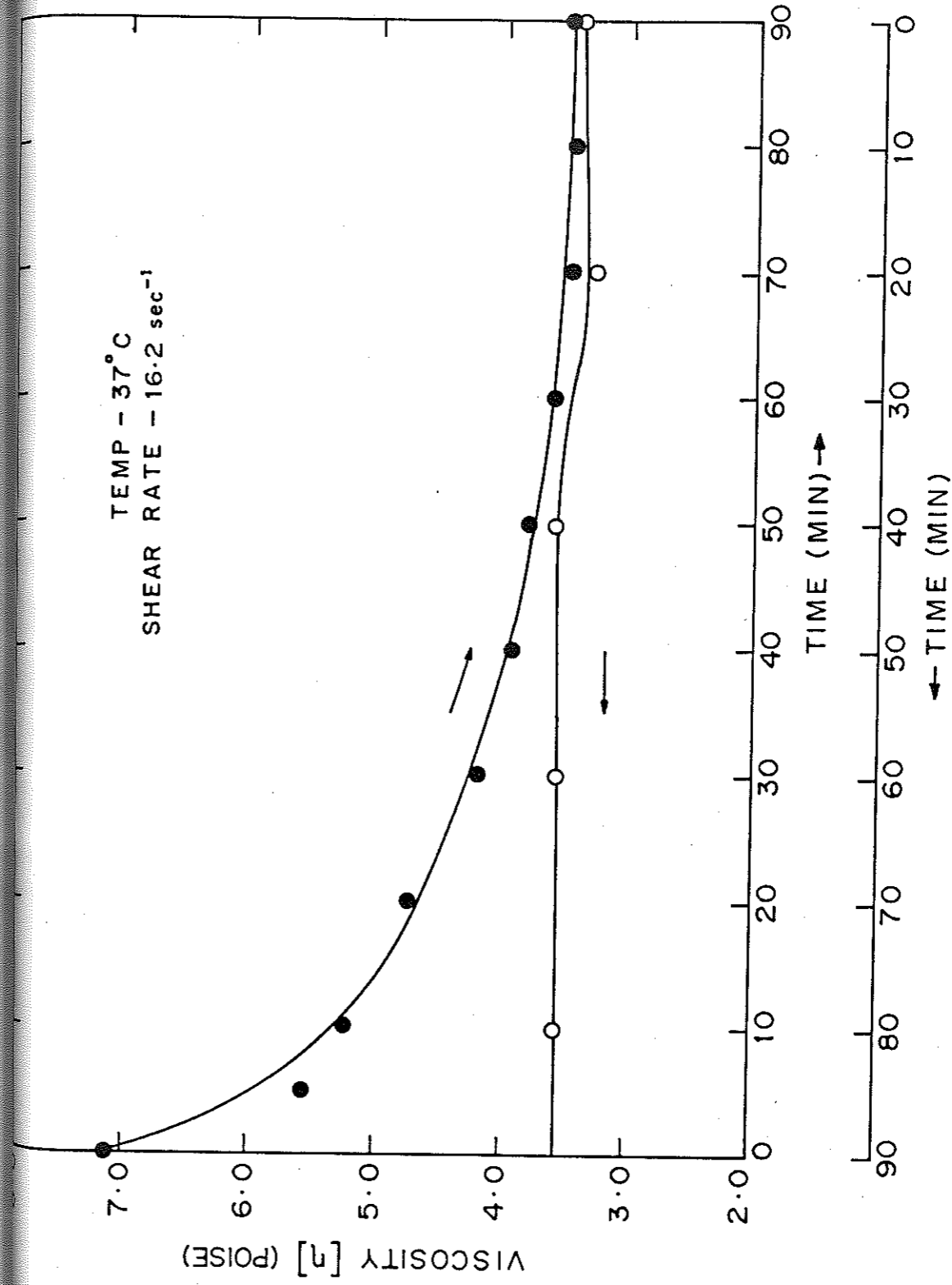


FIGURE 5.3 VISCOSITY vs TIME - HSPAN POLYMER (200% SATURATION)

where,

$$\tau_y = \tau_{y_0} + \lambda_1 \tau_{y_1} + \lambda_2 \tau_{y_2} \quad (5.2)$$

where, (λ_1) (λ_2) are reversible and irreversible structure parameters, (τ_y) denotes the yield stress, (τ_{y_0}) is yield stress of the gel when it has reached equilibrium state, (τ_{y_1}) , (τ_{y_2}) denote yield stresses due to 'reversible' and 'irreversible' structures respectively, (k) and (n) are consistency index and flow behaviour index and $(\dot{\gamma})$ denotes the shear rate. The reversible and irreversible structures are independent of each other.

$$\frac{d\lambda_1}{dt} = a(\lambda_1^0 - \lambda_1) - b\lambda_1 \dot{\gamma} \quad (5.3)$$

and

$$\frac{d\lambda_2}{dt} = -c\lambda_2 \dot{\gamma} \quad (5.4)$$

where,

a = recovery parameter for structure 1

b = breakdown parameter for structure 1

c = breakdown parameter for structure 2

We note that structure 1 is reversible, whereas, structure 2 is irreversible.

Integration of equations (5.3) and (5.4) gives,

$$\lambda_1 = \frac{a\lambda_1^0}{(a+b\dot{\gamma})} + \frac{b\dot{\gamma}\lambda_1^0}{(a+b\dot{\gamma})} e^{-(a+b\dot{\gamma})t} \quad (5.5)$$

and

$$\lambda_2 = \lambda_2^{\circ} e^{-c\delta t} \quad (5.6)$$

where, $\lambda_2 = \lambda_2^{\circ}$ at $t=0$

$\lambda_1 = \lambda_1^{\circ}$ at $t=0$

Note that

$$\lambda_1^{\circ} + \lambda_2^{\circ} = 1.0$$

$$\text{AS, } t \rightarrow \infty, \lambda_2 \rightarrow 0 \text{ and } \lambda_1 \rightarrow \frac{a\lambda_1^{\circ}}{(a+b\delta)} \quad (5.7)$$

Recovery of the broken down gel

Assume that recovery starts after $t = t_{\infty}$ when,

$$\lambda_2 = \lambda_2^{\infty}, \lambda_1 = \lambda_1^{\infty}$$

During recovery, $\delta = 0$

hence, equations (5.3) and (5.4) become

$$\frac{d\lambda_1}{dt} = a(\lambda_1^{\circ} - \lambda_1) \quad (5.8)$$

$$\frac{d\lambda_2}{dt} = 0 \quad (5.9)$$

Integration of equations (5.8) and (5.9) gives,

$$\lambda_2 = \text{Constant} = \lambda_2^{\infty} \quad (5.10)$$

$$\lambda_1 = \lambda_1^{\circ} - (\lambda_1^{\circ} - \lambda_1^{\infty}) e^{-at} \quad (5.11)$$

where, $\lambda_2 = \lambda_2^{\infty}$ at $t=t_{\infty}$ and $\lambda_1 = \lambda_1^{\infty}$ at $t=t_{\infty}$

Here, the time t_{∞} may not be very large for the full breakdown to occur. If the recovery is assumed to start after shearing for a long time, but not for 'infinite time', the value of the structural parameters (when the recovery starts) will have to be calculated from the equations (5.5) and (5.6) by substituting, the appropriate values for time 't'. If, however, the recovery starts after shearing for an 'infinite' time, then λ_1^{∞} and λ_2^{∞} will be given by the equation (5.7).

Evaluation of various parameters

(1) Data at infinite time ($t = \infty$) [i.e. fully broken down 'virgin' gel].

The plots of τ vs $\dot{\gamma}$ can be made. At large values of $\dot{\gamma}$, the τ - $\dot{\gamma}$ data will be linear on logarithmic scales. The equation, $\tau = k \dot{\gamma}^n$ can be fitted and the values of k and n can be determined.

(2) At lower values of $\dot{\gamma}$, we can calculate the difference $\tau - k \dot{\gamma}^n$, which is equal to τ_y .

Since,

$$\tau_y = \tau_{y_0} + \lambda_1 \tau_{y_1} + \lambda_2^{\infty} \tau_{y_2} \quad (5.12)$$

and $\lambda_1^{\infty} = \frac{a \lambda_1^0}{(a + b \dot{\gamma})}$, $\lambda_2^{\infty} = 0$

we get,

$$\tau_y = \tau_{y_0} + \frac{a \tau_{y_1} \lambda_1^0}{a + b \dot{\gamma}} \quad (5.13)$$

By fitting the data one can evaluate $a\tau_{y_1} \lambda_1^\circ$, a and b and hence $\lambda_1^\circ \tau_{y_1}$, a and b .

(3) Breakdown of a recovered gel

$$\text{at } t = 0, \tau = \tau_{y_0} + \lambda_1^\circ \tau_{y_1} + k\delta^n \quad (5.14)$$

$$\text{at } t = t, \tau = \tau_{y_0} + \lambda_1 \tau_{y_1} + k\delta^n \quad (5.15)$$

Therefore,

$$\lambda_1 \tau_{y_1} = \tau - \tau_{y_0} - k\delta^n \quad (5.16)$$

$$\lambda_1^\circ \tau_{y_1} = \tau - \tau_{y_0} - k\delta^n \quad (5.17)$$

dividing (5.16) by (5.17) we get

$$\frac{\lambda_1}{\lambda_1^\circ} = \text{expression (at various } t \text{ and } \delta \text{ values)} \quad (5.18)$$

However,

$$\lambda_1 = \frac{a\lambda_1^\circ}{(a+b\delta)} + \frac{b\delta\lambda_1^\circ}{a+b\delta} e^{-(a+b\delta)t}$$

$$\lambda_1 = \lambda_1^\circ \left\{ \frac{a}{(a+b\delta)} + \frac{b\delta e^{-(a+b\delta)t}}{(a+b\delta)} \right\}$$

We have, $\lambda_1 / \lambda_1^\circ$ at various t and δ values. By fitting the data to the above equation, λ_1° can be evaluated by interpolation technique and hence, $\lambda_2^\circ = (1 - \lambda_1^\circ)$ can be determined.

(4) We already know the product of $\lambda_1^\circ \tau_{y_1}$. Hence,

$$\tau_{y_1} = \frac{\text{product}}{\lambda_1^\circ}$$

(5) The initial or zero time data of a virgin gel is given as,

$$\tau = \tau_{y0} + \lambda_1^{\circ} \tau_{y1} + \lambda_2^{\circ} \tau_{y2} + k \dot{\gamma}^n$$

We know

$$\tau_{y0}, \lambda_1^{\circ}, \lambda_2^{\circ}, \tau_{y1}, k \text{ and } n$$

therefore the value of τ_{y2} can be evaluated.

(6) Data of 'virgin' gel at various times is given by,

$$\tau = \tau_{y0} + \lambda_1 \tau_{y1} + \lambda_2 \tau_{y2} + k \dot{\gamma}^n$$

One can calculate λ_1 at various times 't' and $\dot{\gamma}$ by using the above equation.

By knowing λ_1 the value of λ_2 can be given as ,

$$\lambda_2 = \frac{\tau - \tau_{y0} - \lambda_1 \tau_{y1} - k \dot{\gamma}^n}{\tau_{y2}}$$

however,

$$\lambda_2 = \lambda_2^{\circ} e^{-c \dot{\gamma} t}$$

'So, by data fitting, the value of 'c' can be evaluated.

Conclusion

The model proposed above consists of nine parameters and a procedure for evaluating the parameters has been described. The model could not be verified experimentally due to limitations of the equipment. However, it can explain atleast qualitatively the rheological behaviour of the gel systems investigated.

REFERENCES

1. 'Ion Exchange Technology', edited by Nadeu and Streat (1984), Ellis Horwood Ltd., England.
2. Chrambach A. and Rodbard D. Science 172, 440 (1971).
3. Peterfi T., Arch. Entwicklungsmech. Org. 112, 680, (1927).
4. Mewis J., Jl. of Non-Newtonian Fluid Mech. 6, 1 (1979).
5. Cheng D.C.H. 'The characteristics of thixotropic behaviour' Research Report No. LR 157 (MH) Stevenage: Warren Spring Laboratory (1971).
6. Taylor N.W. and Bagley E.B., Jl. of Appl. Polym. Sci. 18, 2747 (1974).
7. Taylor, N.W. and Bagley E.B., Jl. of Appl. Polym. Sci. 21, 113 (1977).

NOTATION

for

- a recovery parameter/structure - 1
- b breakdown parameter for structure - 1
- c breakdown parameter for structure - 2
- k consistency index
- n flow behaviour index
- $\dot{\gamma}$ shear rate
- t time of shear
- τ stress
- τ_y yield stress
- τ_{y0} yield stress of gel at equilibrium
- τ_{y1} yield stress due to reversible structure
- τ_{y2} yield stress due to irreversible structure
- λ_1 reversible structure parameter
- λ_2 irreversible structural parameter

CHAPTER-VI

SUPERABSORBENT POLYMERS IN SEPARATIONS

Introduction

In the area of separation technology, separations involving polymeric systems are gaining importance. The area where polymers themselves are used as separators comprise polymeric membranes, ion exchange resins, polymer flocculants, etc. Recently some new advances have been made in the area of separation technology, for example, the polymeric mechanochemical devices, made up of perm selective membranes act as chemical valves for effecting separations (1).

Synthetic polymers are being increasingly used to remove organic species from an aqueous medium by physicochemical adsorption and also for extraction of metals (2). There are very few references on separation of dilute proteins or polymer solutions through size selective superabsorbent polymers. In this chapter the use of superabsorbent polymers in separation is discussed.

Separations of biological molecules from dilute aqueous solutions is a challenging task, since the viability of number of processes depends entirely on whether the economically viable separation technique has been developed. There are a number of instances, where the 'bioconversion' process has been carried out successfully but the failure has occurred essentially because 'bioseparation' process has not been possible. The problem of separation processes focussing around concentration of

dilute solutions of organic or biological materials are becoming increasingly important. Specific examples include the removal of water from starch and cheese whey, the concentration of antibiotics in fermentation broths and the recovery of protein products of genetically engineered microorganisms.

Conventional Separations

Various methods have been used for concentrating dilute solutions of macromolecules. The conventional techniques developed in the past include ultrafiltration (UF), dialysis, reverse osmosis (RO), freeze drying, etc. A representative summary of these techniques is given in Table-6.1.

In most of the techniques enumerated above, a polymeric membrane is used as a separation device. A wide range of polymeric membranes which offer fluxes of the order of $0.02 - 4.0 \text{ g/cm}^2 \cdot \text{min} \cdot \text{atm}$. and specific molecular weight cut off (MWCO) limits are now commercially available. However, these membrane techniques suffer from a number of disadvantages. For instance, the performance of the device often deteriorates because of concentration polarization near the membrane surface. This inevitably results in a large pressure drop. Additionally, there is a possibility of degradation of shear sensitive macromolecules such as DNA and some proteins (3). The problem of denaturation can be overcome by using

a freeze-drying technique. However, this process is slow and expensive. Further a disadvantage of the freeze drying is that the salts also get concentrated. The cost of the capital equipments in most membrane separation processes is rather high.

Towards Alternative Solutions to Separation Problems

We do not want to give an impression that membrane processes are full of problems. Indeed in some cases they may be indispensable. However, there is a definite scope for looking at cheaper and elegant alternatives for macromolecular separations from aqueous solutions. The problem is essentially that of sieving biological macromolecules from an aqueous solution, without sacrificing the viability or activity of macromolecules such as an enzyme. A new concept which involves the use of cross-linked polymeric gels or superabsorbents for concentration of dilute macromolecular solutions is being extensively investigated in recent years. Cross-linked gels based on dextran (Sephadex)(4), polyacrylamide and hydrolysed polyacrylamide for the concentrations and separation processes have been used with varying levels of success.

Vartak et al. (5) have reported the use of acrylamide-acrylic acid copolymeric gels in the form of small sticks for the concentration process. This process is effected by immersing the gel sticks in the solution to be concentrated (Fig. 6.1). Proteins having wide range

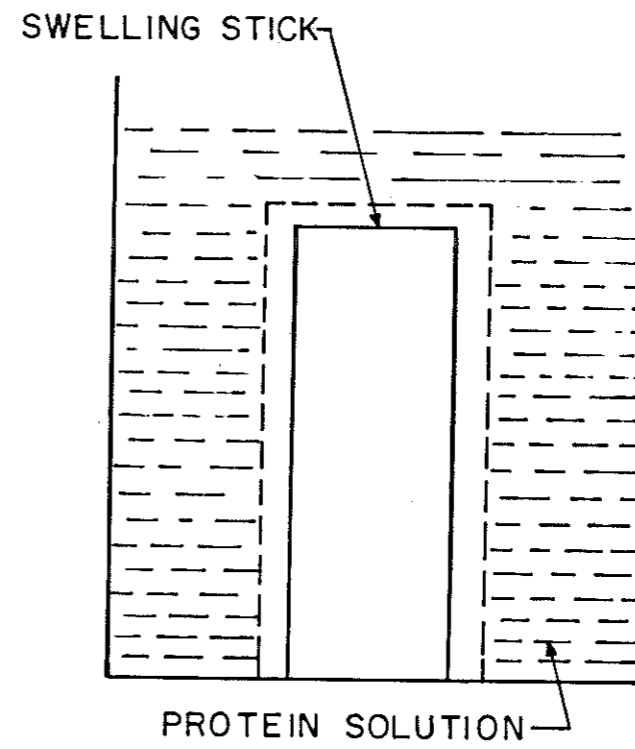


FIGURE 6-1: DIRECT CONTACT OPERATION-USE OF GEL STICK

of molecular weights (10,000-4,50,000) were concentrated and 5-10 fold concentrations were achieved (Table-6.2). However, no efforts were made to regenerate these gel sticks.

Cussler et al. (6) went a step further in providing a technologically viable scheme for using partially hydrolysed cross-linked polyacrylamide gels as size selective extraction solvents. Wide range of macromolecular solutes were concentrated (Table-6.3). Observing that the swelling characteristics of gel is a strong function of pH (Fig. 6.2) and temperature, an elegant regeneration step was developed by varying pH (6,7) and temperature (8). The swelling and collapse phenomena of these gels could be described by semiempirical relationships based on Flory's theory (9).

In this chapter, a technique which is based on the use of cross-linked polystyrene sulfonate gels (namely Swellex gels) which were synthesized and characterized earlier (Chapter-II) has been reported. These gels were prepared in the form of beads and packed in a column in the dry state (Fig. 6.4). The dilute macromolecular solution was passed through the column and concentration could be effected. The swellex gels are rigid, therefore the integrity of the swollen bead is retained which prevents the blockade of the column. Thus a simple batch process can be made semicontinuous or continuous with proper design of the column. During the process of

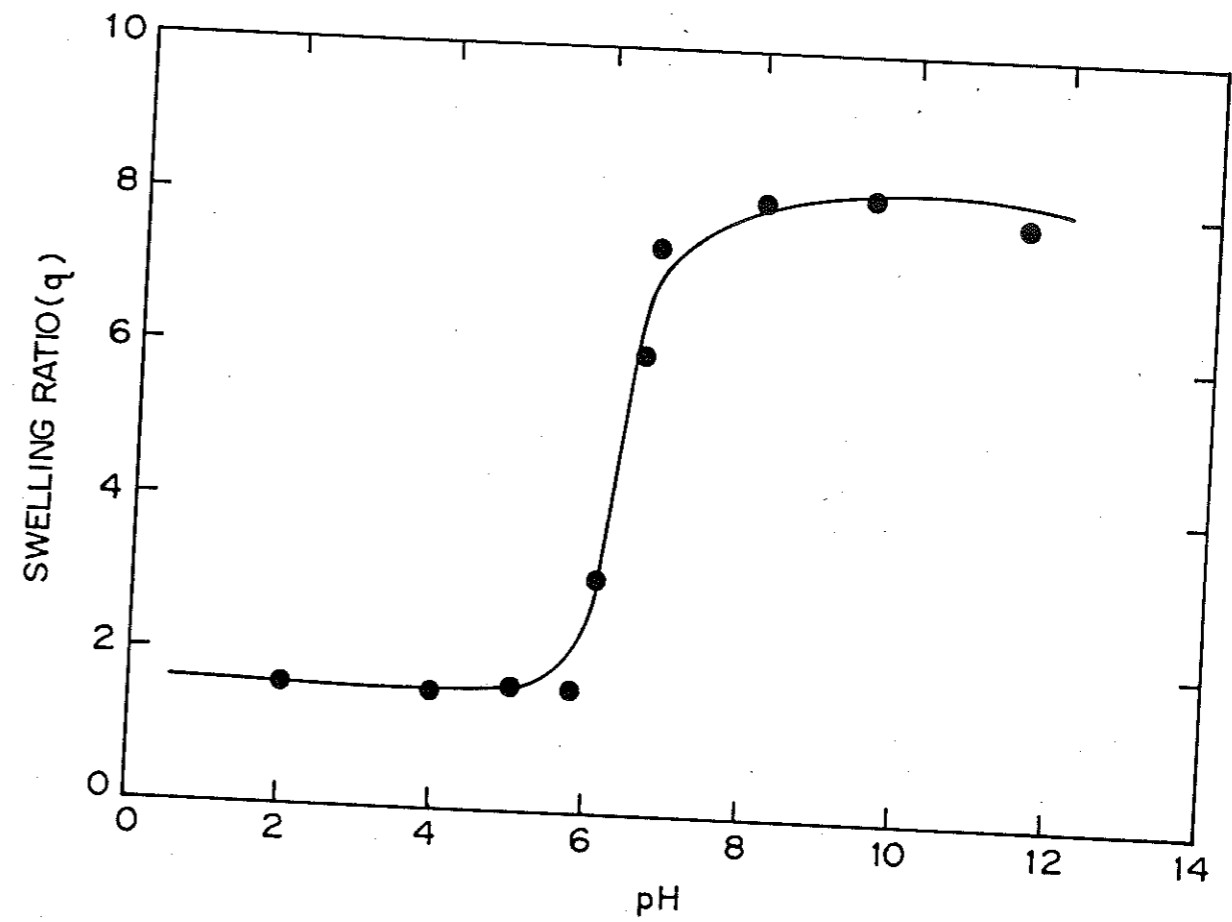


FIGURE 6.2 : SWELLING RATIO CONTROLLED BY VARIATION OF pH

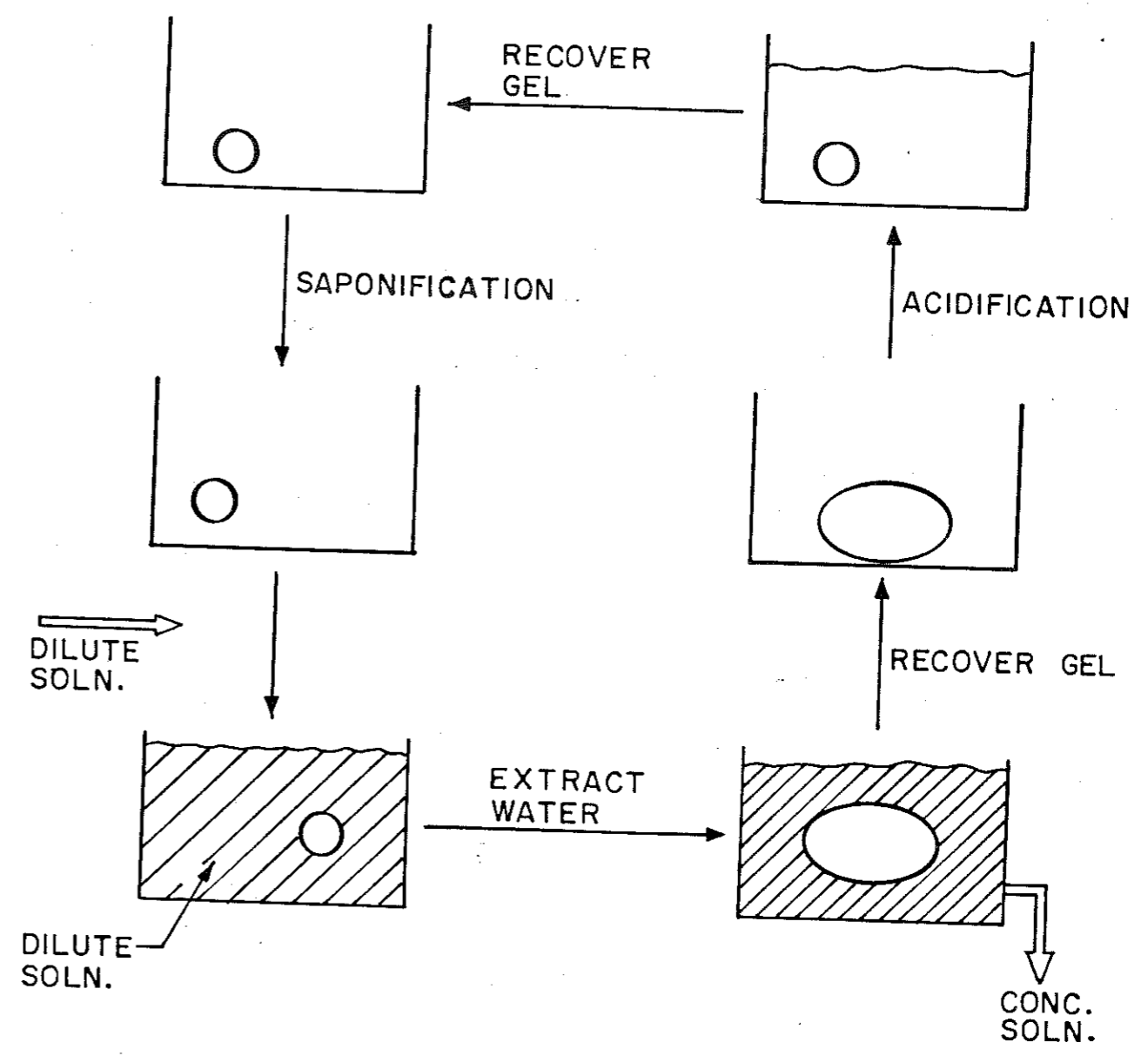


FIGURE 6-3: REGENERATION STRATEGY BASED ON pH DEPENDENT SWELLING

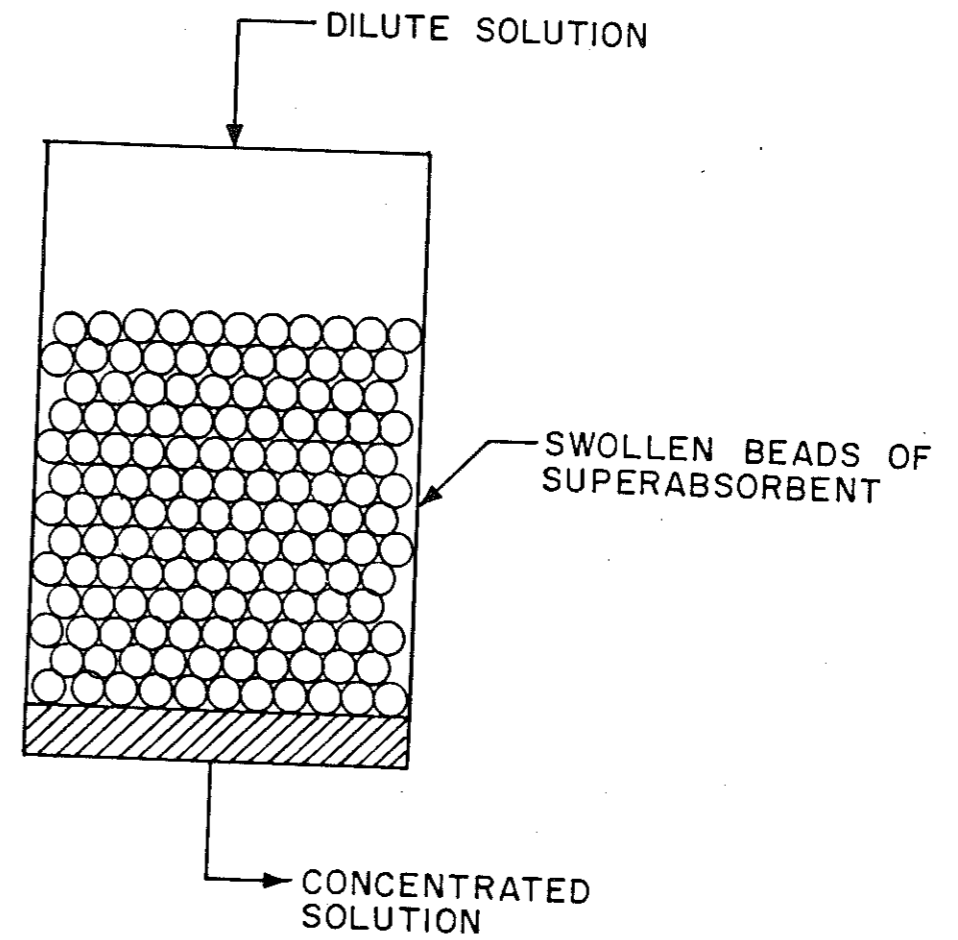


FIGURE -6.4 : CONCEPTUAL DESIGN OF DIRECT CONTACT SEPARATIONS

concentration the gel beads swell and selectively absorb low molecular weight substances like water and exclude macromolecular substances. By varying the composition, the swellex gels of specific mesh sizes (ξ) and cut-off levels can be tailor-made for specific systems. Moreover, the swelling behaviour of swellex gels is less sensitive to pH and external electrolytes present as compared to other gels used earlier. Therefore the efficiency of the separation process is less affected by the presence of salts in dilute macromolecular solution. Apart from packed bed, other separation processes based on liquid gel assisted membrane have been discussed in this chapter. While examining the performance of these processes vis-a-vis other competitive separation processes, number of aspects related to the percentage recovery, extent of separation, absorption fluxes, size exclusion and ease of recovery have been explained in this chapter. These new class of separation processes appear to have a considerable potential in concentrating biological macromolecules both on the laboratory scale as well as on large scale.

Theoretical Aspects

The separation process proposed by Cussler et al. (6) relies on regenerating the gel by changing its volume with variation in the pH. They have extended Flory's theory to predict the change in gel volume by the addi-

tion of a base. However, many assumptions have been made in their theory for which there are no justifications. The chemical potential of the solvent (μ_1) in the gel was given as,

$$\mu = \mu_1^0 + RT \left\{ \ln v_1 + v_2 + \chi v_2^2 + k_1 v_2^{1/3} \right\} \quad (6.1)$$

where, v_1 and v_2 are volume fractions of solvent and the gel and 'k' is the measure of gel elasticity. On the right hand side of the equation, the effect of non-Gaussian chain and the entropy of cross-links have been neglected. By solving the above equation, they arrived at,

$$\left(\frac{V_{\text{swollen}}}{V_{\text{dry}}} \right)^{-2/3} = \frac{k_1}{iz} \quad (6.2)$$

where, 'i' is the degree of ionization and 'z' is the maximum concentration of counterions produced by one mole of gel. The above equation deduces the relationship between the degree of ionization and swelling of the gel (10). Based on their prediction, the gel volume to the $(-2/3)$ power varies linearly with the reciprocal of the amount of added sodium from the base. It follows,

$$V_{\text{swollen}}^{-2/3} \propto \left\{ 1 + \frac{([\bar{R}] + K^{-1})}{[Na^+]} \right\} \quad (6.3)$$

where, $[\bar{R}]$ is the total concentration of potentially ionic groups, K is equilibrium constant and ' V_{swollen} ' is volume of the swollen gel. The above analysis did not hold good for swellex gels because of their strong ionic groups.

The swelling and deswelling behaviour of swellex gels, particularly the effect of ionic strength (i.e. presence of electrolytes) on the swelling has been explained in Chapter-II by making use of Flory's theory of swelling for ionic networks. The above studies indicated that the presence of electrolyte (increased I_0) reduces the extent of swelling markedly, which is reversible i.e. upon washing away the electrolytes again increases the swelling. This provides a means of controlling the swelling and deswelling of gels in a remarkably easy way.

Design Considerations

While examining the performance of these processes based on superabsorbent polymers vis-a-vis other competitive separation processes, it is important to investigate five different aspects related to percentage recovery, extent of separation, absorption fluxes, size exclusion and ease of recovery.

The first relates to percentage recovery, which is defined as,

$$\text{Percentage recovery} = 100 \times \frac{\text{Change in concentration}}{\text{Change in concentration expected due to volume change}}$$

100 percent recovery will be ideally desired, since it will rule out any loss of valuable macromolecules due to physical entrapment, adsorption etc.

The second important factor is the extent of separation that becomes possible over the original dilute solution identified by the concentration factor. The third relates to the fluxes achievable. Conventionally the transfer area figuring in these fluxes (as is commonly mentioned in membrane separation) corresponds to the active membrane area across which the transfer occurs. In the case of processes based on superabsorbent polymers it is not always easy to define it. However, it can be approximately defined for gel by knowing the size and density of the dry gel. The fourth important factor relates to size exclusion. This can be checked by controlling the mesh size of the network.

Based on Flory's theory of swelling, the swelling and deswelling behaviour of ionic network can be predicted and can be controlled at will and this would give an indication as to how much solvent (H_2O) can be removed in a given network. It does not, however, give any indication about the mesh size (ξ) which is related to the ability of the network to 'sieve'. Recently there

has been an active interest in predicting the mesh size (ξ) and relating to the characteristics of the network provided, the volume fraction of the network (v_2), average mol.wt. between cross-links (M_c) and end-to-end distance in the unperturbed state (r_0) is known (11,12,13). Accordingly, we have determined the mesh sizes of our swellex gels and described in detail in chapter-II. It can be readily seen that as the degree of cross-linking increases the mesh size decreases.

It then follows, that by using more tightly cross-linked gels, one can obtain a smaller mesh size and concentrate lower and lower molecular weight solutes. Finally, the fifth and most critical parameter is the ease of recovery and reuse of the gel. Different techniques can be adopted and in each case the viability will depend upon the value of the product to be recovered. Considering the above factors and depending upon the type and scale of operation, one could conceive a variety of strategies for effecting separation of biological macromolecules from their aqueous solutions.

In this work two types of experiments were carried out. The first one describes the separation process based on direct contact operations where there is a direct contact between the superabsorbent and a macromolecular solution, whereas in the second a membrane-gel composite process is described.

EXPERIMENTAL

Swellex gels used were based on polystyrene sulfonate and their method of preparation is given in Chapter-II. Casein, dextran, bovine serum albumin (BSA) and insulin were obtained from Sigma Chemical Company, USA and used as such.

The absorption capacities of swellex gels varied from 20-150 g/g depending on the degree of cross-linking and degree of ionization. The characterization of these gels in terms of average molecular weight between cross-links (M_c) and mesh sizes (ξ) are given in Chapter-II.

Concentration of Dilute Solutions

The dry swellex gel was thoroughly washed with (70/30) mixture of acetone and water and dried in oven at 60°C. The dried gel was sterilized at 120°C for 15 minutes. Then the requisite quantity of dry gel was packed in a glass column fitted with a sintered disc at the bottom (Fig. 6.4). The dilute macromolecular solution was passed through the column by a peristaltic pump. After 30 minutes, the raffinate was collected and its concentration was estimated spectrophotometrically (SHIMADZU UV-240) at appropriate wavelengths. The polyacrylamide concentration was estimated by starch-triodide method.

RESULTS AND DISCUSSION

Direct Contact Operation

The strategies discussed by Vartak et al. and

Cussler et al. imply the batch handling of swellable polymeric superabsorbents which may not be amenable to scale up. Therefore a concept of continuous or semicontinuous operation where rigid gel beads are used in a packed bed (Fig. 6.4) with a strategy of regeneration employed in suitable cycles would be very attractive. Therefore efforts were focussed on developing such a technique. Accordingly the glass column was packed with a swellex gel and dilute solution of macromolecular solute having wide range of molecular weights ($6000 - 10^6$) were used. The effectiveness of such an operation can be seen from Table-6.4, where data on concentration of macromolecular solutions especially proteins are presented. High recoveries with good concentration factors were obtained.

SELECTIVITY

The size exclusion characteristics or the selectivity of the gels were examined by devising gels of different mesh sizes (ξ) by controlling the molecular weight between cross-links (M_c). Figure 6.5 shows how the degree of cross-linking varies the mesh sizes and average molecular weight between cross-links. Protein having molecular weights from 14000 to 1,15,000 were concentrated by using gels of different mesh sizes. The results are summarized in Table-6.5. It can be seen that the concentration of lower molecular weight protein could be effected by using gels of lower M_c values i.e. highly cross-linked gels.

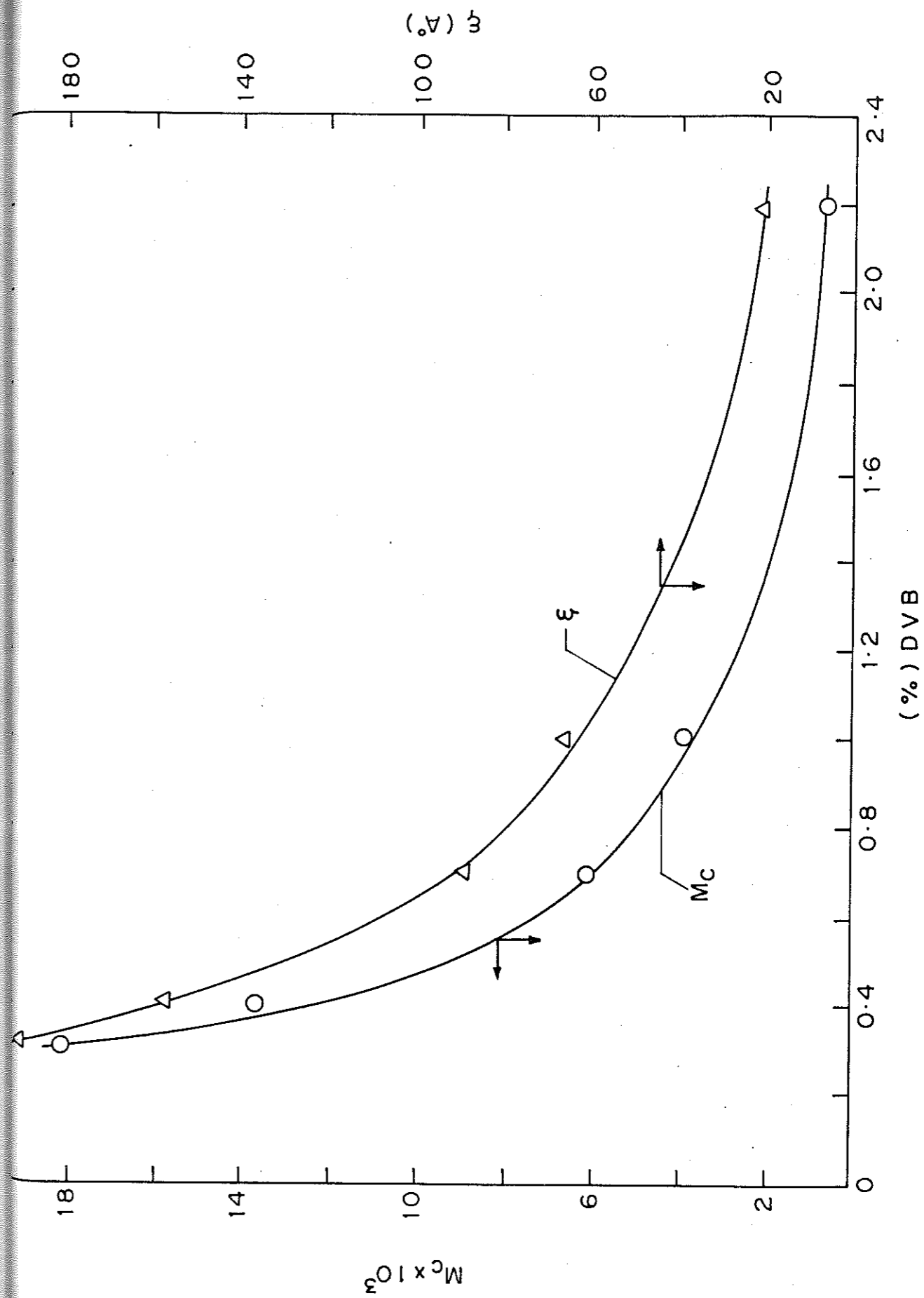


FIGURE 6.5: CROSS LINKING AGENT CONTROLS Mol.wt. BETWEEN CROSS LINKS (M_c) AND MESH SIZE (ξ)

REGENERATION

A crucial test of the viability of the separation technique rests with the ability to regenerate, recycle the gels easily. A strategy to effect such regeneration has been evolved on the basis of science of swelling and deswelling that has been described in the foregoing. When the proteins are separated, it is easy to effect the regeneration by cycling electrolyte solution shown schematically in Fig. 6.6. The latter Fig. 6.7 shows the influence of regeneration on the ability of polymeric beads to regain their absorbency characteristics. The first case shows that upto 75% of the original water absorption capacity can be regained by such cycling. This is presumably due to the retention of small amounts of electrolyte. A further washing with water ensures that the original absorption capacity can be easily regained.

Membrane/Gel Composite Processes

In the foregoing separations based on direct contact operations are discussed. However, in some cases, it may be desirable to avoid any direct contact between the polymeric gel and the macromolecular solution being concentrated. In such cases it may be desirable to use a semipermeable membrane to separate the gel and the protein solution. The membrane should be suitably chosen so that it will have the necessary flux and cut off values.

In our case the cellulose acetate membrane of 12,000

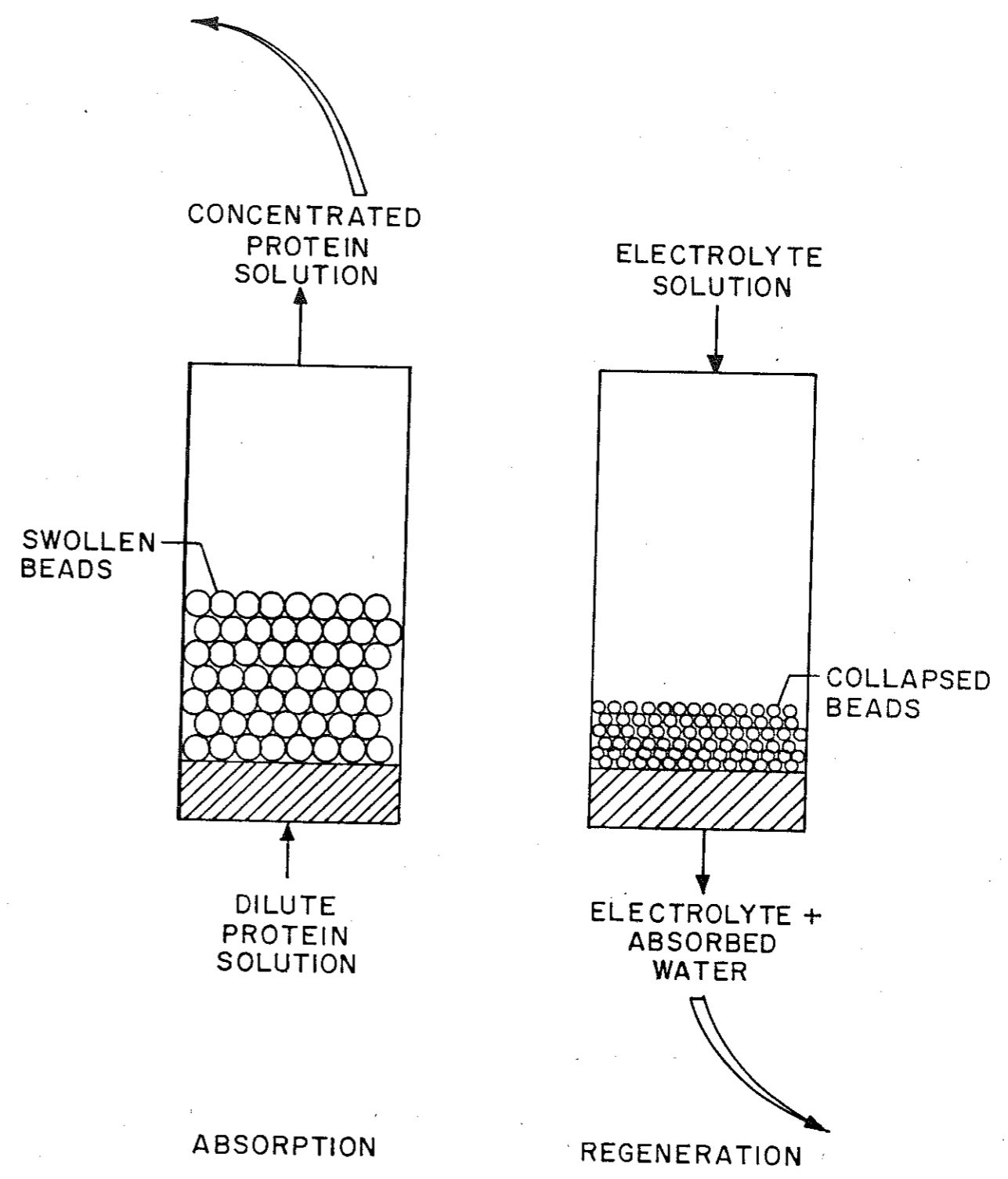


FIGURE 6.6: REGENERATION STRATEGY FOR PACKED BED OPERATION BASED ON ELECTROLYTE ELUTION

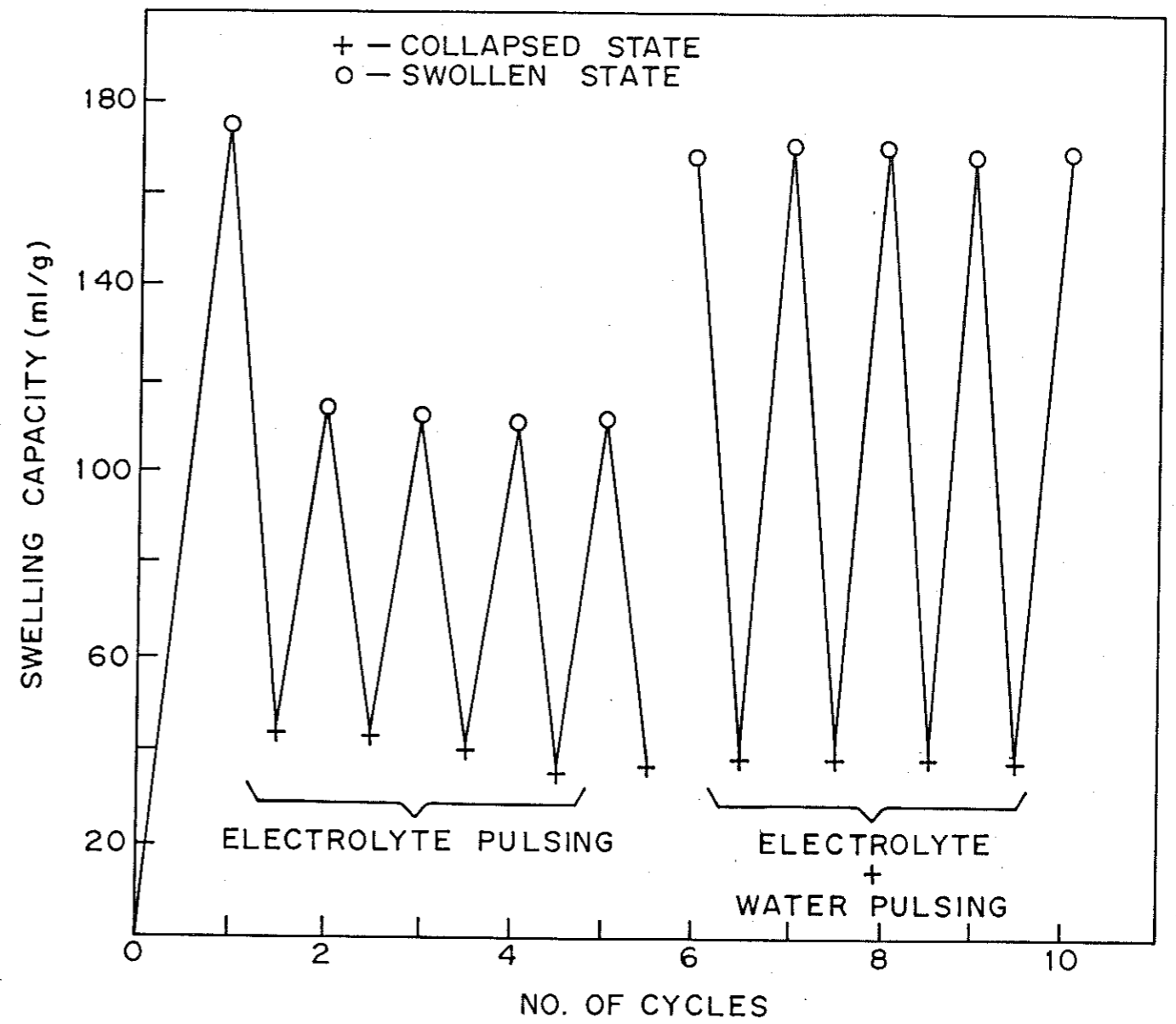


FIGURE 6.7 : INFLUENCE OF REGENERATION BY ELECTROLYTE ELUTION ON SWELLING CAPACITY

molecular weight cut off (MWCO) value (Sigma Chemical Corporation, USA) was used.

Liquid Gel Assisted Batch Dialysis

The diagram illustrating the separation concept is shown in Fig. 6.8. Here the protein solution to be concentrated is simply held in a dialysis bag, which is immersed in a superabsorbing liquid gel (Na-polyacrylate) with a concentration range of 2 to 7 percent. The efficiency of such an operation in specific cases can be seen from Table-6.6. Good concentration factors and reasonably good recoveries can be seen. However, these processes are slow and the separation times required are quite long. These could be in the range of 16-24 hrs. This is obviously due to the concentration polarization at the surface.

Liquid Gel Assisted Continuous Operation

The concept of this separation is shown in Fig. 6.9. A superabsorbing Na-polyacrylate solution (2-7%) was used. The ranges of molecular weights of Na-polyacrylate used can be seen from Table-6.7. A separation column made out of 2 cm diameter cellulose acetate membrane tubing (supported on a glass column) was used. The superabsorbing gel solution was circulated on the outside and the protein solution circulated on the inside. The detailed results are presented in Table-6.7. Although the fluxes appear to be quite reasonable, there is a

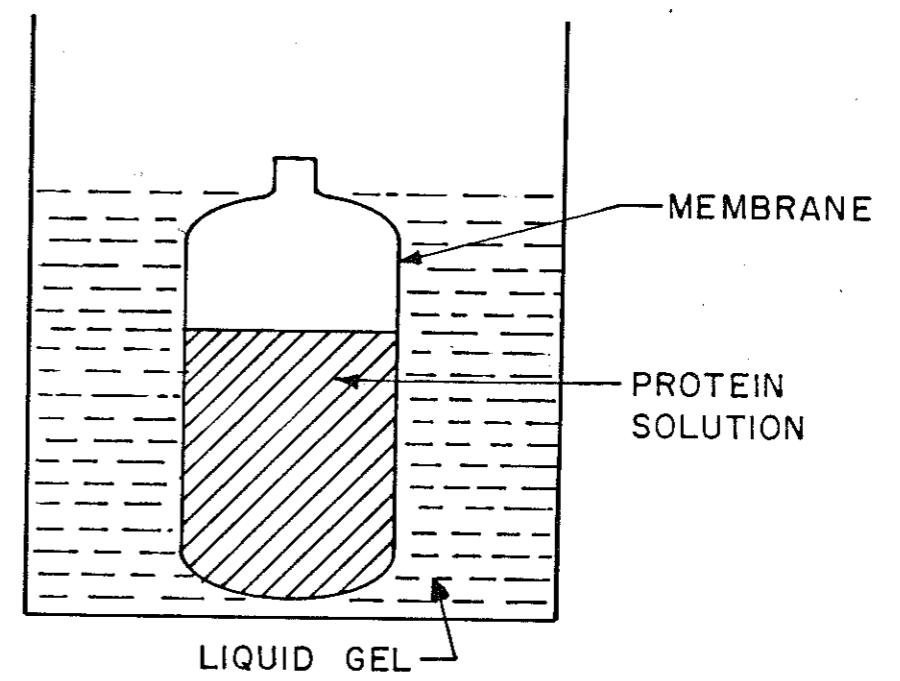


FIGURE 6-8: INDIRECT CONTACT OPERATION - BATCH DIALYSIS

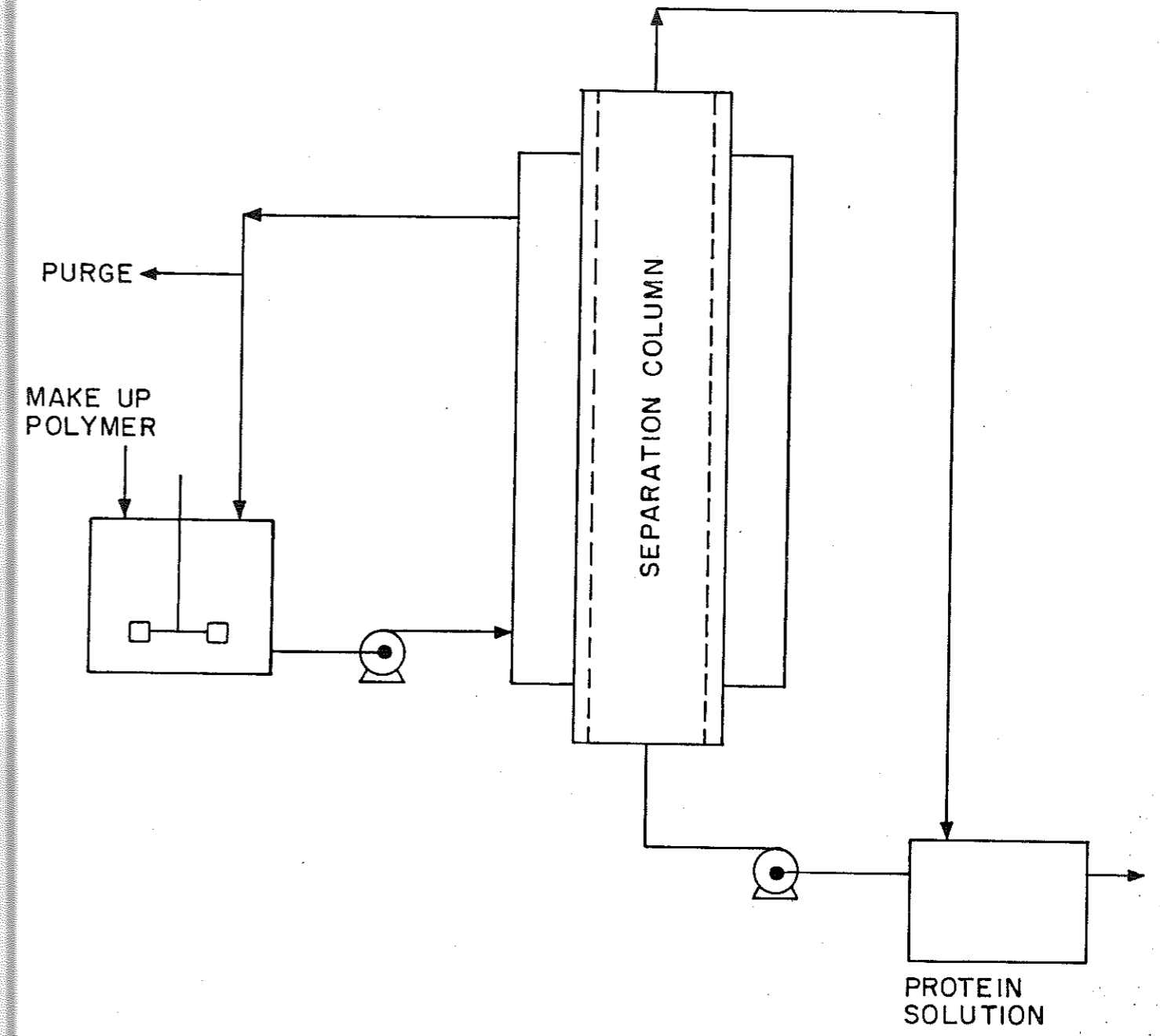


FIGURE 6.9: CONCEPTUAL DESIGN FOR INDIRECT CONTACT SEPARATIONS

scope for the improvement in the operation of such a device by making further innovation in design such as, for instance, by using the concept of 'shell and tube heat exchanger', where the liquid gel will flow continuously on the 'shell side', and the protein solution will flow on the 'tube side'.

Industrial Applications of Separation Process Based on Superabsorbent Polymers

In the preparation of vaccine, a dilute virus solution from allantoic fluid isolated from the chick or the cell culture, contains lot of water and useful proteins. Separation and removal of water is a crucial aspect of the vaccine preparation. In order to try this concept, the sample of superabsorbent polymer (Swellex) was submitted to an industrial organisation.

Dialysis, which is routinely used was known to take about 12 to 15 hrs for concentrating 100 ml fluid. By making use of the process described in the foregoing as 'continuous packed bed separation process', it was possible to concentrate 100 ml fluid in 30 minutes without sacrificing the activity of macromolecules. The concentration and activity in terms of haemagglutination (HA) was estimated before and after the concentration. The initial activity of 1:256 HA and final activity of 1:2406 HA clearly indicated that the process of concentration can be done without any loss in activity.

scope for the improvement in the operation of such a device by making further innovation in design such as, for instance, by using the concept of 'shell and tube heat exchanger', where the liquid gel will flow continuously on the 'shell side', and the protein solution will flow on the 'tube side'.

Industrial Applications of Separation Process Based on Superabsorbent Polymers

In the preparation of vaccine, a dilute virus solution from allantoic fluid isolated from the chick or the cell culture, contains lot of water and useful proteins. Separation and removal of water is a crucial aspect of the vaccine preparation. In order to try this concept, the sample of superabsorbent polymer (Swellex) was submitted to an industrial organisation.

Dialysis, which is routinely used was known to take about 12 to 15 hrs for concentrating 100 ml fluid. By making use of the process described in the foregoing as 'continuous packed bed separation process', it was possible to concentrate 100 ml fluid in 30 minutes without sacrificing the activity of macromolecules. The concentration and activity in terms of haemagglutination (HA) was estimated before and after the concentration. The initial activity of 1:256 HA and final activity of 1:2406 HA clearly indicated that the process of concentration can be done without any loss in activity.

Conclusion

In the foregoing, a number of separation processes based on superabsorbent polymers have been described. This new class of separation processes appears to have a considerable potential in concentrating biological macromolecules both at the laboratory scale as well as on a large scale. There is also a scope for undertaking fundamental investigations on the synthesis and functioning of superabsorbent polymers and especially about the possibility of highly selective and efficient separations, which are amenable to scale up.

89

89

he
ed
ly
in

REFERENCES

1. Osada Y. and Takeuchi Y., J. Polym. Sci. (Letters Edn), 19, 303 (1981).
2. Mashelkar R.A., J. of Indian Chem. Soc. 63, 149, (1986).
3. Narendranathan T.J. and Dunhill P., Biotechnol. Bioeng. 24, 2103 (1982).
4. Flodin P., Gelotte B. and Porath J., Nature, 188, 493 (1960).
5. Vartak H.G., Rele M.V., Rao M. and Deshpande V.V., Anal. Biochem. 133, 260 (1983).
6. Cussler E.L., Stokar M.R. and Verberg J.E., AIChE J. 30, 578 (1984).
7. Freitas R.F.S. and Cussler E.L., Chem. Engg. Sci. 42, 97 (1987).
8. Freitas R.F.S. and Cussler E.L., Sep. Sci. and Technol. 22 (2&3), 911 (1987).
9. Flory P.J., 'Principles of Polymer Chemistry', Cornell Univ. Press Ithaca, NY. (1953)
10. Gehrke S.H., Andrews G.P. and Cussler E.L., Chem. Engg. Sci. 41, 2153 (1986).
11. Bar-Howell B.D. and Peppas N.A., J. Appl. Polym. Sci. 30, 4583 (1985).
12. Regas F.P. and Valkanas G.N., Polymer, 25, 245 (1984).
13. Regas F.P., Polymer, 25, 249 (1984).

TABLE-6.1

Conventional techniques for concentration of
biological macromolecules

Technique	Resolving power	Operational difficulties
Industrial scale		
Precipitation	Poor	Inactivation possible Not universally applicable
Ultrafiltration	Poor	Fouling, cleaning shear denaturation
Laboratory scale		
Gel filtration	Moderate	Poor flow rates High packing costs
Electrophoresis	High	Limited experience on large scale

TABLE-6.2

Concentration of macromolecules using gel-stick method

Macromolecules	Mol. wt.	Concentration factor	Recovery (%)
Subtilisin inhibitor	10,000	7.75	85
Cytochrome C	12,500	8.0	80
Myoglobin	17,000	7.4	81
Soybean trypsin inhibitor	21,000	8.0	80
B.S.A.	68,000	8.2	90
Ferritin	450,000	8.0	93
DNA	-	8.0	80

Source: Vartak et al. (5).

TABLE-6.3

Concentration of dilute aqueous solution using
gel-bead batch operation

Macromolecules	Mol.wt.	Concentration factor	Recovery (%)
Polystyrene latex	-	1.53	82
B.S.A.	66,000	2.23	93
Haemoglobin	64,500	1.72	91
PEG	3,700	1.94	91
Sucrose	342	1.09	6
Urea	60	1.0	0

Source : Cussler et al. (6).

89

89

he
ed
ly
in

TABLE-6.4

Macromolecular separation by continuous packed bed
operation

Macromolecule	Mol. wt.	*Recovery (%)	Flux (g/cm ² .min.atm)
Casein	1,15,000	94.6	0.816
Dextran	71,500	96.8	0.418
B.S.A.	68,000	98.6	0.816
Egg albumin	45,000	98.5	0.825
PEG	9,000	80.8	0.543
Insulin	6,000	60.8	0.272

$$* (\%) \text{ Recovery} = 100 \times \frac{\text{Changes in concentration}}{\text{Change in concentration expected due to volume change}}$$

TABLE-6.5

Selectivity in continuous packed bed operation

Proteins	Mol. wt.	Gels of different Mc values				
		18,116	13,759	6,137	3,979	655
Casein	1,15,000	o	+	+	+	
Dextran	71,000	o	o	+	+	+
B.S.A.	68,000	o	o	+	+	+
Egg albumin	45,000	o	o	o	o	+
Lysozyme	14,000	o	o	o	o	+

o concentration not affected.

+ concentration affected.

he
ed
ly
in

TABLE-6.6

Liquid gel-assisted dialysis/batch operation

Macromolecule	Concentration factor	Recovery (%)
Glucose isomerase	7	89.0
Alkaline protease	11	85.0
Xylanase	17	90.0
Haemoglobin	50	95.0

89

89

he
ed
ly
in

TABLE-6.7

Liquid gel-assisted dialysis/continuous operation

Absorbent mol. wt. x 10 ⁻⁴	Gel conc. (%)	BSA conc. factor	Flux (g/min.cm ² ,atm)	BSA residence time (hrs)
1.10	7.0	1.35	2.06x10 ⁻³	1.11
2.54	7.0	1.21	2.21x10 ⁻³	1.11
27.0	2.0	1.23	1.46x10 ⁻³	1.27
41.0	2.0	1.14	2.21x10 ⁻³	1.27

89

89

he
,
ed
ly
in

SUMMARY AND CONCLUSIONS

Synthesis and characterization of two types of superabsorbent polymers viz. poly (2-acrylamido-2-methyl propane sulfonic acid) and sulfonated cross-linked polystyrene divinyl benzene is reported. Based on the swelling ratio measurements (q), parameters such as volume fraction of the network (V_2), average molecular weight between cross-links (M_c) and mesh sizes (ξ) of the network polymer have been estimated.

The effect of parameters like pH, composition and presence of electrolytes has been elucidated on the basis of Flory's theory. It has been shown that these polymers also absorb organic solvents to a large extent and these absorption characteristics have been correlated in terms of the solubility parameter of polymer and solvent.

In order to understand the structure and dynamics of superabsorbent polymers, extensive NMR investigations were undertaken. Proton magnetic relaxation has been used to elucidate the state of water in superabsorbent polymers. The proton nuclear spin-lattice relaxation times (T_1) were measured as a function of polymer concentration by using standard pulse sequences. The results of the experiments were interpreted by using a simple

exchange model which reveals the existence of two states of water namely bound and free water. Based on the analysis, about 90% of total water seemed to be present as free water and the remaining as bound water.

It has also been shown that in the superabsorbent polymeric systems it is possible to obtain a very high resolution proton spectrum by MASS technique. Since the polymer proton signals can be resolved, it is possible to undertake studies where specific polymer sites can be probed for structural and dynamical information.

The deformation dependent superabsorption and phase transitions has been demonstrated. The superabsorbent polymer, when subjected to deformation undergoes a structural change which is reflected on the superabsorption. The results of this finding have been explained on the basis of the permanent and semipermanent cross-links in the network structure. The existence of two types of cross-links is further corroborated by NMR and rheological measurements.

The viscosity behaviour of superabsorbent polymers has been investigated. The results predict the existence of both reversible and irreversible structures in the polymer. Based on the above studies a model has been developed which explains results qualitatively.

A number of alternative separation processes based on superabsorbent polymers as well as regeneration/recycle possibilities have been described. The performance of these processes have been evaluated in terms of size exclusion, percentage recovery and ease of regeneration.

189

189

he
ed
ly
in

SUGGESTIONS FOR FUTURE WORK

Synthesis and characterization of two types of superabsorbent polymers based on sulfonic acid monomers has been reported. Based on the swelling ratio measurements the mesh-sizes of these polymers have been estimated. Subsequently these polymers are used in the separation of dilute macromolecular solutions. Selectivity could be achieved by varying the mesh sizes. These superabsorbents also absorb organic solvents. Therefore application of these polymers in specific solvent extraction systems could be investigated.

The state of water, high resolution proton NMR and ^{13}C NMR of superabsorbent polymer such as PAMPS and HSPAN have been reported. The hydration and specific hydration sites in superabsorbent polymers can be investigated.

The existence of two types of cross-links and the breakdown of cross-links which enhances the superabsorption has been qualitatively explained by modification of Cheng's model. The model parameters have been evaluated theoretically. The experimental verification of these parameters would be a worthwhile exercise.

It has been shown that the deformation can be effected

by rapid motion of solvent due to centrifugal force. The verification of the structural changes brought about by this treatment could not be verified by NMR. It could be an interesting investigation.

89

89

he

,

ed

ly

in

B.U.P.—J. R.O./214-5,000-8-88.

University of Bombay



No. Th/ 591 of 1989

Bombay, 24-1-1989

Shri Manohar Virupax Badiger,
Chemical Engineering Division,
National Chemical Laboratory,
Pune-411008.

Dear Sir/~~Madam~~,

With reference to the thesis submitted by you for the degree of Doctor of Philosophy (Science) in Chemistry, I have pleasure in informing you that you have been declared eligible for the said degree. The degree will be formally conferred on you at a Convocation on your applying for it in the prescribed form at the proper time.

Yours faithfully,


for University Registrar.